Functional characterization of the 5-oxo-ETE receptor OXE-R and identification of the first small molecule antagonist with a novel mechanism of ligand bias

Dissertation

zur

Erlangung des Doktorgrades (Dr. rer. nat.)

der

Mathematisch-Naturwissenschaftlichen Fakultät

der

Rheinischen Friedrich-Wilhelms-Universität Bonn

vorgelegt von

Stefanie Blättermann

aus

Düsseldorf

Bonn 2011

Angefertigt mit Genehmigung der Mathematisch-Naturwissenschaftlichen Fakultät der Rheinischen Friedrich-Wilhelms Universität Bonn.

1. Gutachter: Prof. Dr. Evi Kostenis

2. Gutachter: Prof. Dr. Klaus Mohr

Tag der Promotion: 07.10.2011

Erscheinungsjahr: 2011

Die vorliegende Arbeit wurde in der Zeit von Oktober 2006 bis November 2010 am Institut für Pharmazeutische Biologie der Rheinischen Friedrich-Wilhelms Universität Bonn unter der Leitung von Frau Prof. Dr. Evi Kostenis durchgeführt.

Meinen Eltern

Index

1 Introduction

1.1 G protein coupled receptors

G protein coupled receptors (GPCRs) are signaling proteins which are found on the cell surface and transduce signals from outside the cell to the inside of a cell, thus allowing communication between cells, tissues and organs by responding to a wide range of modulators, such as hormones, neurotransmitters, lipids, peptides, nucleotides, ions and photons (Gether and Kobilka, 1998; Lagerström et al., 2008). With about 800 receptors, GPCRs represent the largest gene family in the mammalian genome, and, as widely expressed in the human body, GPCRs are involved in a vast range of physiologic and pathologic processes relying on cell signaling (Lundstrom, 2006). Related to their involvement in diseases like hypertension, pain, asthma, allergy and cancer, GPCRs are important pharmacological targets in drug development (Jacoby et al., 2006; Lappano and Maggiolini, 2011). About one third of currently used drugs are targeted against GPCRs, acting on approximately thirty receptors (Overington, 2006).

GPCRs consist of a single polypeptide chain spanning through the cell membrane seven times with three intracellular loops (ICLs) and three extracellular loops (ECLs), resulting in an extracellular N terminus and an intracellular C terminus. Structural comparison amongst GPCRs prove that the transmembrane (TM) helices contain highly conserved amino acid features, whereas the extra- and intracellular regions vary, which is due to the divergent ligands and signaling molecules interacting with GPCRs. Within the highly conserved TM helices, a highly conserved DRY motif at the C-terminal end of TM III and a highly conserved NPXXY motif in TM VII are most prominent and have been determined to stabilize the inactive receptor conformation. Important regions for receptor-G protein interaction are the intracellular loops 2 and 3, and intracellular loop 3 also contains recognition sites for protein kinases, presented by serine and threonine residues (Burstein et al., 1995; Krupnick and Benovic, 1998).

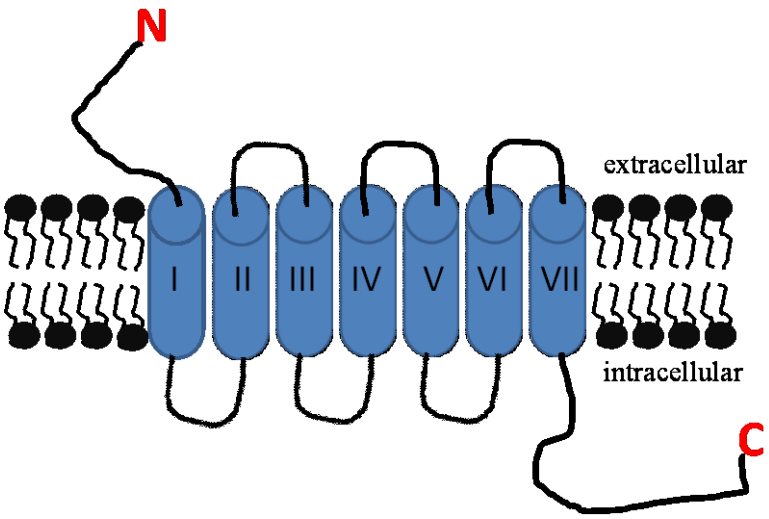

Figure 1: Scheme of a G protein coupled receptor.

GPCRs can be divided into five major subfamilies: the Rhodopsin-like receptors, the Secretin receptors, the Adhesion receptors, the Glutamate receptor family and the Frizzled/Taste2 receptors.

1.2 G proteins

Heterotrimeric G proteins are membrane-associated polypeptides serving as most common signal transducers of GPCRs. They consist of the subunits Gα, Gβ and Gγ, and in humans, there are fifteen genes encoding for Gα, five for Gβ and eleven for Gγ (Hurowitz et al., 2000). In the inactive state, the three subunits form a heterotrimer with a GDP bound to the Gα subunit (Gα-GDP). Upon G protein activation, GDP is released and exchanged for GTP, and subsequently Gα-GTP either dissociates from Gβγ or, alternatively, Gαβγ undergoes intramolecular rearrangement (Rosenzweig et al., 2007; Digby et al., 2006). Subsequently, Gα as well as Gβγ interact with cellular effectors close to the cell membrane, hereby inducing production of second messengers, which in turn activate further cellular pathways. G proteins are classified into four subfamilies due to structural determinants of the Gα subunit: $G\alpha_s$, $G\alpha_{i/o}$, $G\alpha_{q/11}$ and $G\alpha_{12/13}$ (Simon et al, 1991, Milligan and Kostenis, 2006).

Gαs was the first G protein to be discovered (Northup, et al., 1980, Ross, E. M. and Gilman, 1980) and is the stimulatory protein for adenylyl cyclase, leading to an increase of intracellular levels of the second messenger cAMP. The Gαs subfamily is comprised of $G\alpha_{olf}$ and the $G\alpha_s$ gene splice variants $G\alpha_{s(L)}$ and $G\alpha_{s(XL)}$ (Milligan and Kostenis,

2006). $G\alpha_s$ proteins are ubiquitously expressed, whereas $G\alpha_{olf}$ is mainly found in olfactory neurons and in certain CNS ganglia (Milligan and Kostenis, 2006).

Gα proteins belonging to the subfamily of $G\alpha_{i/o}$ proteins inhibit activity of adenylyl cyclase (Bokoch, et al., 1984, Sternweis and Robishaw, 1984), which results in a decrease of cellular amounts of cAMP. The $G\alpha_{i/o}$ subfamily comprises the subunits $G\alpha_{i1}$, $G\alpha_{i2}$, $G\alpha_{i3}$, and $G\alpha_o$, which are abundantly expressed.

Gα proteins from the $G\alpha_{q/11}$ subfamily activate β-isoforms of phospholipase C, which induces production of inositol phosphate and diacylglycerol, which in turn triggers cellular events resulting in calcium flux from intracellular stores. Thus, inositol phosphate and calcium are the second messengers produced upon activation of Gα proteins belonging to the $G\alpha_{q/11}$ subfamily (Cockcroft and Gomperts, 1985; Milligan and Kostenis, 2006). The $G\alpha_{q/11}$ G protein subfamily comprises $G\alpha_q$, $G\alpha_{11}$, $G\alpha_{14}$, $G\alpha_{15}$, $G\alpha_{16}$, where $G\alpha_q$ and $G\alpha_{11}$ are almost ubiquitously expressed in contrast to $G\alpha_{14}$, $G\alpha_{15}$, $G\alpha_{16}$ which are more restrictedly expressed in hematopoietic cells (Wilkie et al., 1991).

Activation of $G\alpha_{12}$ and $G\alpha_{13}$ proteins does not result in second messenger formation, but in increasing activity of the downstream effector small GTPase RhoA, which is mediated by a subgroup of guanine nucleotide exchange factors for Rho. $G\alpha_{12}$ and the $G\alpha_{13}$ proteins are expressed ubiquitously (Kurose, 2003, Kelly et al., 2007; Worzfeld et al., 2008).

1.3 GPCR signaling

GPCR signaling is initiated upon agonist binding to the receptor, causing a conformational change of receptor structure, which enables the receptor to interact with intracellular effectors. These intracellular effectors in turn induce cellular signaling cascades and hereby transfer the agonist-induced receptor stimulation into a cell response. GPCR signaling can mechanistically be divided into G protein-dependent and G protein-independent signaling.

At G protein dependent signaling, heterotrimeric G proteins located at the cell membrane are activated by agonist-stimulated GPCRs, causing a conformational change in the G protein heterotrimer, which leads to release of GDP from the nucleotide

binding pocket of Gα. Receptor-mediated G protein activation is thought to be initiated through contact between the activated GPCR and the Gβγ subunit of the G protein heterotrimer (Bourne, 1996; McIntire, 2009). After GDP release from Gα, subsequently a GTP binds to Gα. The Gα-GTP as well as the Gβγ subunit can interact with cellular effectors and during these processes, the Gα-GTP can either remain bound to Gβγ or dissociate from the Gβγ dimer, as evidence exists for the occurrence of both states (Janetopoulos et a., 2001; Bünemann et a., 2003). Cellular effectors and processes activated by G protein-dependent signaling are K+ channels, Src tyrosine kinases and the tubulin GTPase ($G\alpha_s$ and $G\alpha_{i/o}$), protein kinase A, the exchange protein directly activated by cAMP and the transcription factor cAMP response element binding protein (Gαs), protein kinase C and guanine nucleotide exchange factors ($G\alpha_{q/11}$), phospholipase C ($G\alpha_{q/11}$ and Gβγ), phosphoinositol kinase 3 (Gβγ) as well as Rho kinases and serum response transcription factor ($G\alpha_{12/13}$) (Siehler, 2009; Milligan and Kostenis, 2006; Oldham and Hamm, 2009; Woehler and Ponimaskin, 2009).

G protein-dependent signaling of GPCRs is terminated by G protein coupled receptor kinases (GRKs), which phosphorylate the receptor and enable binding of Arrestins to the receptor that in turn sterically interdicts further receptor-G protein contact.

Despite its function to terminate G protein-dependent GPCR signaling, Arrestins also play a role for G protein-independent GPCR signaling by acting as scaffold proteins, linking the GPCR to intracellular effectors such as the mitogen-activated protein kinases (MAPK) including extracellular-regulated kinase 1/2 (ERK 1/2), the c-Jun N-terminal kinase 3 (JNK3) and p38 (DeFea et al., 2000). Other GPCR signaling processes and effectors reported to be activated G protein independently involve GRKs, PDZ domain containing proteins, janus protein kinase/signal transducers and activators of transcription (JAK/STAT), or Src-protein tyrosine kinases (Woehler and Ponimaskin, 2009; Sun et al., 2007; Millar and Newton, 2010).

1.4 5-oxo-eicosatetraenioc acid

The fatty acid 5-oxo-eicosatetraenoic acid (5-oxo-ETE, OXE) belongs to the group of eicosanoids, which comprises oxygenated metabolites of arachidonic acid (AA) featuring a twenty carbon chain structure. OXE is a metabolite of the 5-lipoxygenase (5-LO) pathway of AA (**fig. 2**), which is abundantly present in cell membrane phospholipids. At the 5-LO pathway of AA, the fatty acid is converted into 5-

hydroperoxy-eicosatetraenoic acid (5-HpETE) via oxidation (Funk, 2001). 5-HpETE is further transformed by 5-LO into the leukotriene precursor leukotriene A4 (LA4) or is reduced to 5-hydroxy-eisosatetraenoic acid (5-HETE) by peroxidases, which is then further converted into OXE.

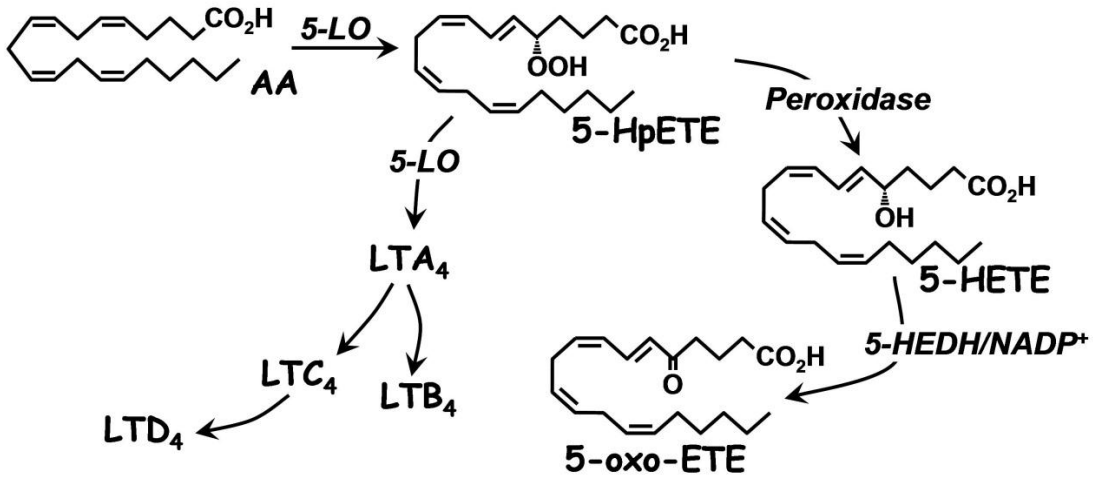

Figure 2: Formation of 5-oxo-ETE and other 5-lipoxygenase products from arachidonic acid. Taken from *OXE and the OXE receptor, Grant et al. (2009)*.

Conversion of 5-HETE into OXE is implemented by 5-hydroxyeicosanoid dehydrogenase (5 HEDH), which is highly selective for 5S-HETE and needs NADP+ as cofactor at high intracellular levels (Powell et al., 1992; Erlemann, 2007). Naturally, NADP+ is found at low intracellular levels due to its preferred complement NADPH. In neutrophils, increasing intracellular levels of NADP+ were determined to be produced by respiratory burst and oxidative stress due to activation of NADPH oxidase-2 (NOX2), converting NADPH into NADP+ by oxidation (Powell et al., 1994), thus inducing increased OXE formation. OXE production has been reported for monocytes (Zhang et al., 1996), dendritic cells (Zimpfer et al., 2000), platelets (Powell et al., 1999), endothelial (Erlemann et al., 2006), epithelial (Erlemann et al., 2007) and airway smooth muscle cells (Erlemann et al., 2007; Grant et al., 2009). OXE induces calcium mobilization, actin polymerization, CD11b expression and L selectin shedding, and as it is determined to be a potent chemoattractant for eosinophils and neutrophils (Powell et al., 2005), OXE is suggested to play a pivotal role in inflammatory diseases (Zimpfer et al., 1998; Jones, 2006; Grant et al., 2009).

1.5 5-oxo-ETE receptor

5-oxo-ETE was recently identified as endogenous ligand for a G_i coupled GPCR. The receptor gene was independently cloned by three groups (Hosoi et al., 2002; Jones et al., 2003; Takeda et al., 2002). Due to the agonist 5-oxo-ETE (OXE), the receptor was named OXE-receptor (OXE-R) by the International Union of Pharmacology (Brink et al., 2004). There are differences between the OXE-R sequence cloned by the groups of Hosoi and Takeda (also referred to as TG1019), and the OXE-R sequence cloned by Jones et al. (referred to as R527): The N terminus of TG1019 is 39 amino acids longer than that of R527 and possesses leucine at position 368 instead of valine. However, these differences do not alter the biological activity of the receptor, indicating that the N terminus of the OXE-R plays a minor role in signaling (Brink et al., 2004).

Phylogenetically, the OXE-R is closest related to the hydroxy-carboxylic acid receptors GPR109A (also referred to as HM74A) and the GPR81 (Ahmed et al., 2009), with 40 % sequence identity at the amino acid level (Jones et al., 2005). The OXE-R was determined not to respond to a variety of prostaglandins, leukotrienes and lipoxins (Hosoi et al., 2003), respectively, but agonistic activity on the OXE-R was determined for the mead acid metabolites 5-hydroxy-6,8,11-eicosatrienoic acid, 5-oxo-20:3 and two 6-trans isomers of leukotriene B(3) (Patel et al., 2008) as well as for bioactive peptides discovered by Sasaki et al. (2008).

Expression of the OXE-R was determined in peripheral leukocytes, lung, kidney, liver, spleen and a variety of tumor cells (Jones et al., 2003; Sundaram and Ghosh, 1998; O´Flaherty et al., 2005). The OXE-R was suggested to couple to Gαi/o proteins, since it had been shown that OXE induced calcium increase in neutrophils and inhibited forskolin-stimulated adenylyl cyclase-dependent cAMP production in CHO and HEK293 cells transfected with the OXE receptor (Hosoi et al, 2002, Jones et al., 2003). OXE-R coupling to $G\alpha_{i/o}$ proteins was confirmed by the use of PTX (Powell et al., 1996; Norgauer et a., 1996; O´Flaherty et al., 1996), a toxin which inactivates Gαi/o proteins by irreversible ADP-ribosylation (Kaslow, et al., 1987). Since OXE-mediated calcium mobilization and chemotaxis of transfected CHO cells were inhibited by PTX and by the phospholipase C inhibitor U73122, it was suggested that these responses were mediated by Gβγ signaling of $G\alpha_{i/o}$ proteins (Hosoi et al., 2005). It was also shown that OXE activates phosphoinositide-3 kinase (PI3K), which was suggested to be involved in chemotaxis of transfected CHO cells since the PI3K inhibitor LY294002

was able to block this reaction (Hosoi et al., 2005). Further cellular events induced by OXE-R signaling are phosphorylation of ERK 1/2 as shown for neutrophils (O´Flaherty, 1996), eosinophils (Langlois et al, 2009; O´Flaherty et al., 1996), PC3 cells (O´Flaherty et al., 2002) and OXE-R transfected CHO cells (Hosoi et al., 2005), as well as protein kinase C-delta (PKC-delta) and PKC-zeta signaling (Langlois et al., 2009). Since OXE is produced by inflammatory cells and elicits immune cell infiltration to inflammatory sites, OXE-R signaling is supposed to be related to inflammatory diseases like asthma (Jones, 2005), cancer (Grant et al., 2009), and cardiovascular diseases (Grant et al., 2009).

An OXE-R antagonist would be of great advantage to evaluate the receptor´s role in inflammation and diseases related to inflammatory processes. To date, no synthetic small molecule OXE-R antagonist has been published. Until now, only endogenously formed OXE metabolites of the 12-LO pathway, such as 5-oxo-12-HETE or 8-trans-5-oxo-12-HETE have been found to block OXE-mediated calcium mobilization in neutrophils, probably due to biological inactivation (Powell et al., 1999). Additionally, polyunsaturated fatty acids such as docosahexaenoic acid (DHA), eicosapentaenoic acid (EPA), dihomo-y-linolenic acid and eicosa-11Z,14U,17Z-trienoic acid have been reported to exhibit antagonistic activity against the OXE-R in GTPγS binding assays (Hosoi et al., 2002).

1.6 Aim of this work

The aim of this work was to discover small molecule OXE-R antagonists and to explore their antagonistic efficacy on the various signaling pathways of the OXE-R in a recombinant human cell line engineered to overexpress the receptor.

Toward this goal, a number of functional assays had to be established allowing to monitor G protein-dependent and G protein-independent effector activation of the OXE-R (calcium mobilization, cAMP inhibition, dynamic mass redistribution, β-Arrestin recruitment). The putative OXE-R antagonists should then be tested on endogenously expressed OXE-R in primary human eosinophils and neutrophils to determine their functionality in the receptor´s natural environment and to explore the consequences of OXE-R activation for primary cell function.

The very aim of this work therefore was to carefully dissect the various OXE-R signaling pathways and to evaluate antagonistic efficacy of OXE-R inhibitors on all

pathways with the goal to identify a small molecule antagonist that is competent to inhibit OXE-R signaling in both recombinant and primary human cells and therefore serve as a valuable tool for studies on the pathophysiological role of the OXE-R in inflammatory diseases.

2 Material and methods

2.1 Material

2.1.1 Chemicals, enzymes and reagents

5-oxo-6E,8Z,11Z,14Z-eicosatetraenoic acid, 5-oxo-ETE	Cayman, distributed by Biozol, Eching, DE, #34250
Agar	Fluka, Hamburg, DE, #05040
Agarose UltraPure	Invitrogen™, Darmstadt, DE, #15510-27
Ampicillin sodium salt	Roth, Karlsruhe, DE #K029.1
Bovine serum albumin, fatty acid free	Sigma, Taufkirchen, DE, #A6003
Bromphenol blue	Fluka, Hamburg, DE, #32712
Calcium chloride, dehydrate	Sigma, Taufkirchen, DE, #C3306
Carbachol	Sigma, Taufkirchen, DE, #C4382
Coelenterazine 400 a	Gold Biotechnology, St. Louis, USA, #C-320-10
compounds selected from virtual screening (ZINC codes depicted):	
- 682471	Molport, Riga, LT, #MolPort-002-826-987
- 938141	Enamine, Kiev, UA, #T5398912
- 1071153	Labotest, Niederschöna, D, #LT02891795
- 1087122	Aronis, Moscow, RUS, #m09511
- 3022900	Molport, Riga, LT, #MolPort-007-924-797
- 9030109	Molport, Riga, LT, #MolPort-000-501-445
- 9925404	UORSY, Kiev, UA, #PB-90138328
- 11852816	Interchim, Montlucon cedex, F, # F0817-0134
Dextran T-500	Roth, Karlsruhe, DE, #9219.2
Disodium hydrogen phosphate, dihydrate	Roth, Karlsruhe, DE, #4984
Dimethyl sulfoxide	Riedel-de Haen, Seelze, DE, #60153

DNA ladder 1 kb	New England BioLabs®, MA, US, #N3272
Ethylenediaminetetraacetic acid, disodium salt dihydrate	Roth, Karlsruhe, DE, #8040.3
Ethanol	KMF Optichem, Lohmar, DE, #08-205
Forskolin	Tocris, Bristol, UK, #1099
D-(+)-glucose	Sigma, Taufkirchen, DE #G7021
Geneticin	Gibco, Paisley, UK, #11811
HEPES	AppliChem, Darmstadt, DE, #A1069.0500
Hydrochloric acid	Applichem, Darmstadt, DE #0659
Hygromycin B	Invivogen, Toulouse, FR, #ant-hm-1
Interleukin-8	Peprotech, London, UK, #200-08M
3-Isobutyl-1-methylxanthine	Tocris, Bristol, UK, #2845
Magnesium chloride, hexahydrate	Fluka, Hamburg, DE, #63068
Magnesium sulphate, heptahydrate	Applichem, Darmstadt, DE, #A10373
(N-Morpholino)propanesulfonic acid	Sigma, Taufkirchen, DE, #M-1254
Nicotinic acid	Roth, Karlsruhe, DE, #3815.1
Oregon Green® BAPTA-1/AM	Molecular Probes, Darmstadt, DE, #O6807
Pertussis toxin	Sigma, Taufkirchen, DE, #2980
Pluronic®-F127	Molecular Probes, Darmstadt, DE, #P6867
Poly-D-Lysin	Sigma, Taufkirchen, DE, #P-6407
Potassium acetate	Merck, Darmstadt, DE, #1.04820
Potassium carbonate	Fluka, Hamburg, DE, #60110
Potassium chloride	Fluka, Hamburg, DE, #60128
Potassium dihydrogen phosphate	ZVE, D-53121 Bonn; #234984
Prostaglandin D2	Cayman, MI, US, #12010
Restriction endonucleases:	New England BioLabs®, MA, US
-BamHI	#R0136S
-EcoRI	#R0101S
-HindIII	#R0104S
-KpnI	#R0142S
-XbaI	#R0145S

-XhoI	#R0146S
Rubidium chloride	Merck, Darmstadt, DE, #107615
Sodium acetate	Applichem, Darmstadt, DE, #4555
Sodium chloride	Fluka, Hamburg, DE, #71376
Sodium dihydrogen citrate, 99%	Sigma, Taufkirchen, DE, #234265
Sodium dihydrogen phosphate	Roth, Karlsruhe, DE, #T878.2
Disodium hydrogen phosphate	Roth, Karlsruhe, DE, #T876.2
Sodium hydrogen carbonate	Merck, Darmstadt, DE, #1.06323.2500
Sodium hydroxide	Fluka, Hamburg, DE, #71689
Sulfuric acid	Merck, Darmstadt, DE, #1007311000
Tris(hydroxymethyl)-aminomethane	Roth, Karlsruhe, DE, #5426
Tryptone	Roth, Karlsruhe, DE, #8952.1
Yeast extract	Applichem, Darmstadt, DE, #3732

2.1.2 Kits

Calcium 4 assay kit FLIPR	Molecular devices, CA, USA, #R8142
cAMP dynamic 2 HTRF® assay kit	Cisbio Bioassays, BP 84175, France, #62AM4PEC
LANCE® Ultra cAMP assay kit	Perkin Elmer, Rodgau, DE, #TRF0262
NucleoBond® Xtra Maxi kit	Macherey Nagel, Düren, DE, #740414.50

2.1.3 Devices

Autoclave	3850 ELV, Systec
	Brunswick Scientific, NJ 08818-4005, USA
Balances	TE64, Sartorius, Göttingen, DE (precision balances)
	TE6101, Sartorius, Göttingen, DE (analytical balances)
Cell counting chamber	Neubauer, Brand, Wertheim, DE
Centrifuges	MiniSpin, Eppendorf, Hamburg, DE
	5810, Eppendorf, Hamburg, DE
	6K10, Sigma, Osterode, DE

Dry block heater	QBT2, Grant Instruments, Cambridge, UK
Electroporation device	Gene Pulser Xcell™, BioRad®, CA, US
Electrophoresis chambers	Mini-Sub® cell GT, Bio Rad, CA, USA
	Wide Mini-Sub® cell GT, Bio Rad, CA, USA
Freezer (-80°C)	Herafreeze, Heraeus, Hanau, DE
Incubator/shaker (bacteria)	HT-INFORS, Buch+Holm, CH
Incubator (cells)	HERAcell 240, Thermo Fisher, Dreieich, DE
Liquid nitrogen tank	MVE-Tec 3000, GermanCryo, Jüchen, DE
Microbiological safety cabinets	S@fe flow 1.2, Nunc™, NY, USA
Microplate readers	NOVOstar®, BMG Labtech, Offenburg, DE
Mithras LB940 Multimode reader	Berthold Technologies, Bad Wildbad, DE
Microscope	CKX31, Olympus, Hamburg, DE
Microwave	Microwave 800, Severin, Sundern, DE
Pipettes 0.5-10 µl; 10-100 µl; 20-200 µl; 100-1000 µl	Eppendorf, Hamburg, DE
Pipettes, multichannel	Alpha, Genex, Torquay, UK
Power supply	Power Pac HC, BioRad®, CA, US
pH meter	SevenEasy, Mettler Toledo, Giessen, DE
Sterile bench (cell culture)	HeraSafe, Thermo Fisher, Schwerte, DE
Thermomixer	Thermomixer® comfort, Eppendorf, Hamburg, DE
Spectrophotometer	Smart Spec Plus, BioRad®, CA, US
Vortexer	Reaxtop, Heidolph, Schwabach, DE
Water purification system	Milli Q® Water system, Millipore, MA, US

2.1.4 Buffers and solutions

2.1.4.1 Commercially available buffers and solutions

DMEM	Invitrogen™, Darmstadt, DE, #41965039

DPBS without Ca^{2+} and Mg^{2+}	Invitrogen™, Darmstadt, DE, #14190-094
FCS Sera Plus	Pan Biotech GmbH, Aidenbach, DE, #3702-P290616
Glycerol	Sigma, Taufkirchen, DE, #G2025
HBSS buffer	Invitrogen™, Darmstadt, DE, #14025
Histopaque	Sigma, Taufkirchen, DE, #1077
MEM	Invitrogen™, Darmstadt, DE, #31095-029
Penicillin/streptomycin solution	Invitrogen™, Darmstadt, DE, #15140
Sodium pyruvate MEM 100 mM	Invitrogen™, Darmstadt, DE, #11360039
Trypsin/EDTA 0.05/0.02% in PBS	Pan Biotech GmbH, Aidenbach, DE, #P10-0231SP
Ultra pure water	Invitrogen™, Darmstadt, DE, #10977035

2.1.4.2 Other buffers and solutions

Aqua dem. was used as solvent unless otherwise stated.

Assay buffer for DMR and BRET assays

20 mM HEPES in HBSS, pH 7.2.

$CaCl_2$ solution for calcium phosphate transfection

2 M $CaCl_2$, filter-sterilised (0.2 µm).

Coelenterazine stock solution

1 mg Coelenterazine 400a resuspended in 2500 µl of 99.9% Ethanol (final conc. 1 mM).

Coelenterazine reagent

Coelenterazine stock solution diluted in BRET assay buffer containing 30% ethanol (final concentration 100 µM).

Competent bacteria buffer 1

30 mM CH_3COOK, 50 mM $MnCl_2$ x 4 H_2O, 100 mM $CaCl_2$ x H_2O, 15% glycerine, pH 5.8, filter-sterilised (0.2 µm).

Competent bacteria buffer 2

10 mM RbCl, 75 mM $CaCl_2$, 10 mM MOPS, 15% glycerine, pH 6.8, filter-sterilised (0.2 µm).

DNA loading dye (6x)

Bromphenol blue (0.25% w/v) in equivalent amounts of glycerol and deionized water.

6% Dextran solution

6% Dextran in 0.9% saline.

Electroporation buffer (EB) (5x)

250 mM K_2HPO_4, 100 mM CH_3COOK, 100 mM KOH, pH 7.4 with acetic acid, filter-sterilised (0.2 µm).

HEPES solution (1 M)

1 M HEPES, pH 7.2, filter-sterilised (0.2 µm).

Hepes bufferd saline (HBS) (2x) for calcium phosphate transfection

50 mM HEPES, 280 mM NaCl, 1.5 mM Na_2HPO_4, pH 7.1, filter-sterilised (0.2 µm).

Krebs-HEPES-buffer (KHB)

118.6 mM NaCl, 4.7 mM KCl, 1.2 mM KH_2PO_4, 4.2 mM $NaHCO_3$, 11.7 mM D-glucose, 10 mM HEPES, making a 5x concentrated buffer stored at -20°C. Dilution of 5x KHB buffer with deionized water to 1x, then addition of 1.3 mM $MgSO_4$ and 1.2 mM $CaCl_2$, pH 7.4 with 1 M sodium hydroxide.

Luria Bertani (LB) medium

1% bactotryptone, 0.5% yeast extract, 1% NaCl, pH 7.4, sterilised by autoclaving at 121°C.

$MgSO_4$ solution for electroporation

1 M $MgSO_4$ heptahydrate, filter-sterilised (0.2 µm).

Neutrophil washing buffer

PBS without Ca^{2+} and Mg^{2+}, 10 mM HEPES, 10 mM Glucose, 0.1% BSA fatty acid free, pH 7.4.

Neutrophil DMR assay buffer

PBS with Ca^{2+} and Mg^{2+}, 10 mM HEPES, 10 mM Glucose, 0.1% BSA fatty acid free, pH 7.4.

Oregon Green® stock solution

39.7 µl DMSO were added to 50 µg Oregon Green® 488 BAPTA-1/AM (final concentration 1 mM), 3 µl aliquots of 1 mM stock were stored at -20°C under exclusion of light.

Oregon Green® assay solution

A 3 µl aliquot of Oregon Green® stock solution (1 mM) was diluted in 1994 µl KHB and 3 µl 20% pluronic®-F-127.

Phosphate buffered saline (PBS)

150 mM NaCl, 2.5 mM KCl, 7.5 mM Na_2HPO_4, 1.5 mM KH_2PO_4, pH 7.2 with HCl, sterilised by autoclaving at 121°C.

3.8% sodium citrate

3.8% sodium citrate, filter-sterilised (0.2 µm), stored at 4°C.

Stimulation buffer for HEK293 cell cAMP assays (cAMP dynamic 2 HTRF® assay kit)

HBSS, 20 mM HEPES, 1 mM 3-isobutyl-1-methylxanthine (IBMX).

Stimulation buffer for neutrophil cAMP assays (LANCE® Ultra cAMP assay kit)

HBSS, 5 mM HEPES, 0.5 mM IBMX, 0.1% BSA, pH 7.4, according to LANCE® Ultra assay development guidelines.

Super optimal broth (SOB)

2% Bactotryptone, 0.5% (w/v) yeast extract, 10 mM NaCl, 2.5 mM KCl, pH 7.4, sterilised by autoclaving at 121°C. After autoclaving 1 ml of sterile 1 M $MgCl_2$ and 1 ml of sterile 1 M $MgSO_4$ were added to 100 ml media.

Tris acetate EDTA (TAE) buffer (50x)

40 mM Tris(hydroxymethyl)-aminomethane (Tris), 1 mM EDTA, 5.71% glacial acetic acid. Diluted 1:50 before use.

Tris-EDTA (TE) buffer

10 mM Tris, 1 mM EDTA, pH 8.0 with HCl, filter-sterilized (0.2 µm).

2.1.5 Consumables

Cell culture plastic ware:	
- Plates: 6, 24, 48, 96 well	Corning®, NY, US, #3506, 3512, 3548, 3596
- Flasks: 25, 75 and 175 cm^2	Corning®, NY, US, #430168, 430720, 431079
- Dishes: 6, 10 and 15 cm	Corning®, NY, US, #430161, 430167, 430599
Cryogenic vials 1.5 ml	Nalgene, Thermo Fisher Scientific, NY, USA, #5012
Falcon tubes 15 and 50 ml	Corning®, NY, US
Gene Pulser cuvette, 0.4cm,	BioRad®, CA, US, #1652088
Microplates:	
- 384-well, fibronectin-coated biosensor cell assay microplate (Epic®)	Corning®, NY, US, #5042
- 384-well, biosensor cell assay microplate (Epic®)	Corning®, NY, US, #5040
- 384-well, source plate (Epic®)	Corning®, NY, US, #3657
- 384-well, LIA-plate, white, TC, F-form	Greiner, Frickenhausen, DE, #632102

Greiner bio one 4550 (cAMP assays)	
- 96-well, clear flat bottom, costar cell plate (Calcium mobilization assay)	Corning®, NY, US, #3599
- 96-well, v-bottom, costar plate (Calcium mobilization assay)	Corning®, NY, US, #3357
- 96-well, round bottom, costar plate (Calcium mobilization assay)	Corning®, NY, US, #3795
- 96-well, flat bottom, white, Optiplate (BRET)	Perkin Elmer, Rodgau, DE, # 6005500
Norm-Ject, sterile single-use syringe 20 ml (24 ml)	Henke Sass Wolf, Tuttlingen, DE #4200.000VE
Petri dishes (for bacteria)	Greiner, Frickenhausen, DE, #632102
reaction tubes 1,5 ml and 2,0 ml	Eppendorf, Hamburg, DE
Pipet tips	Sarstedt, Nümbrecht, DE
Tiptrays 384 (for Epic®)	CyBio, Jena, DE, #3800-25-513-N
Venofix winged infusion set, Luer Lock 21G	B.Braun, Melsungen, DE, #4056337

2.1.6 Software

Citavi 3.0	Swiss Academic Software GmbH, Zürich, CH
Office Excel® 2003	Microsoft Corporation, Unterschleißheim, DE
Office PowerPoint® 2003	Microsoft Corporation, Unterschleißheim, DE
Office Word® 2003	Microsoft Corporation, Unterschleißheim, DE
Prism® 4.02	GraphPad Software, Inc, CA, USA
MicroWin 2000 AdvII v4.41	Mikrotek Laborsysteme GmbH, Overath, DE
DeVision G v1.0	Decon Science Tec GmbH, Hohengandern, DE
Assay Development Mode Epic™ V1.22.2	Corning® Incorporated, NY, USA

Microplate Analyzer v1.5 modified for Excel 2002	Corning® Incorporated, NY, USA
NOVOstar® 1.20-0	BMG LABTECH, Offenburg, DE

2.1.7 Bacteria

XL1blue (Stratagene, CA, US), *Escherichia coli*, genotype: *recA1 endA1 gyrA96 thi-1 hsdR17 supE44 relA1 lac* [F´ *proAB lacI*q*Z*Δ*M15* Tn*10* (Tetr)]

2.1.8 Vectors

pcDNA3.1+

pcDNA3.1+ was purchased from Invitrogen™, Darmstadt, DE, #V790-20

OXE-R cDNA in pcDNA3.1+

cDNA of OXE-R *R527* (GenBank accession-number NM_148962) was inserted into pcDNA3.1+ by *Hind*III and *Eco*RI restriction sites. The plasmid originated from an internal source: research group of Prof. Dr. Evi Kostenis, Institute of Pharmaceutical Biology, University of Bonn, Germany.

HM74A cDNA in pcDNA3.1+

cDNA of HM74A (GenBank accession-number NM_177551) was inserted into pcDNA3.1+ by *Hind*III and *Eco*RI restriction sites. The plasmid originated from an internal source: research group of Prof. Dr. Evi Kostenis, Institute of Pharmaceutical Biology, University of Bonn, Germany.

RLuc cDNA in pcDNA3.1+

cDNA of Renilla Luciferase (GenBank accession-number M63501) was inserted into pcDNA3.1+ by *BamH*I and *Xba*I restriction sites. The plasmid originated from an internal source: research group of Prof. Dr. Evi Kostenis, Institute of Pharmaceutical Biology, University of Bonn, Germany.

OXE-R cDNA in pcDNA3.1+-RLuc

cDNA of OXE-R *R527* (GenBank accession-number NM_148962) was inserted into pcDNA3.1+-RLuc by *Hind*III and *Xba*I restriction sites. The plasmid originated from an internal source: research group of Prof. Dr. Evi Kostenis, Institute of Pharmaceutical Biology, University of Bonn, Germany.

HM74A cDNA in pcDNA3.1+-RLuc

cDNA of HM74A (GenBank accession-number NM_177551) was inserted into pcDNA3.1+-RLuc by *Hind*III and *Xba*I restriction sites. The plasmid originated from an internal source: research group of Prof. Dr. Evi Kostenis, Institute of Pharmaceutical Biology, University of Bonn, Germany.

2.1.9 Mammalian cell lines

HEK293 cells

The used HEK293 cell line was from an internal source: research group of Prof. Dr. Evi Kostenis, Institute of Pharmaceutical Biology, University of Bonn, Germany.

HEK293 cells stably expressing OXE-R *R527* and Gα subunit G_{16} (HEK293-OXE-R-G_{16})

HEK293 cells stably expressing OXE-R *R527* and the Gα subunit G_{16} were from an internal source: research group of Prof. Dr. Evi Kostenis, Institute of Pharmaceutical Biology, University of Bonn, Germany. Cells include cDNA of OXE-R *R527* (gene bank accession-number NM_148962) and cDNA of the Gα subunit of human G_{16}. Cells were selected by resistance towards geneticin (G418) and hygromycin B.

HEK293 cells stably expressing GFP^2-labeled β-Arrestin2 (HEK-βARR2-GFP^2)

HEK293 cells stably expressing GFP^2-labeled β-Arrestin2 and were kindly provided by Jesper Mosolff Mathiesen, University of Copenhagen, Copenhagen, Denmark.

HEK293 cells stably expressing GFP^2-labeled β-Arrestin2 and CRTH2 fused to Renilla luciferase (HEK-βARR2-GFP^2-CRTH2-Rluc)

HEK293 cells stably expressing GFP^2-labeled β-Arrestin2 and CRTH2 fused to Renilla luciferase were kindly provided by Jesper Mosolff Mathiesen, University of Copenhagen, Copenhagen, Denmark.

HEK293 cells stably expressing CRTH2 (CRTH2-HEK)

The HEK293 cell line stably expressing CRTH2 was from an internal source: research group of Prof. Dr. Evi Kostenis, Institute of Pharmaceutical Biology, University of Bonn, Germany. Cells include cDNA of CRTH2 (gene bank accession-number NM_004778) fused to a FLAG-tag at the N-terminus. Cells were selected by resistance towards geneticin (G418).

2.2 Methods

2.2.1 Molecular biology protocols

2.2.1.1 Preparation of LB plates

LB was prepared as described in section 2.1.4.2 and 1.5% (w/v) agar was added. The mixture was autoclaved and allowed to cool to 50°C prior to the addition of ampicillin (100 µg/ml). The medium was mixed to ensure equal distribution of antibiotic and approximately 25 ml were poured per 10 cm petri dish. The plates were left at room temperature before being stored at 4°C.

2.2.1.2 Preparation of competent bacterial cells

E. coli K12-XL-blue cells were streaked onto an LB agar plate in the absence of antibiotics and incubated overnight at 37°C. A single colony was inoculated into a 5 ml culture of SOB and grown at 37°C in a shaking incubator at 220 rpm for 16 hours. 1 ml of this culture was used to inoculate 100 ml SOB. The cell suspension was grown at 37°C and 220 rpm until the optical density at 550 nm reached the value of 0.5. The culture was centrifuged in ice-cold falcons for 10 min (3000xg, 4 °C). For the following work steps, chilled tips and falcons were used. The cell pellet was resuspended in 2x 12.5 ml ice-cold competent bacteria buffer 1 and centrifuged for 10 min (3000xg, 4 °C). After

cell pellet resuspension in 8 ml competent bacteria buffer 2, bacteria were aliquoted to 100 µl, frozen in liquid nitrogen and stored at 80°C until required.

2.2.1.3 Transformation of competent bacterial cells

An aliquot of competent bacteria was allowed to thaw on ice. 100 ng of DNA were added and cells were incubated on ice for 20 minutes. Hereafter, cells were subjected to a heat shock at 42°C for 90 seconds and returned on ice for 2 minutes. For recovery and expression of the antibiotic resistance gene needed for positive selection of transformants, 500 µl of LB without antibiotic was added to the cells and cell suspension was incubated at 37°C for 45 minutes in a shaking incubator. 100 µl of the cell suspension was spread onto LB plates containing the appropriate selective antibiotic and plates were incubated overnight at 37°C.

2.2.1.4 Preparation of glycerol stocks from transformed bacteria

A single colony of transformed E. coli cells grown on a LB plate overnight (see 2.2.1.3) was picked with a sterile wooden stick and transferred into 5 ml or larger amounts of LB media containing the appropriate antibiotic. The cell suspension was incubated overnight at 37°C in a shaking incubator at 200 rpm. The overnight culture was supplemented with glycerol to 15% and stored in a cryovial at –80°C.

2.2.1.5 Preparation of plasmid DNA

A 200-500 ml culture of transformed bacteria was pelleted by centrifugation at 7000 rpm at 4°C for 15 min. DNA was isolated with the NucleoBond® Xtra Maxi kit (2.1.2) according to the manufacturer´s instructions.

2.2.1.6 Digestion of DNA with restriction endonucleases

Digests were performed with 500 ng DNA, 0.5 µl of the appropriate restriction enzyme, 2 µl of the appropriate buffer specified by the manufacturer, BSA if required, and purified water (UltraPure, Invitrogen®) in a total volume of 20 µl. Reactions were incubated at 37°C for a minimum of 2 hours and heat-inactivated for 15 min at 70°C.

2.2.1.7 DNA gel electrophoresis

Digested DNA samples were examined using gel electrophoresis. Samples were diluted in 5-fold concentrated DNA loading buffer. A 0.7% agarose gel was prepared by mixing agarose with 1x TAE and boiling the solution in a microwave until the agarose was completely melted. After the solution was cooled down to 60 °C, 2.5 mg/ml ethidi-um bromide was added. The gel was set in a horizontal gel tank and immersed in 1x TAE. Samples and 1 kb DNA marker were loaded and the gel ran at a voltage of 100 V for 30-40 minutes. The DNA fragments were visualised using ultraviolet light and the size of each fragment was assessed by comparison with 1 kb DNA marker. Pictures were taken with the photo documentation system DeVision G v1.0.

2.2.1.8 Quantification of DNA

Quantification of DNA samples was performed by examining the absorbance of a 1:100 dilution of the sample at 260 nm. An A260 value of 1 unit was taken to correspond to 50 µg/ml of double stranded DNA. The A280 value of sample was also measured to assess the purity of the DNA solution. A DNA solution with A260/A280 ratio between 1.7 and 2.0 was considered pure enough for use.

2.2.2 Cell culture protocols

2.2.2.1 Cell culture media

Medium for HEK293 cells

HEK293 cells were cultivated in Dulbecco's Modified Eagle's Medium (DMEM,) supplemented with 10% (v/v) fetal calf serum (FCS), 100 U/ml penicillin and 100 µg/ml streptomycin.

Medium for HEK-OXE-R-G_{16} cells

HEK-OXE-R-G_{16} cells were cultivated in Dulbecco's Modified Eagle's Medium (DMEM) supplemented with 20% (v/v) fetal calf serum (FCS), 400 µg/ml of geneticin 418 (G418) and 250 µg/ml hygromycin B.

Medium for HEK–βARR2-GFP^2 cells

HEK-βARR2-GFP^2 cells were cultivated in Dulbecco's Modified Eagle's Medium (DMEM,) supplemented with 10% (v/v) fetal calf serum (FCS), 100 U/ml penicillin, 100 µg/ml streptomycin and 500 µg/ml of geneticin 418 (G418).

Medium for CRTH2-HEK cells

CRTH2-HEK cells were cultivated in DMEM supplemented with 10% (v/v) FCS, 100 U/ml of penicillin, 100 µg/ml of streptomycin and 500 µg/ml of geneticin 418 (G418).

2.2.2.2 Cell maintenance

Human embryonic kidney cells (HEK293) were grown in an incubator of 5% CO_2 and 95% air humidity at 37°C. Cells were grown in flasks or plates of varying sizes depending on the requirement of cells.

2.2.2.3 Passage of cells

For dividing confluent HEK293 cells, medium was removed, sterile PBS was added to wash the cells and removed. Sterile 0.25% Trypsin was added and flasks were placed in the incubator for 3 minutes. Fresh medium was then directly added to the detached cells and the cells were replated at desired density in new flasks or dishes.

2.2.2.4 Thawing and freezing cells

Liquid nitrogen frozen cells were thawed in a water bath at 37ºC. Cells were immediately transferred to a 15 ml falcon containing 4 ml of warm medium. The cell suspension was pelleted at 800 rpm for 4 min, the supernatant was discarded and the cells were resuspended in medium and transferred to an appropriate culture flask or dish.

To freeze cells, cells were washed, trypsinised, counted and pelleted at 800 rpm for 4 min. The medium was discarded and cells were resuspended with an appropriate amount of freezing solution (90% FCS, 10% DMSO) so that cell density was $3x10^6$

cells/ml. Cells were transferred to a cryogenic vial and placed at -80ºC overnight. The next day, cells were transferred to liquid nitrogen for long term conservation.

2.2.2.5 Cell count

20 µl of a cell suspension were pipetted between the surface of a counting chamber and a cover slip. The cell number of one big square was counted. The cell density and the total cell number was determined by the following terms:

Cell density [cells/ml] = counted cells x dilution factor x 10^4

Total cell number = cell density x volume [ml]

2.2.2.6 Transient cell transfection via calcium phosphate-DNA co-precipitation

24 hours prior to transfection, cells were seeded at $4x10^6$ cells per 10 cm dish in DMEM 10% FCS to achieve 70-80% confluence at the time of transfection. The day of transfection, medium was exchanged with 10 ml of fresh medium (DMEM, 10% FCS).

20 µg of DNA was mixed directly with 60 µl 2 M $CaCl_2$ and filled up with TE (10 mM Tris-HCl, 1 mM EDTA, pH 7.5) to a final volume of 500 µl. This was added dropwise to a volume of 500 µl 2x HBS buffer (50 mM HEPES, 280 mM NaCl, 1.5 mM NaH_2PO_4, pH 7.2) at minimum speed for vortex. After incubation for 45 min at room temperature, the mixture was added dropwise to the cells. The medium was changed after 16 hours to avoid cell toxic effects. In the present work, the total DNA amount consisted of 1:1 receptor DNA and empty vector.

2.2.2.7 Transient cell transfection via electroporation

For BRET assays (2.3.3), pcDNA3.1(+)-OXE-R-Rluc was introduced into stable HEK293-GFP^2-bARR2 cells using the Gene pulser Xcell™ electroporator. 1 µg receptor construct and 4 µg pcDNA3.1(+) were mixed with 20 µl 5x electroporation buffer (EB) and 4 µl of 1 M $MgSO_4$. Afterwards solution was filled up to a final volume of 100 µl with aqua dem. HEK293-GFP^2-βARR2 cells were trypsinised, counted and pelleted per 5 Mio cells. The pelleted cells were resuspended in 30 µl of 1x EB, cells were added to the DNA buffer mix and incubated at room temperature for 10-15 min. Cells were transferred to a 4 mm electroporation cuvette and electroporation was carried

out in the electroporator at 250 V, 500 µF and ∞ Ω. After electropration, cells were removed from the cuvette without cell debris and resuspended in media without antibiotics. Cells were grown for 48 hours prior to the assay.

2.2.2.8 Isolation of neutrophils from human peripheral blood

Peripheral blood from healthy volunteers was collected according to a protocol approved by the Ethics Committee of the medical faculty of the University of Bonn. All volunteers provided informed consent. 20 ml of blood were added to 4.4 ml 3.8% sodium citrate in a 50 ml falcon (**fig. 3**).

Figure 3: 20 ml of human peripheral blood supplemented with 4.4 ml 3.8 % sodium citrate.

Immediately, the falcon was gently inverted to prevent blood coagulation. To remove platelet-rich plasma, the blood was centrifuged at 400xg without brake at room temperature for 20 min. After centrifugation, two phases were obtained: an upper plasma phase and a lower phase containing blood cells (**fig. 4**). The plasma was carefully discarded without touching a white interphase between plasma and blood cells containing leukocytes.

Figure 4: Separation of plasma from blood cells.

For dextran sedimentation of erythrocytes and platelets, 6 ml of 6% dextran was added and the falcon was filled up to 50 ml with 0.9% saline. After gentle shaking, the inside of the falcon lid was cleaned, bubbles were taken out and the falcon was incubated at room temperature for 30 min. Erythrocytes sedimented to the bottom of the falcon and leucocytes remained in the upper phase (**fig. 5**).

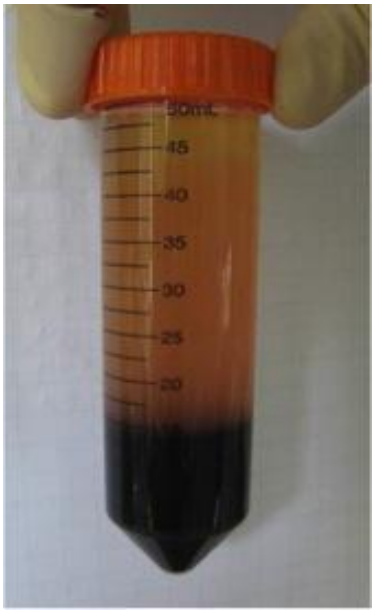

Figure 5: Dextran sedimentation of erythrocytes.

The leukocyte upper phase obtained from dextran sedimentation was carefully placed onto 15 ml of Histopaque® (**fig. 6**) and centrifuged at 400xg without brake for 20 min at room temperature.

Figure 6: Leukocyte phase layered onto 15 ml of Histopaque®

After centrifugation, five phases were obtained (from the top to the bottom, **fig. 7**): saline (yellow), peripheral blood mononuclear cells (PBMCs, white) including monocytes, basophils and lymphocytes, Histopaque® (white transparent), polymorphonuclear leukocytes (PMNL, light red) containing eosinophils and neutrophils and red blood cells (RBC, dark red).

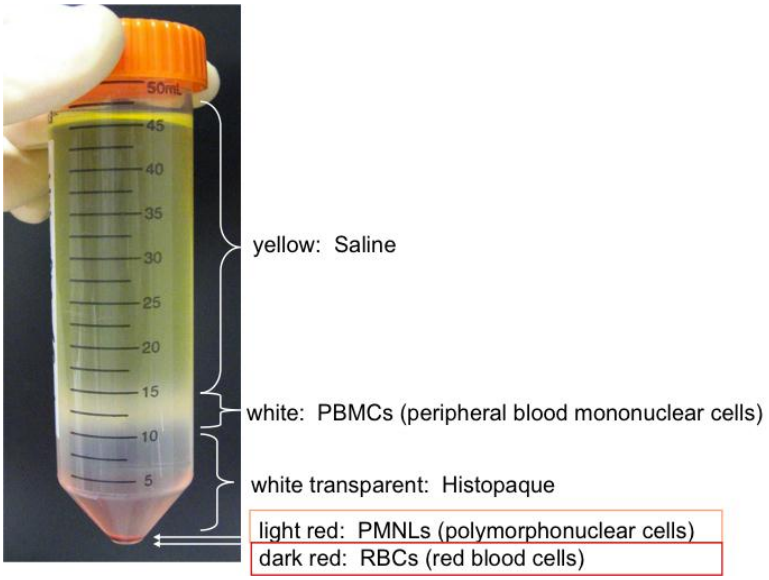

Figure 7: Polymorphonuclear cells are separated from peripheral blood mononuclear cells after Histopaque® density gradient centrifugation.

The saline, the PBMC and the Histopaque phase were discarded and the remaining PMNL pellet was resuspended in 10 ml wash buffer. The cells were pelleted at 400xg

with maximum brake for 7 min (**fig. 8**) and haemolysis was carried out to remove the remaining red blood cells from the leukocytes.

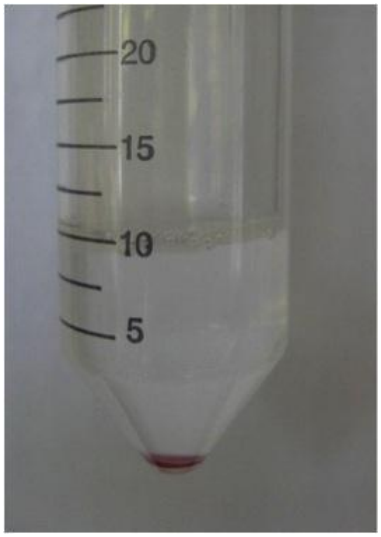

Figure 8: Cell pellet of leukocytes containing red blood cells

Thereforee, the supernatant was discarded, the pellet was resuspended in 1 ml 0.2% saline, and immediately 10 ml of 1.6% saline were added. After addition of further 10 ml washing buffer, cells were centrifuged at 400xg with maximum brake for 7 min. The supernatant including disrupted erythrocytes was discarded, the remaining neutrophils were washed twice with 10 ml wash buffer and cells were counted in a cell chamber (section **2.2.2.5**). With this method, cell purity was 98% with the majority of contaminating cells being eosinophils.

2.2.3 Cell based assays

2.2.3.1 Calcium mobilization assay

Calcium mobilization assay principle and protocol

Calcium release from intracellular stores is triggered by Phospholipase C activation followed by Inositol phosphate 3 accumulation, which triggers calcium release from the endoplasmic reticulum. For detection of released calcium, cells are loaded with a cell membrane permeable dye. Intracellular esterases convert the dye into its active form. Released calcium is bound to the dye and the fluorescence properties of the dye change.

Calcium measurements were performed using a NOVOstar® microplate reader with a built-in pipetor (BMG Lab Tech, Offenburg, Germany).

24 hours prior to the assay, cells were detached, counted and seeded into a PDL-coated 96-well plate at a cell number of 50.000 cells/well for transiently transfected cells and at a cell number of 60.000 cells/well for stable cells, and cells were incubated overnight at 37°C in a 5% CO_2 atmosphere. On the day of the assay, cells were washed twice with 50 µl KHB-buffer, and 20 µl Oregon Green® 488 BAPTA-1/AM or 50 µl of Ca4 solution, respectively, were added to each well. Cells were incubated at 37° and 5% CO_2 for 60 min. Meanwhile, 10-fold concentrated agonist was added to the 96-well agonist plate. KHB was added to the cells up to a final volume of 180 µl per well. Both the test and compound plate were transferred to the NOVOstar® and kept at 37°C under exclusion of light for 15 min until the measurement was started. The gain of the test plate was determined. For agonist assays, 20 µl compound solution was injected sequentially per well and fluorescence intensity was monitored at 520 nm (bandwith 20 nm) for 25 seconds at 0.4 s intervals. Excitation wavelength was 485 nm (bandwidth 25 nm). Antagonist assays were performed by addition of agonist after pre-incubation with antagonist for 30 min at 37 °C. The maximum fluorescence intensity was determined for each data set, and the mean value of a triplicate was plotted against agonist or antagonist concentration, respectively using GraphPad Prism®. Dose response curves were generated by a non-linear sigmoidal fit.

2.2.3.2 cAMP accumulation assays

In cAMP accumulation assays, the G_i mediated inhibition of forskolin-stimulated adenylyl cyclase of the OXE receptor was analysed by measuring cAMP production. For experiments with HEK293-OXE-R-G_{16} cells, the HTRF®-cAMP dynamic 2 kit from Cisbio was used, and for neutrophil cAMP accumulation assays, the LANCE® Ultra cAMP kit from Perkin Elmer was used.

HTRF®-cAMP dynamic 2 assay principle and protocol

The HTRF®-cAMP dynamic 2 assay is based on time-resolved resonance energy transfer (HTRF®) using a competition immunoassay where cellular cAMP competes with a labeled form of cAMP for binding to an anti-cAMP antibody. The anti-cAMP antibody used as donor is labeled with europium cryptate, and cAMP labeled to the dye d2 is used as acceptor.

Light excitation (320 nm) at anti-cAMP conjugates leads to emission of light (620 nm). When the cAMP-d2 molecule binds to the anti-cAMP conjugate, fluorescence resonance energy transfer (FRET) between the europium cryptate and the dye d2 occurs, resulting in fluorescence caused emission of light (655 nm). Results are calculated from the ratio of absorbance at 665 nm/620 nm. Obtained ratio values are corrected by a negative control, consisting of buffer and europium cryptate, and calculations are performed according to following formula:

$$\text{Delta F} = \frac{\text{Ratio}_{\text{sample}} - \text{Ratio}_{\text{neg}}}{\text{Ratio}_{\text{neg}}} * 100$$

Due to the inverse relationship between signal and cAMP concentration, accumulation of cAMP will result in a decreased signal.

HEK-OXE-R-G_{16} cells were detached, counted and resuspended in stimulation buffer at a cell number of 10^6/ml. Cells were dispersed into a 384-well microplate at a density of 50.000 cells per well (5 µl), briefly centrifuged and incubated at 37°C for 30 min. For agonist assays, cells were stimulated with 5 µl compound solution consisting of 2.5 µl 4-fold concentrated agonist or buffer, respectively, and 2.5 µl 4-fold concentrated forskolin and incubated for 30 min at 37°C. For antagonist assays, cells were incubated with 2.5 µl antagonist solution 4-fold concentrated or buffer, respectively, for 30 minutes at 37 °C, followed by stimulation with 2.5 µl compound solution consisting of 1.25 µl 8-fold concentrated agonist or buffer, respectively, and 1.25 µl 8-fold concentrated forskolin. After agonist stimulation, reactions were stopped by addition of 5 µl lysis buffer containing anti-cAMP conjugate and 5 µl lysis buffer containing cAMP-d2. The cell plate was incubated for 60 min at room temperature, and time-resolved FRET signals were measured at an excitation wavelength of 320 nm using the Mithras LB 940 multimode reader.

Data was analysed using the fluorescence ratio of light emitted by d2 labeled cAMP at 665 nm over light emitted by europium cryptate-labeled anti-cAMP at 620 nm. Levels of cAMP were normalised to the amount of cAMP elevated by 0.5 µM forskolin.

LANCE® Ultra cAMP assay principle and protocol

The LANCE Ultra cAMP assay is a homogeneous time-resolved fluorescence resonance energy transfer (TR-FRET) immunoassay where sample cAMP competes with Europium chelate-labeled cAMP for binding to anti-cAMP antibody labeled with U*Light*™ dye. When antibodies are bound to the Eu-labeled tracer and a light pulse at 320-340 nm excites the europium chelate molecule of the tracer, energy is emitted and transferred by FRET to U*Light*™ molecules on the antibody, which in turn emit light at 665 nm. Residual energy from the europium chelate will produce light at 615 nm. Data is expressed as ratio of emitted light at 665 nm and 615 nm as described by the following term:

$$\text{Ratio } (665/615*10^4)$$

In the absence of free cAMP, maximal HTRF signals at 665 nm are obtained, whereas when native, free cAMP competes with the Eu-cAMP tracer for binding to the U*Light*™-labeled antibodies, a decrease in HTRF signals at 665 nm is measured.
Neutrophils were resuspended in neutrophil stimulation buffer, seeded into a 384-well microplate at a density of 12.000 cells per well (5 µl) and briefly centrifuged. For agonist assays, cells were incubated with 5 µl agonist solution, consisting of 2.5 µl 4-fold concentrated agonist and 2.5 µl 4-fold concentrated forskolin solution. After 30 min, 5 µl 4-fold concentrated Eu-cAMP tracer working solution and 5 µl ULight-anti-cAMP working solution were added, and the plate was incubated at room temperature for 1 h. Fluorescence signals at 665 and 615 nm were detected using the Mithras LB 940 multimode reader (Berthold Technologies).
For antagonist assays, seeded cells were incubated with 2.5 µl 4-fold concentrated antagonist solution for 15 minutes before adding 2.5 µl of 4-fold concentrated agonist solution, consisting of 1.25 µl 8-fold concentrated agonist and 1.25 µl 8-fold concentrated forskolin solution.

Data derived from cAMP accumulation assays were collected using the MicroWin2000 software (Berthold Biotechnologies) and GraphPad Prism® software was used for dose response curves fitted with nonlinear regression and sigmoid dose-response equation.

2.2.3.3 BRET assay

BRET assay principle and protocol

Bioluminescence resonance energy transfer (BRET) technology is a proximity assay, based on non-radiative transfer of energy between a bioluminescent donor and a fluorescent acceptor. Fluorescence can only be measured if energy donor and acceptor moieties are less than 100 Å apart. The enzyme Renilla luciferase (Rluc) is used as bioluminescent donor and the chromophore GFP (Green Fluorescent Protein) as complementary fluorescent acceptor. BRET is monitored in real time and can be measured in living cells. If luciferase and GFP are attached to two proteins, e.g. the luciferase to a receptor and GFP to β-Arrestin2 (βARR2), the occurence of BRET can be taken as a result of the interaction of these two proteins.

Upon oxidation of a coelenterazine substrate by the luciferase, blue light is emitted which overlaps with the excitation spectrum of GFP, which then produces green light. There are different coelenterazine substrates to be used for different BRET techniques (Pfleger et al., 2006). In the present work, BRET^2 was utilized with Coelenterazine 400 a (also known as DeepBlueC) as luciferase substrate and GFP^2 as fluorescent acceptor. Oxidation of Coelenterazine 400 a results in an emission peak at 400-420 nm that exites GFP^2 producing light emission with a peak at around 510 nm. The BRET signal is determined by monitoring the ratio of green light (515 nm) over blue light (410 nm).

HEK293 cells stably expressing GFP^2 linked to βARR2 were electroporated with the OXER(R527)-Rluc construct. 48 h after transfection, cells were detached, counted and washed with assay buffer. Cells were resuspended in assay buffer at a cell number of 10^6/ml and incubated at 28°C with shaking at 160 rpm for at least 30 min. 10 µl 19-fold concentrated agonist or buffer were added to a white 96-well plate. Cells were added to agonist with a cell density of 180.000/well and incubated at 300 rpm for 10 min. 10 µl of 100 µM Coelenterazine 400 a was injected automatically by the Mithras and readings were collected immediately.

For antagonist assays, cell number was adjusted to 1.059×10^6/ml. 10 µl 19(or 18)-fold concentrated antagonist were added to a white 96-well plate, cells were added and incubated at 300 rpm for 30 min. 10 µl 19-fold concentrated agonist were added and cells were incubated at 300 rpm for another 10 min before measurement.

Data were collected using the MicroWin2000 software (Berthold Biotechnologies) and BRET signal was expressed in mBRET units of BRET ratio. GraphPad Prism® software

was used for dose response curves fitted with nonlinear regression and sigmoid dose-response equation.

GFP^2 control

150 µl assay buffer and 50 µl of suspended cells per well were added to a black 96-well plate, which was incubated at room temperature for 60 min. GFP^2 fluorescence was read by the Mithras with excitation wavelength of 400 nm and emission wavelength of 515 nm.

RLuc control

140 µl assay buffer per well was added to a white 96-well plate. 50 µl of suspended cells per well were added and cell suspension was incubated at room temperature for 60 min. 10 µl of 100 µM Coelenterazine 400 a per well were injected by the Mithras and RLuc luminescence was read immediately at emission wavelength of 400 nm for 10s.

2.2.3.4 Dynamic mass redistribution (DMR) assays

DMR assay principle and protocol

DMR assays were performed using a beta version of the Corning® Epic® System consisting of a temperature-control unit, an optical detection unit and an on-board robotic liquid handling device. The DMR assay is a holistic method which monitors GPCR-mediated cellular responses in real time and which is able to detect complex GPCR signaling (Fang et al., 2007; Schröder et al., 2010;). In this assay, changes in the local index of refraction upon mass redistribution within a cell monolayer grown onto a surface of a biosensor are measured. Cells are cultivated in a 384-well Epic® microplate containing a resonant waveguide grating biosensor in the bottom of each well. Broadband light illuminates the biosensor, and light of a given wavelength is guided to travel parallel to the bottom of the well. The light extends for a depth of 150 nm into the adjacent cells, is reflected and the wavelength of the reflected light is measured. Within the cell, mass movement of signaling molecules or cytoskeleton rearrangement due to ligand-induced G-protein signaling appears. This leads to a change of local optical density affecting the passing light, resulting in a wavelength shift of the reflected light. The magnitude of this wavelength shift is proportional to the amount of DMR, and

increase of mass contributes positive and decrease negative to the overall DMR response.

24 hours prior to the assay, cells were seeded at a cell number of 20.000/well in 30 µl medium onto fibronectin-coated 384-well Epic® biosensor microplates and centrifuged for 5 s at 200xg. Cells were cultivated (37°C, 5% CO_2) to obtain confluent monolayers. 1 hour before the assay, cells were washed twice with HBSS containing 20 mM HEPES (DMR assay buffer) by aspirating the medium with an eight channel manifold with 10 µl buffer remaining in each well. Cells were washed with 30 µl of assay buffer added to each well. In case the compound solutions contained dimethyl sulfoxide (DMSO), cells were washed in assay buffer containing the same percentage of DMSO as the later added compounds, because DMSO can induce bulk refractive index differences. After the last aspiration, the total volume was set to 30 µl by adding 20 µl of assay buffer. The microplate was centrifuged at 200xg for 5 s and kept for at least 1 hour in the Epic® reader at a constant temperature of 28°C.

Neutrophils were seeded at a cell number of 70.000/well in 30 µl of assay buffer onto fibronectin-coated Epic® biosensor microplates and centrifuged for 5 s at 200xg. The plate was directly transferred into the Epic® reader and incubated for approximately 2 hours.

For compound addition, a 384-well source plate was prepared by loading 20 µl per well of 4-fold concentrated substance solutions and hereafter was kept in the Epic® reader for at least 1 h prior to the assay. If antagonists were added in a first addition, a separate antagonist compound plate was prepared with 20 µl 5-fold concentrated antagonist per well, which was also pre-incubated for 1 hour in the Epic® reader. For the second addition of agonist hereafter, the agonist compounds were prepared in 5-fold concentration.

After starting the assay, the sensor plate was scanned and a baseline optical signature was recorded for 300 s. 10 µl of compound solutions were then transferred into each well of the sensor plate by an on-board liquid handling device and DMR was monitored for at least 3600 seconds.

Data were collected using Microplate Analyzer v1.5 (Corning® Incorporated). For quantification of DMR responses in dose response curves, the maximum response value within the time line from 500-1800 s was used. Dose response curves were established

with the GraphPad Prism® software and curves were fitted with a nonlinear regression and sigmoid dose-response equation.

2.2.3.5 Functional assays at primary human leukocytes

Assays at human eosinophils and neutrophils cells were performed by Petra Luschnig from the group of Prof. Dr. Akos Heinemann, Department of Experimental and Clinical Pharmacology, Medical University of Graz, Austria.

Eosinophil and neutrophil Calcium flux assay

Calcium flux assays at primary human eosinophils and neutrophils were performed as described previously (Heinemann et al., 2003).

2.2.4 Computational modeling

Computational modeling analyses were performed by Angel Gonzalez from the group of Prof. Dr. Leonardo Pardo, Laboratory of Computational Medicine, Universitat Autònoma de Barcelona, Barcelona, Spain.

Computational modeling of complexes between OXE-R antagonists and the OXE receptor

A homology model of the OXE-R was created with Modeller v9.5 (Martí-Renom et al., 2000) based on the crystal structure of the chemokine CXCR4 receptor (PDB code 3ODU). The relative orientation of the side chains at the extracellular side 2 is modified by TM 2 of CXCR4 (Wu et al., 2010), making a tighter helical turn at the TxP2.58 motif (NxP1482.58 in the OXE-R). For compiling Gü 1157, Gü 1158 and compound 11852816, the general Amber force field (GAFF) with HF/6-31G*-derived RESP atomic charges was used, and the Sander module of AMBER 10 (Case et al., 2008) was used to energy-minimize the ligand-receptor complexes.

Virtual screening of commercially available compounds with predicted antagonistic activity on the OXE-R

Molecules presenting the characteristic properties of Gü 1157 and Gü 1158, which are a molecular weight in the range of 350-450 and the number of hydrogen bond donors and acceptors ≤ 3, were filtered from the ZINC data base of commercially available compounds (URL http://zinc.docking.org 4; Irwin et al., 2005). PyPx and AutoDock Vina virtual screening tools 5 were used to dock the resulting hits into the binding pocket of the OXE-R, which was ascertained within a 20Å radius sphere around the centroid of Gü 1157 and Gü 1158 in their complex with the OXE-R model, as depicted in **fig. 12**. For selection of the best 100 compounds, the Autodock scoring function was used.

3 Results

3.1 OXE-R antagonist screening in calcium mobilization assays

3.1.1 Determination of calcium mobilization capabilities of the OXE-R in HEK293 cells

For OXE-R antagonist screening in calcium mobilization assays, a HEK293 cell line stably expressing the OXE-R *R527* as well as the promiscuous Gα subunit G_{16}, referred to as HEK-OXE-R-G_{16}, was used, which was provided by the group of Prof. Dr. Evi Kostenis. In an initial assay, the OXE potency in the HEK-OXE-R-G_{16} cell line was determined using calcium mobilization assays (section **2.3.1**). An OXE concentration effect curve was established, yielding a pEC_{50} for OXE of 7.75 ± 0.04 (**fig. 9a**). However, this OXE potency determined for the HEK-OXE-R-G16 cell line used by our group was 10-fold increased compared to the OXE potency obtained by Jones et al. (2003) for their stable HEK-OXE-R-G_{16} cell line.

Due to the findings of Hosoi et al. (2002) that the OXE-R *TG1019* is able to mobilize calcium via G_i in CHO cells, it was examined if calcium mobilization via Gi could also be detected for the OXE-R version *R527* in HEK293 cells. Therefore, HEK293 cells were transiently transfected with either the OXE-R alone or in combination with the OXE-R and the promiscuous Gα subunit of G_{16} (cDNAs used are according to section 2.1.8). 48 h after transfection, cells were analysed for OXE triggered calcium mobilization. Calcium flux could be detected in HEK293 cells co-transfected with the OXE-R and $G\alpha_{16}$, but not in cells lacking the promiscuous Gα protein (**fig. 9b**).

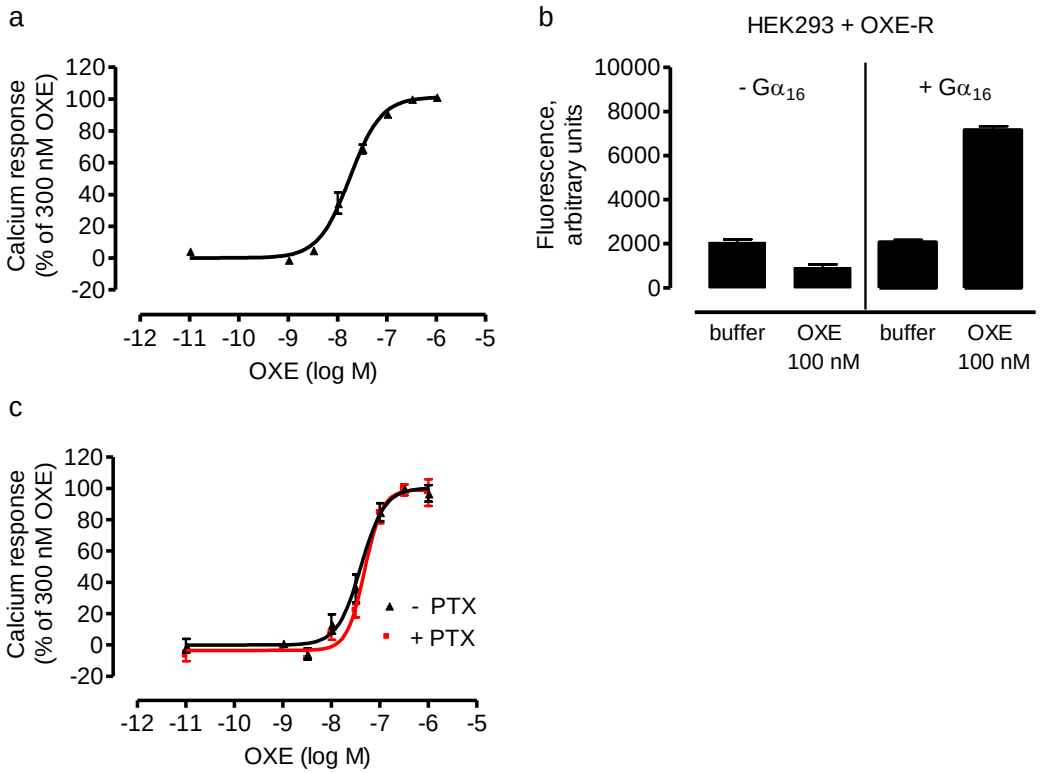

Figure 9: Effects of OXE on calcium mobilization in HEK293 cells expressing the OXE-R. (**a**) Concentration effect curve for OXE in HEK293 cells stably expressing OXE-R and $G\alpha_{16}$, resulting from calcium mobilization. The calcium response was normalized to the maximal calcium response achieved with 300 nM OXE. The pEC_{50} for OXE was 7.75 ± 0.04. (**b**) HEK293 cells transiently transfected with pcDNA3.1-OXE-R (*R527*) alone do not mobilize calcium after treatment with 5-oxo-ETE. However, HEK293 cells transiently co-transfected with pcDNA3.1-OXE-R and pcDNA3.1-$G\alpha_{16}$ show a calcium release. Calcium mobilization was measured as increase in fluorescence, expressed as arbitrary units. Shown are representative data (+ SEM) of at least three independent experiments performed in triplicates. (**c**) OXE-induced calcium mobilization in HEK-OXE-R-G_{16} cells is not blunted after pre-treatment with 50 ng/ml pertussis toxin (PTX) for 18 h. Data are shown as mean values (± SEM) of three independent experiments, each performed in triplicates.

Obviously, it is necessary to funnel the OXE-R *R527* to the G_q pathway by a promiscuous G protein to obtain detectable amounts of calcium in HEK293 cells. In order to examine if OXE-R G_{16} signaling in HEK293 cells is affected by endogenously expressed G_i proteins, HEK-OXE-R-G_{16} cells were exposed to OXE after pre-treatment with PTX (50 ng/ml, 18 h). As depicted in **fig. 9c**, G_{16}-mediated calcium flux was not affected when G_i proteins were inactivated by PTX. Hence, it was concluded that G_i signaling does not contribute to or affect G_{16} signaling of the OXE-R in HEK-OXE-R-G_{16} cells.

3.1.2 OXE-R antagonist screening of a compound library in calcium mobilization assays

About a hundred compounds from the in house compound library of the group of Prof. Evi Kostenis were tested on HEK-OXE-R-G_{16} cells for their ability to inhibit OXE-induced intracellular calcium increase. The antagonist screening was based on two measurements: In a first measurement, the compounds were assayed for OXE-R agonism, in order to exclude a false-positive effect in antagonism testing. To this end, 10 µM of each compound was added to the cells, and the cell response was recorded immediately after compound addition. After compound incubation for 30 min, antagonistic activity was analysed by addition of 500 nM OXE, the OXE EC_{80} value determined from OXE concentration effect curves established in section **3.1.1**, **fig. 9a**. No compounds were found to exhibit inhibitory activity at OXE triggered calcium mobilization of HEK-OXE-R-G_{16} cells, until a subset of compounds, which was obtained from Prof. Dr. Gütschow, Institute of Pharmaceutical Chemistry, University of Bonn, was analysed. Two compounds were found to exhibit inhibitory effects at OXE-induced calcium release (**fig. 10b**), without displaying agonistic effects on the cells (**fig. 10a)**: Gü 1157 (**fig. 10c**) and Gü 1158 (**fig. 10d**), two structurally related benzothiazin derivatives.

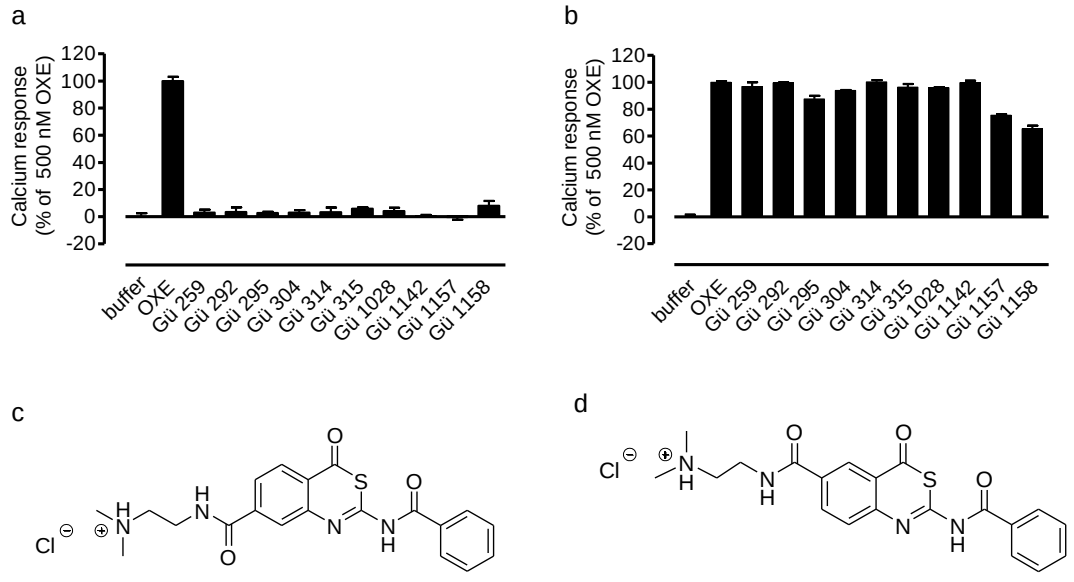

Figure 10: Screening for compounds with antagonistic activity on the OXE receptor in calcium mobilization assays. (**a**) No calcium mobilization could be detected after addition of 10 µM compound to HEK-OXE-R-G_{16} cells. (**b**) After incubation for 30 min, cells were challenged with 500 nM OXE. Gü 1157 (**c**) and Gü 1158 (**d**) exhibited antagonistic activity on calcium response of the OXE-R. Shown are representative data (+ SEM) of at least three independent experiments in triplicates. Structures of the tested compounds are depicted in section **8**.

Both compounds were chosen to be further characterized for antagonistic effects on the OXE-R.

3.1.3 Elucidation of unspecific cellular effects of Gü 1157 and Gü 1158

Before Gü 1157 and Gü 1158 were further explored for OXE-R antagonism in more detail, they were subjected to an additional test using the DMR technology in order to analyse unspecific, compound-triggered cellular effects. Briefly, in DMR assays the cell response to GPCR activation is measured as intracellular change of molecules in real time. Polarized light is passed through the bottom of cells located on a biosensor, and the reflected light is measured. After GPCR activation, resulting in G-protein signaling, intracellular reactions take place, and intracellular mass changes are detected as a shift in wavelength of the reflected light. Due to the ability of the DMR technology to detect whole cell responses, the DMR assay is a well suited tool for the analysis of unspecific cell reactions upon compound treatment, which might lead to false-positive results in further experiments.

In DMR assays, Gü 1157 and Gü 1158 were analysed on HEK293 cells stably expressing the G_i coupled GPCR chemoattractant receptor-homologous molecule expressed on Th2 cells (CRTH2). Prior to the assay, HEK-CRTH2 cells were seeded into fibronectin-coated biosensor microplates according to the DMR assay protocol in section **2.3.4**, and were grown for 24 hours till the assay. For analysis of unspecific compound effects, HEK293-CRTH2 cells were challenged with 3, 10 and 30 µM Gü 1157 or Gü 1158, respectively, or buffer as control. Meanwhile, the DMR response was recorded. During compound incubation for 30 minutes, negative DMR responses of CRTH2-HEK cells could be observed at compound concentrations of 30 µM of Gü 1157 (**fig. 11a)** and 10 and 30 µM of Gü 1158 (**fig. 11b**). These negative DMR responses probably depict cell stimulation due to Gü 1157 and Gü 1158. In order to analyse if cell responsiveness to the CRTH2 agonist PGD2 would be affected due to cellular stimulation, cells were challenged with 30 nM PGD2. The recorded DMR traces revealed that the PGD2 mediated cell response was not affected by Gü 1157 (**fig. 11c**) and Gü 1158 (**11d**), respectively. Gü 1157 and Gü 1158 also triggered negative DMR responses when tested on native HEK293 cells (data not shown), proving that cellular responses upon compound treatment were not related to interaction with CRTH2.

These findings revealed that Gü 1157 and Gü 1158 induced unspecific negative DMR responses in HEK293 cells, but did not alter cell responsiveness to agonist. In conclusion, both compounds were chosen to be further characterized for antagonistic activity on the OXE-R.

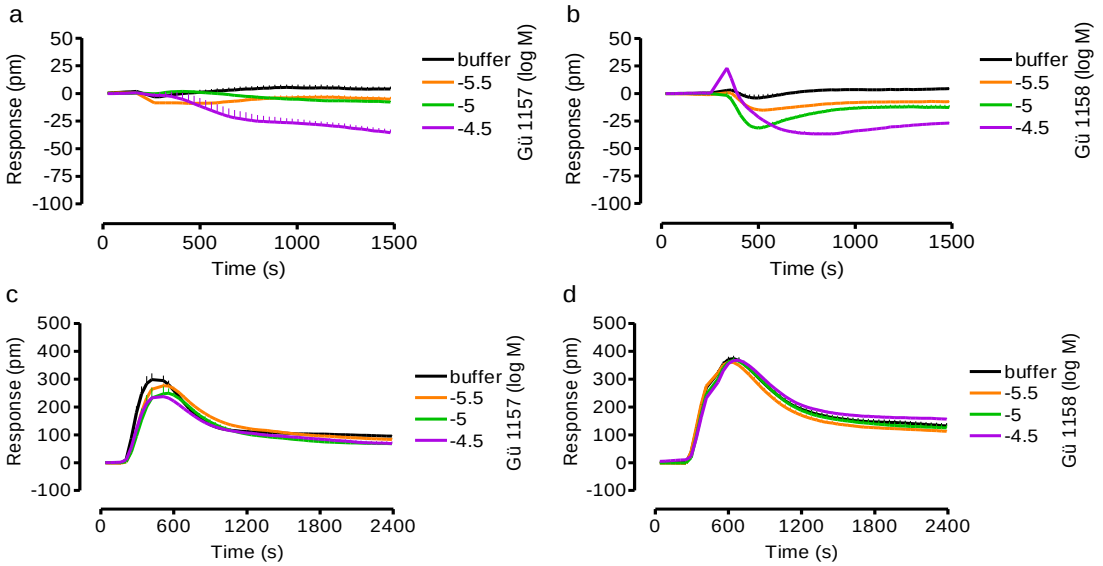

Figure 11: Analysis of potential unspecific cellular effects of Gü 1157 and Gü 1158 on the DMR response of HEK-CRTH2 cells to PGD2. Stable HEK-CRTH2 cells were incubated with increasing concentrations of Gü 1157 (**a**) and Gü 1158 (**b**) and responded with negative DMRs to concentrations of 30 µM Gü 1157 and 10 and 30 µM Gü 1158, respectively. The HEK-CRTH2 cell response to 30 nM PGD2 is not affected by Gü 1157 (**c**) and Gü 1158 (**d**), respectively. Shown are representative data (mean + SEM) of at least three independent experiments, each performed in triplicates.

3.1.4 Computational modeling of compounds with antagonistic activity on the OXE-R devoid of unspecific cellular effects

Based on the structures of Gü 1157 and Gü 1158, a virtual screening using computational modelling was performed in order to detect an OXE-R antagonist that might be devoid of unspecific cellular effects. The computational modelling was performed by Angel Gonzalez from the group of Leonardo Pardo, Laboratory of Computational Medicine, Universitat Autònoma de Barcelona, Barcelona, Spain.

An OXE-R model was built, as previously described in section **2.3.6**, using the crystal structure of the chemokine receptor CXCR4 as template, and the OXE-R was analysed for structural features interacting with molecule structures of Gü 1157 and Gü 1158.

In the CXCR4-based OXE-R model, charged amino acids within the TM helices ($R150^{2.60}$, $R176^{3.36}$ and $E260^{5.46}$) were found to point towards the binding site crevice, and in the middle of the transmembrane helices (TM) bundle, the bulky and very polar

group of R176$^{3.36}$ is interacting with E260$^{5.46}$ in TM5 and S311$^{6.51}$. It was presumed that the protonated amine group of Gü 1157 and Gü 1158 forms an ionic interaction with E260$^{5.46}$, and (**fig. 12a** for Gü 1157 and **fig. 12b** for Gü 1158), that the aromatic moiety of the compounds forms hydrogen bond interactions between their carbonyl groups and R176$^{3.36}$ and R150$^{2.60}$, respectively. Additionally, aromatic-aromatic interactions with F337$^{7.35}$and edge-to-face interaction between the terminal phenyl ring of the ligands and W158 in ECL1 were presumed.

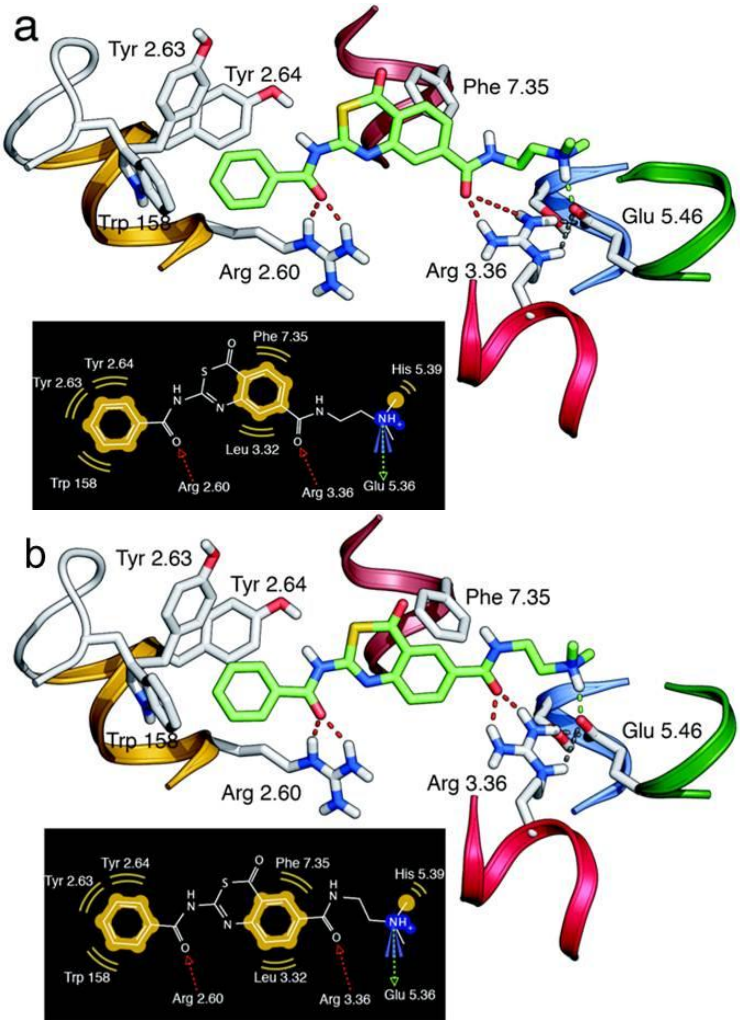

Figure 12: Computational models of the complex between Gü 1157 (a) and Gü 1158 (b), respectively, and the OXE receptor. The color code of the helices is: TM 2 (yellow), TM 3 (light red), 5 (green), 6 (blue), and 7 (pink).

Due to these findings, the ZINC database 4 (Irwin and Shoichet, 2005) was screened for commercially available compounds possessing structural features required for interaction with the OXE-R, as defined by the computational models. The best 100 compounds were chosen and docked into the OXE-R model (**fig. 13**), and the best 10 compounds were selected and ordered.

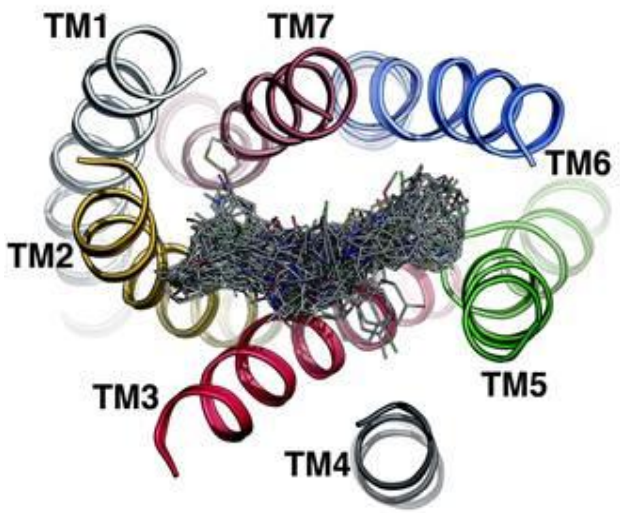

Figure 13: 100 compounds selected from ZINC database screening of commercially available compounds were docked into the OXE-R model.

Eight compounds were obtained and tested in calcium mobilization assays for antagonistic activity on the OXE-R. None of the compounds did trigger calcium flux of HEK-OXE-R-G_{16} cells when added to the cells (**fig. 14a**), but only one compound, 11852816, exhibited significant inhibitory effects on OXE mediated calcium mobilization, as compared to 10 µM Gü 1157 and Gü 1158, respectively (**fig. 14b**).

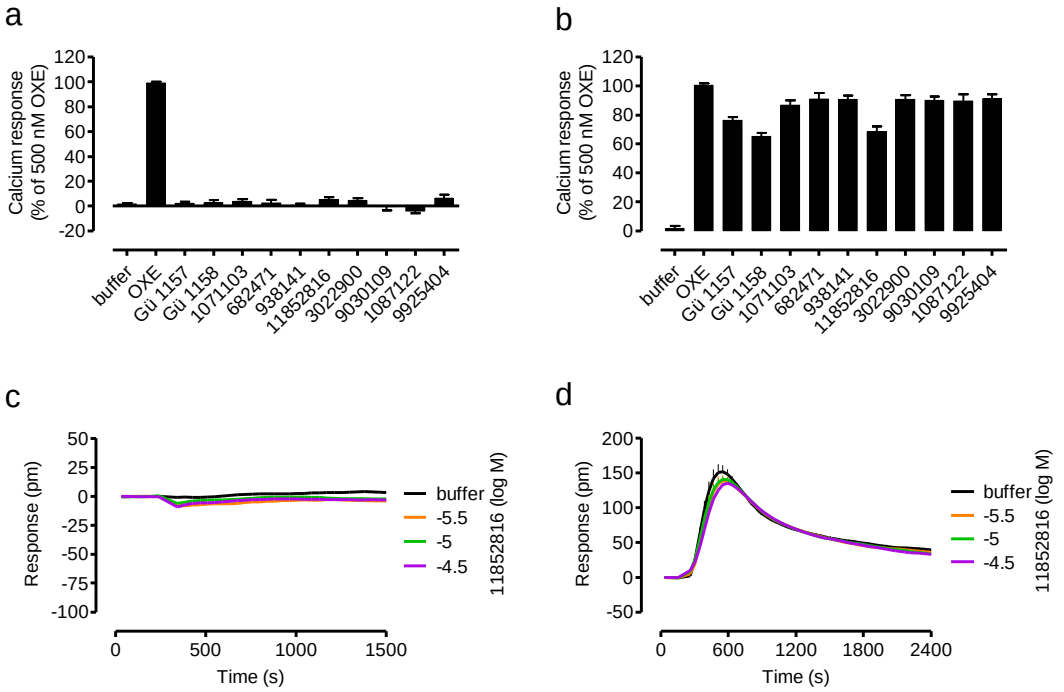

Figure 14: Analysis of antagonistic activity of virtual screening hits derived from the ZINC database in calcium mobilization assays and analysis of unspecific cellular effects of compound 11852816 in DMR assays. After addition of 10 µM 11852816 to HEK-OXE-R-G_{16} cells, no calcium mobilization could be detected (**a**). After pre-incubation with the indicated ligands for 30 min, cells were challenged with 500 nM OXE. Compound 11852816 displayed antagonistic activity at the calcium response of the OXE-R as compared to 10 µM Gü1157 and Gü1158, respectively (**b**). HEK-CRTH2 cells do not respond with a DMR response to increasing concentrations of 11852816 (**c**). After compound pre-incubation for 30 minutes, the 30 nM PGD2 DMR response is not affected (**d**). Shown are representative data (+ SEM) of at least three independent experiments, each performed in triplicates. Structures of the tested compounds are depicted in section **8**.

Following these results, compound 11852816 was also tested for unspecific effects on CRTH2-HEK cells in DMR assays, in order to analyse if the computational modeling approach indeed yielded an OXE-R antagonist devoid of unwanted effects. It could be shown that compound 11852816 neither triggered unspecific DMR responses in HEK-CRTH2 cells (**fig. 14c**), nor did the substance affect the PGD2 mediated CRTH2 response (**fig. 14d**).

In contrast to Gü 1157 and Gü 1158, compound 11852816, which is a benzobisthiazole derivative (**fig. 15a**), lacks the protonated amine group, but $R176^{3.36}$ and $E260^{5.46}$ also form ionic interaction $R176^{3.36}$ and $E260^{5.46}$ in the ligand-unbound receptor (**fig. 15b**). Compound 11852816 mainly interacts with the OXE-R by hydrogen bonds between $R176^{3.36}$ and $R150^{2.60}$ and by aromatic-aromatic interactions with $F337^{7.35}$. The two terminal phenyl rings of compound 11852816 occupy the two different aromatic

pockets of the OXE-R, formed by either W158 in ECL1 and Tyr151$^{2.63}$ Tyr152$^{2.64}$ in TM2, thus representing another significant structural feature of this compound.

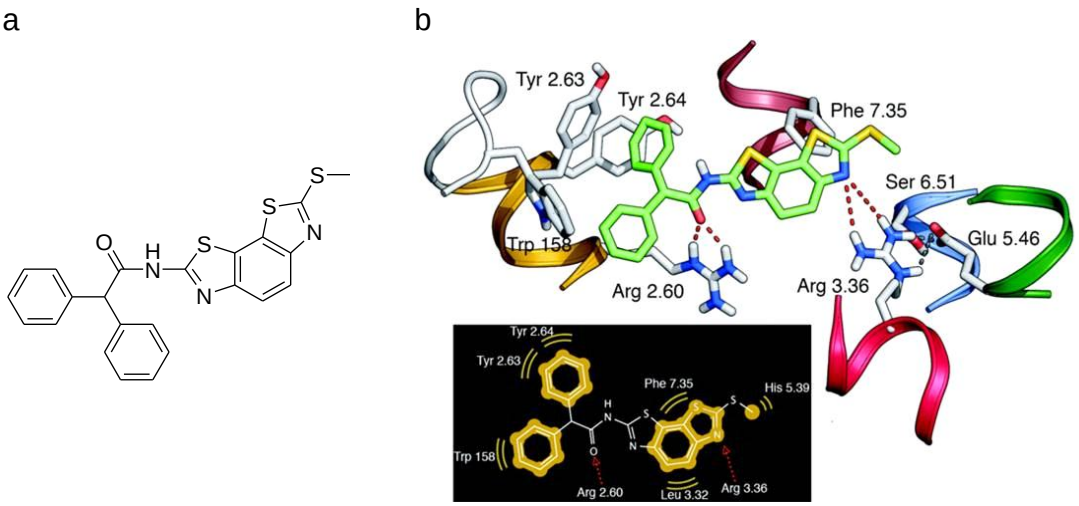

Figure 15: Structure of compound 11852816 and computational model of the complex between compound 11852816 and the OXE-R. (**a**) Molecule structure of compound 11852816. (**b**) Computational model of the complex between compound 11852816 and the OXE-R. The color code of the helices is: TM 2 (yellow), TM 3 (light red), 5 (green), 6 (blue), and 7 (pink).

In order to analyse if particular structural features of compound 11852816 are responsible for antagonistic activity on the OXE-R, molecular fragments of 11852816 were synthesized by Philipp Ottersbach from the group of Prof. Dr. Gütschow, Institute of Pharmaceutical Chemistry, University of Bonn. In addition, compound 11852816 was also re-synthesized.

3.1.5 OXE-R antagonist screening of compounds derived from fragment based synthesis of compound 11852816

Eight compounds were derived from the fragment based synthesis of compounds structurally related to compound 11852816. The new synthesized compounds and the re-synthesized compound 11852816, hereafter named Gü 1654, were tested for antagonistic activity on the OXE-R in calcium mobilization assays. None of the newly synthesized compounds displayed antagonistic effects on the OXE-R (**fig. 16b**), thus proving that all structural features of the molecule described in section **3.1.4** are required for biological activity of compound 11852816. However, Gü 1654 was shown to exhibit equal antagonistic activity on the OXE mediated calcium response as the original compound 11852816.

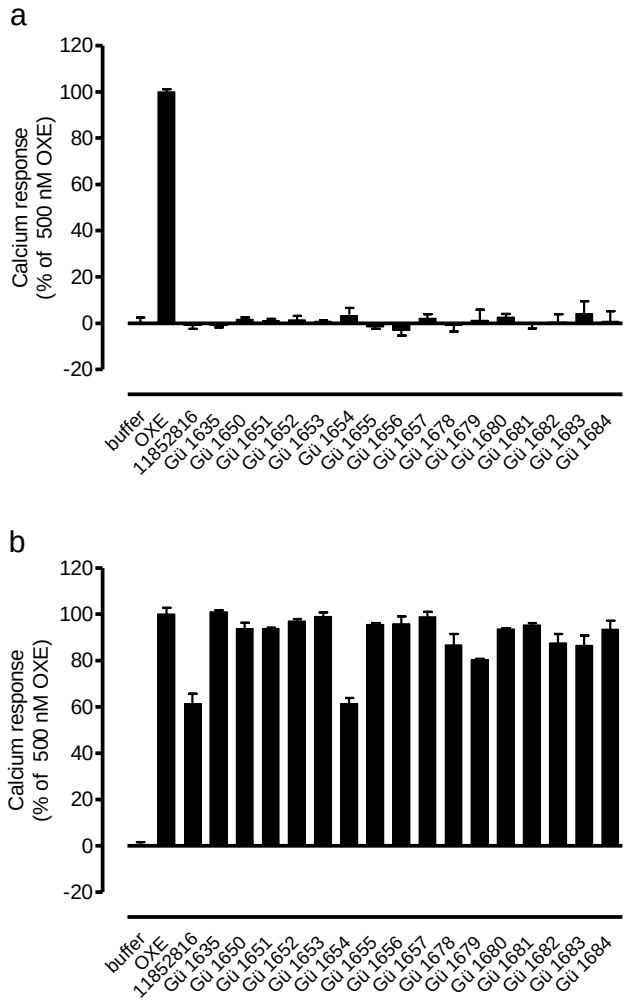

Figure 16: Screening of new synthesized compounds based on the structure of compound 11852816 for antagonistic activity on the OXE-R. (**a**) After addition of 10 µM per compound to HEK-OXE-R-G_{16} cells, no calcium flux was obtained. (**b**) After compound pre-incubation for 30 min, cells were challenged with 500 nM OXE. Except for compound 11852816 and its re-synthetized analogue Gü 1654, no other compound displayed antagonistic activity at the OXE-R calcium response. Shown are representative data (mean + SEM) of at least three independent experiments. Structures of the tested compounds are depicted in section **8**.

Data derived from calcium mobilization assays proved Gü 1654 to be a putative OXE-R antagonist devoid of unspecific cellular effects. Together with Gü 1157 and Gü 1158, Gü 1654 was chosen to be further examined for antagonism on the OXE-R in calcium mobilization assays.

3.1.6 Characterization of the nature of antagonism of Gü 1157, Gü 1158 and Gü 1654 in calcium mobilization assays

OXE concentration effect curves were elaborated after cell pre-incubation with 3, 10 and 30 µM Gü 1157, Gü 1158, and Gü 1654, respectively, or buffer as control. A

concentration-dependent decrease in the maximal OXE response was produced by all compounds, indicating insurmountable antagonism of Gü 1157 (**fig. 17a**), Gü 1158 (**fig. 17b**) and Gü 1654 (**fig. 17c**) at the OXE-R.

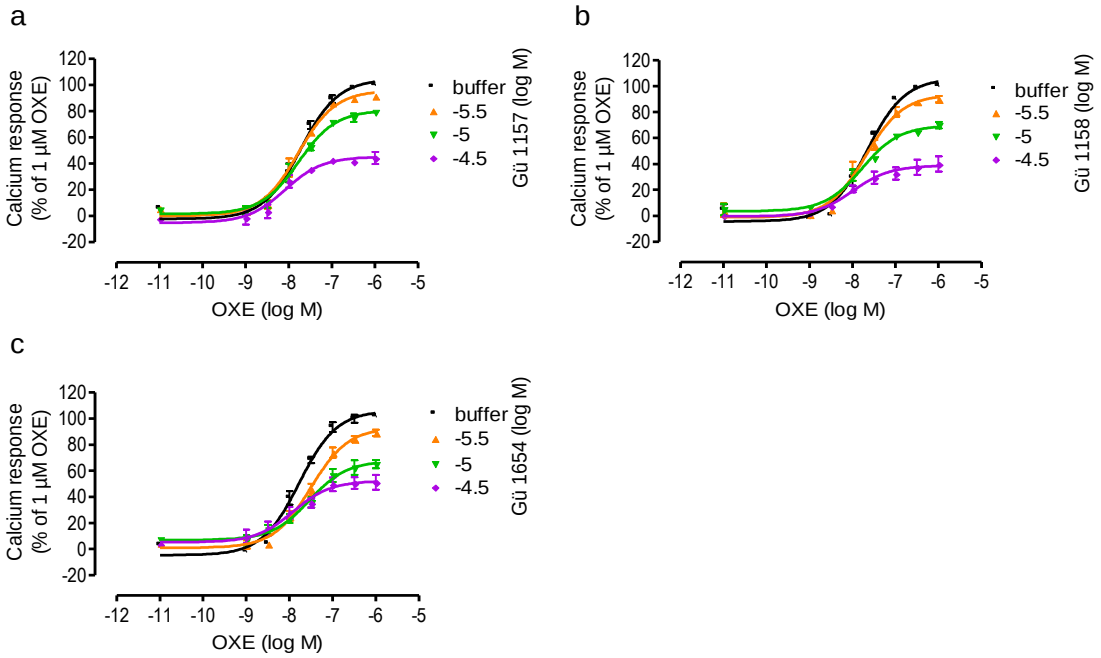

Figure 17: Insurmountable antagonism of Gü 1157, Gü 1158 and Gü 1654 on the OXE-R calcium response of HEK-OXE-R-G_{16} cells. HEK-OXE-R-G_{16} cells pre-treated with the indicated concentrations of Gü 1157 (**a**), Gü 1158 (**b**) and Gü 1654 (**c**), respectively, for 30 min were challenged with increasing concentrations of OXE. Increasing compound concentrations depressed maximal OXE efficacy. All data are means ± SEM of at least three independent experiments, each performed in triplicates.

Together, Gü 1157, Gü 1158 and Gü 1654 were found to exhibit inhibitory activity on the G_{16} pathway of the OXE-R, displaying insurmountable antagonism when tested in increasing concentrations. The next aim of this work was to test these compounds for their ability to inhibit OXE-R signaling on the native G_i pathway of the receptor.

3.1.7 Discussion

From an OXE-R antagonist screening, two compounds were obtained with antagonistic activity on the OXE-R, Gü 1157 and Gü 1158. Because both compounds were found to exhibit unspecific cellular effects, a virtual screening was performed in order to detect an "improved" compound with antagonistic activity on the OXE-R but devoid of unwanted cellular effects. The virtual screening indeed yielded a compound only possessing the wanted properties: Gü 1654. Synthesized molecule fragments of Gü

1654 did not exhibit antagonistic activity on the OXE-R, proving that all structural features of Gü 1654 were necessary to maintain antagonistic activity.

The nature of antagonism of Gü 1157, Gü 1158 and Gü 1654 was investigated. OXE concentration effect curves were established after cell pre-incubation with increasing compound concentrations, and a decrease in the maximal OXE response was observed, implying insurmountable antagonism. Insurmountable antagonism after compound pre-incubation can either result from competitive antagonism by a slow-dissociating orthosteric antagonist or from non-competitive antagonism by an allosteric antagonist.

An orthosteric antagonist binds to the same receptor binding site as the receptor agonist, therefore both ligands compete for binding to the same site. When antagonist and agonist are added at the same time, the competitive antagonist produces a rightward shift of the agonist concentration effect curves which increases with increasing antagonist concentrations. In the present work, the OXE-R was pre-incubated and thus pre-equilibrated with antagonist before agonist was added. Assuming that the binding of Gü 1157, Gü 1158 and Gü 1654 to the receptor is slowly reversible, antagonist liberation from the OXE-R by agonist would take so long that the agonist cannot interact with the receptor at the time when the agonist response is measured. Thus, the maximal agonist response cannot be attained and a decrease of the maximal agonist response is produced (Kenakin et al., 2006; Vauquelin and Szczuka, 2007).

An allosteric antagonist binds to a site distinct from the orthosteric receptor binding site. Antagonist binding to the receptor cannot be reversed by the agonist, so that the agonist response is affected and decreased for the maximal response.

The molecular mechanism of antagonist-receptor interaction underlying insurmountable antagonism can be analysed by radioligand binding assays (Mathiesen et al., 2006), but as radiolabelled OXE is not commercially available, such experiments were not performed. In conclusion, Gü 1157, Gü 1158 and Gü 1654 were found to display insurmountable antagonism at G_{16} signaling of the OXE-R. The next aim of this work was to analyse the compounds for antagonistic activity on the native G_i pathway of the OXE-R.

3.2 Investigations of antagonistic activity of Gü 1157, Gü 1158 and Gü 1654 on the OXE-R G_i pathway in cAMP accumulation assays

Three compounds were found to exhibit insurmountable antagonism on the G_{16} pathway of the OXE-R: Gü 1157, Gü 1158 and Gü 1654. In order to analyse the antagonistic activity of these compounds on the native G_i pathway of the OXE-R, the compounds were also tested for inhibitory effects on OXE mediated inhibition of forskolin-stimulated adenylyl cyclase activity in cAMP accumulation assays. In this assay, cAMP production is quantified by time-resolved fluorescence resonance energy transfer technology, based on a competition immunoassay as described in section **2.3.2**.
Measurement of G_i signaling of over-expressed OXE-R via cAMP accumulation assays has already been described in the literature: Jones et al. (2003) reported OXE mediated inhibition of forskolin-stimulated adenylyl cyclase for their stable HEK-OXE-R-G_{16} cell line in a radiochemical cAMP accumulation assay, gaining an EC_{50} value for OXE of 0.33 ± 0.1 nM. Hosoi et al. (2002) measured OXE dose-dependent inhibition of cAMP formation in CHO cells transiently transfected with the OXE-R in a cAMP enzyme immunoassay, where an EC_{50} value of 33 ± 19 nM was detected. As in this work the same cell system was used as by Jones et al., a similar OXE potency for inhibition of forskolin-stimulated adenylyl cyclase in cAMP accumulation assays was expected to be obtained.

Until now, antagonistic activity on the G_i pathway of the OXE receptor has only been reported for the 12-LO metabolites 5-oxo-12-HETE and 8-trans-5-oxo-12-HETE (Powell et al., 1999), as examined by G_i calcium flux assays with in neutrophils endogenously expressed OXE-R. As these OXE metabolites are endogenously formed substances, Gü 1157, Gü 1158 and Gü 1654, respectively, would be the first small molecule compounds to be found exhibiting antagonistic activity on the G_i pathway of the OXE-R.

3.2.1 Determination of G_i signaling of the OXE-R by cAMP accumulation assays

Forskolin was tested in different concentrations in cAMP accumulation assays for its adenylyl cyclase stimulation capabilities in HEK-OXE-R-G_{16} cells. Adenylyl cyclase stimulation with 0.5 µM forskolin turned out to create an optimal assay window (data

not shown), so that for adenylyl cyclase stimulation in the following cAMP accumulation experiments a forskolin concentration of 0.5 µM was applied.

An OXE dose effect curve was established in cAMP accumulation assays using HEK-OXE-R-G_{16} cells. Forskolin-induced cAMP formation was concentration-dependently inhibited by increasing concentrations of OXE with a pEC_{50} value of 6.67 ± 0.1 (**fig. 16**), which is a 648 fold decreased OXE potency compared to the data published by Jones et al. (2003) using the same cell system. Treatment of HEK-OXE-R-G_{16} cells with 50 ng/ml PTX for 18 hours completely abolished the OXE mediated inhibition of forskolin-stimulated cAMP production, confirming that adenylyl cyclase inhibition is G_i-mediated (**fig. 18**).

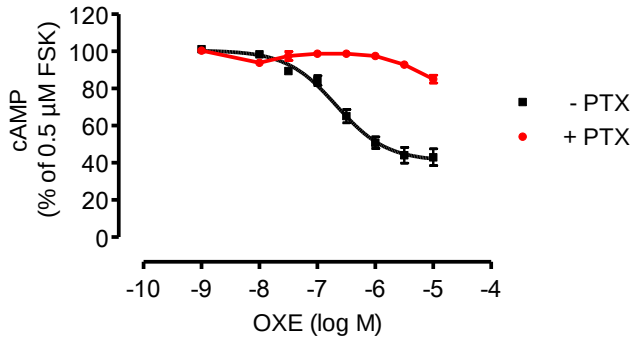

Figure 18: OXE mediates inhibition of forskolin stimulated adenylyl cyclase in HEK-OXE-R-G_{16} cells. cAMP production by forskolin-stimulated adenylyl cyclase was concentration dependently inhibited by increasing concentrations of OXE and is G_i mediated as proven by the use of PTX (50 ng/ml for 18 h). cAMP values are calculated as percent inhibition of 0.5 µM forskolin. Data are mean ± SEM of at least three independent experiments, each performed in triplicates.

3.2.2 Analysis of antagonistic activity of Gü 1157, Gü 1158 and Gü 1654 on the G_i pathway of the OXE-R

Before Gü 1157, Gü 1158 and Gü 1654 were tested for antagonistic activity exclusively on the G_i pathway of the OXE-R, the compounds were analysed for stimulating and inhibitory effects on the adenylyl cyclase in HEK-OXE-R-G_{16} cells. As shown in **fig. 18a**, Gü 1157, Gü 1158 and Gü 1654 did neither inhibit forskolin-stimulated adenylyl cyclase, nor did the compounds act as adenylyl cyclase stimulants.

For analysis of antagonistic activity on the G_i pathway of the OXE receptor, OXE dose effect curves were established after pre-incubation with 3 µM, 10 µM and 30 µM of each compound. Surprisingly, no antagonistic effect on OXE mediated inhibition of forskolin- stimulated adenylyl cyclase was detected for all three compounds (**fig. 18b, c,**

d), indicating that Gü 1157, Gü 1158 and Gü 1654 do not act as antagonists on the G_i pathway.

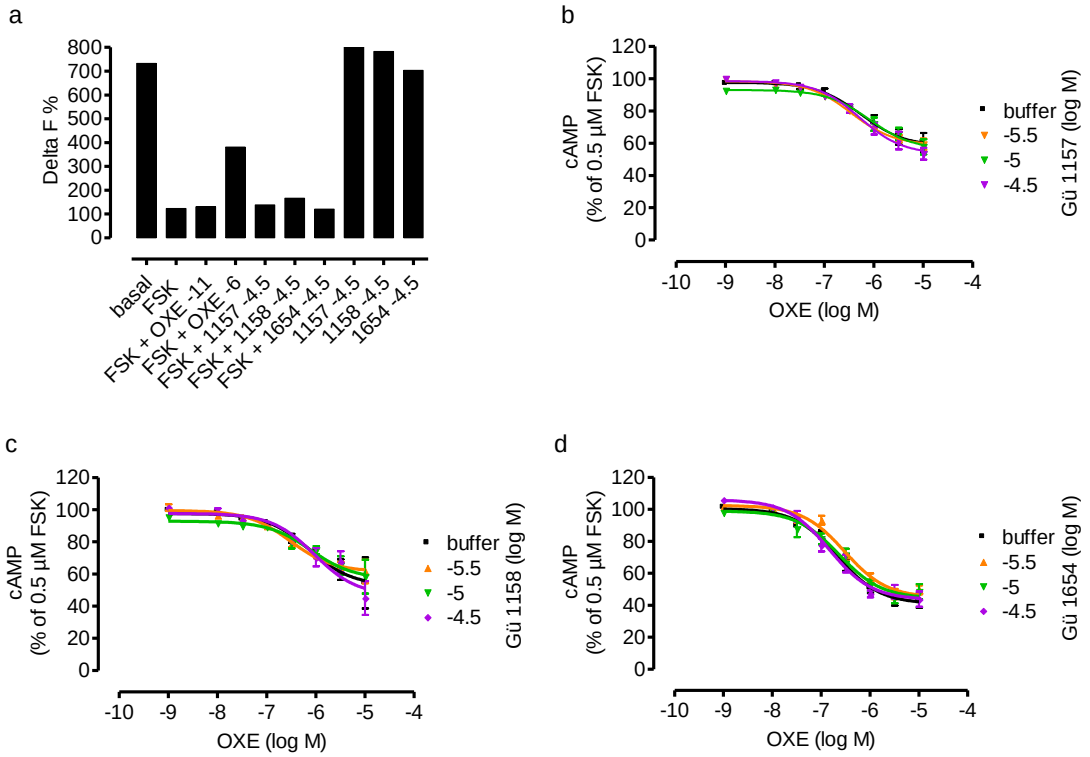

Figure 18: Analysis of Gü 1157, Gü 1158 and Gü 1654 for inhibitory effects on OXE mediated inhibition of cAMP production in HEK-OXE-R-G_{16} cells. Adenylyl cyclase was neither stimulated nor inhibited by individual effects of 30 µM Gü 1157, Gü 1158 and Gü 1654, respectively (**a**). None of the compounds displayed antagonistic activity on OXE mediated inhibition of adenylyl cyclase stimulated with 0.5 µM forskolin (Gü 1157: **b**, Gü 1158: **c**, Gü 1654: **d**). Data shown are mean values and SEM of three independent experiments, each performed in triplicates.

Because Gü 1157, Gü 1158 and Gü 1654 exhibited antagonistic activity on the G_{16} but not on the G_i pathway of the OXE-R, data suggest that these compounds are able to discriminate between G protein subfamilies and thus may act as "biased antagonists". To confirm this hypothesis, Gü 1157, Gü 1158 and Gü 1654 needed to be analyzed for inhibitory effects on G_{16} and G_i signaling in a different assay.

3.2.3 Discussion

In the present chapter, Gü 1157, Gü 1158 and Gü 1654 were tested for antagonistic activity on the native G_i pathway of the OXE-R in cAMP accumulation assays using the same cell line as previously used for calcium mobilization assays. Remarkably, none of the compounds exhibited inhibitory effects on the OXE mediated inhibition of forskolin-stimulated adenylyl cyclase. Data indicates that Gü 1157, Gü 1158 and Gü

1654 are able to discriminate between G_{16} and G_i signaling of the OXE-R, exhibiting a so-called "biased antagonism" for different G protein subfamilies. Most GPCR antagonists inhibit all G protein subtypes a receptor couples to. Until now, the ability of antagonists to discriminate between GPCR signaling via different G proteins has only been reported by two groups: (i) A sequential binding process of the orthosteric NK2R agonist neurokinin A (NKA) to the tachykinin NK2 receptor (NK2R) was found to stabilize the receptor in two active conformations (Holst et al., 2001), each of which were shown to specifically activate the G_q or the G_s pathway. Maillet et al. (2007) discovered the compound LPI805 to inhibit G_s signaling of the NK2R, whereas at the same time G_q signaling of the NK2R was not inhibited, rather, G_q mediated calcium responses were found to be enhanced in the presence of LPI805. LPI805 was found to act as allosteric antagonist. (ii) Dowal et al. (2011) determined biased antagonism at G protein signaling for a small molecule exhibiting antagonistic activity at the thrombin receptor PAR1, a GPCR endogenously expressed on platelets, which is known to signal via G_q, $G_{12/13}$ and G_i protein α subunits (Swift et al., 2006). Dowal et al. found the cyclopentaquinoline-derivative JF5 to act as PAR1 antagonist, and further investigations on PAR1 signaling in platelets revealed that JF5 specifically inhibits G_q but not G_{12} mediated signaling of the PAR1 receptor. Although the molecular mechanism of this biased antagonism remained unknown, Dowal et al. showed that JF5 is a non-orthosteric antagonist, and mutagenesis studies indicated that antagonistic activity of JF5 is conferred through the intracellular eighth helix of the PAR1 receptor, which functions in coupling to Gα subunits.

Possibly, Gü 1157, Gü 1158 and Gü 1654 could also act as intracellular allosteric antagonists on the OXE-R leading to an altered receptor conformation resulting in a modified G protein binding site which would explain the ability of the antagonistic compounds to discriminate between G_{16} and G_i signaling of the OXE-R. Since the aim of this work was to investigate the antagonistic activity on different signaling pathways of the OXE receptor and its impact on OXE mediated effects in primary cells, no studies for the analysis of the molecular mechanism of the presumed "biased antagonism" of Gü 1157, Gü 1158 and Gü 1654 were realized. Instead, it was decided to analyse the three compounds once more in a different assay system for their ability to discriminate between inhibition of G_i and G_{16} to see if these experiments would conform the hypothesis of biased antagonism.

Additionally, the receptor specificity of G_{16} inhibition remained to be analysed, meaning that it had to be tested whether there is only inhibition of OXE-R mediated G_{16} coupling and not a GPCR independent inhibition of G_{16} signaling. Since specific G protein inhibitors exist, as e.g. YM-254890, which acts as inhibitor of the GDP/GTP exchange reaction of the alpha subunit of G_q proteins (Nishimura et al., 2010), a universal inhibition of G_{16} by Gü 1157, Gü 1158 and Gü 1654 needs to be considered as a possible reason for the antagonistic effect on G_{16}, but not on G_i signaling. Thus, after confirmation of the putative biased antagonism of Gü 1157, Gü 1158 and Gü 1654 at OXE-R signaling, appropriate experiments should be performed to address the possibility that these compounds act as universal G_{16} inhibitors.

3.3 Investigations of the biased antagonism of Gü 1157, Gü 1158 and Gü 1654 on the OXE-R using DMR assays

In previous cAMP accumulation assays, Gü 1157, Gü 1158 and Gü 1654 did not show inhibitory activity on the G_i pathway of the OXE-R. The results from cAMP assays were in contrast to the results derived from calcium assays, where the compounds had been discovered for their antagonistic activity on the G_{16} pathway of the OXE-R. These findings implicated that Gü 1157, Gü 1158 and Gü 1654 were able to discriminate between different G protein subfamilies. To confirm by another assay that these compounds are really inactive on the G_i pathway but not on the G_{16} pathway of the OXE-R, dynamic mass redistribution (DMR) assays were performed.

The DMR technology has been evaluated as an approved method to analyse GPCR signaling of all four G protein classes (Schröder et al., 2010). Distinct from the previously used second messenger assays, the DMR method captures the downstream cellular effects of all G proteins, resulting in a whole cell response. Thus, this method provided a valuable tool to prove the hypothesis of the "biased antagonism" from a holistic point of view.

If a GPCR couples to G proteins of different G protein classes at the same time, in the DMR assay a complex DMR signal will be obtained consisting of mixed signatures from all different G protein pathways. To dissect and visualize a single pathway component of a complex DMR signal, toxins or pharmacological pathway inhibitors can be used (Schröder et al., 2010). For example, the G_i pathway can be abrogated with PTX, G_s signaling can be masked by CTX and G_q signaling can be abolished by the G_q inhibitor YM-254890 (Schröder et al., 2010). In HEK-OXE-R-G_{16} cells, the OXE-R couples to co-expressed promiscuous $G\alpha_{16}$ and to endogenously expressed G_i proteins. Thus, DMR recordings of OXE-R signaling in these cells would disclose a mixed G_i-G_{16} DMR signal.

To confirm antagonism of Gü 1157, Gü 1158 and Gü 1654, respectively, on the G_{16} pathway of the OXE-R in DMR assays, HEK-OXE-R-G_{16} would have to be treated with PTX to deactivate G_i proteins and accordingly obtain an isolated OXE-R G_{16} response.

To analyse the antagonistic activity of Gü 1157, Gü 1158 and Gü 1654 on the isolated G_i response of the OXE-R in HEK-OXE-R-G_{16} cells, the G_{16} pathway would need to be blocked, but currently no G_{16} inhibitor exists. Although G_{16} belongs to the $G_{q/11}$ family of G proteins, and YM-254890 is known to be a potent and selective inhibitor for $G_{q/11}$ proteins, this compound has lately been reported not to exhibit inhibitory activity at G_{16} proteins (Nishimura et al., 2010). Thus, analysis of Gü 1157, Gü 1158 and Gü 1654 on the G_i pathway of the OXE-R in DMR assays had to be performed in HEK293 cells transiently transfected with the OXE-R in order to detect isolated G_i signaling of the OXE-R.

3.3.1 Visualization of isolated OXE-R G_{16} signaling in DMR assays

HEK-OXE-R-G_{16} cells were analyzed for OXE-R signaling via G_{16} in DMR assays. Therefore, HEK-OXE-R-G_{16} cells were challenged with increasing concentrations of OXE in the presence and absence of PTX, and the cell response was recorded and visualized as wavelength shift (**fig. 20a,b**). Both the cumulative G_i-G_{16} and the isolated G_{16} response displayed robust and concentration-dependent signals to the agonist. For comparison, HEK293 cells were challenged with OXE, where no DMR response was observed which proved the OXE-R specificity of the OXE mediated cell response (**fig. 20c**).

To quantify both the mixed G_i-G_{16} DMR and the isolated G_{16} responses, the maximum values between 400 and 1800 seconds of the DMR response were selected from each OXE concentration, and OXE concentration effect curves were established (**fig. 20d**). Data revealed, that when G_i signaling was abolished by PTX, OXE-R signaling via the G_{16} pathway was reinforced (**fig. 20d,e**).

Remarkably, the potency obtained from OXE-R G_{16} signaling in DMR assays (pEC_{50} 5.39 ± 0.09) was about 225 fold decreased compared to the potency obtained from OXE-R G_{16} signaling in calcium mobilization assays (pEC_{50} 7.75 ± 0.04; section **3.1.2**).

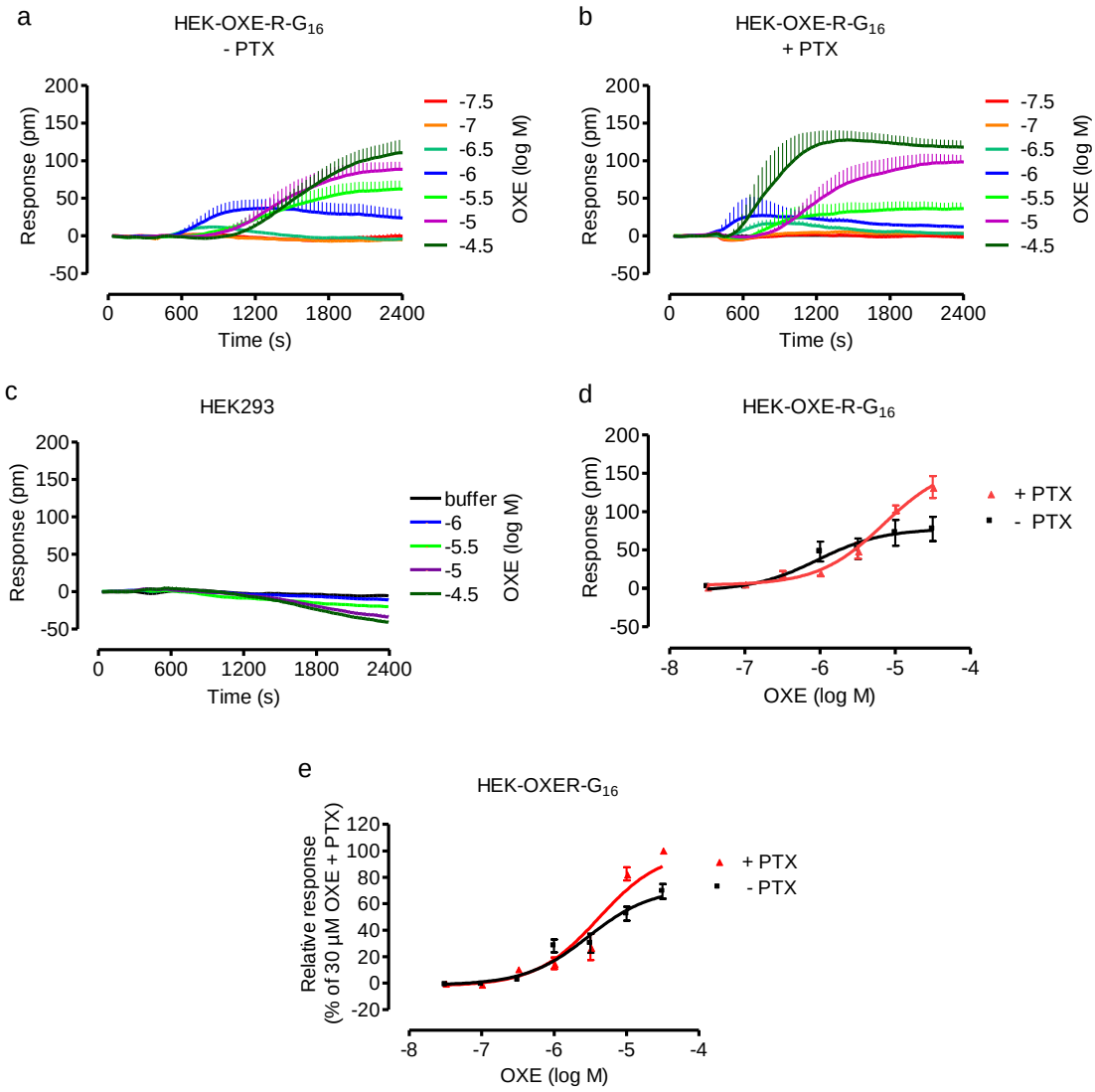

Figure 20: Visualization of OXE triggered G_i-G_{16} signaling and isolated G_{16} signaling of HEK-OXE-R-G_{16} cells in DMR assays. DMR responses were obtained from HEK-OXE-R-G_{16} cells due to G_i-G_{16} signaling (**a**) and G_{16} signaling after PTX treatment (50 ng/ml for 18 h) (**b**), but not from native HEK293 cells (**c**). Concentration effect curves in (**d**) were established for OXE from the maximal DMR values between 400-1800 s from (**a**) and (**b**), and mean data (+ SEM) from three independent experiments were normalized for the maximum response of 30 µM OXE in PTX-treated cells (**e**). The pEC_{50} value of OXE is 5.39 ± 0.09 for G_{16} signaling, and 5.05 ± 0.08 for complex G_i-G_{16} signaling.

3.3.2 Investigations of the antagonism of Gü 1157, Gü 1158 and Gü 1654 on the G_{16} pathway of the OXE-R in DMR assays

Antagonism analyses were performed on the isolated G_{16} response of HEK-OXE-R-G_{16} cells. PTX-treated cells were pre-incubated for 30 minutes with 30 µM Gü 1157, Gü 1158 and Gü 1654, respectively, or buffer as control, and were challenged with increasing concentrations of OXE. The OXE mediated DMR response was not affected by Gü 1157 and Gü 1158. However, OXE concentration effect curves displayed a bell-

shape here. In contrast, Gü 1654 exhibited consistent and potent inhibition of the G_{16} cell response to OXE (**fig. 21**).

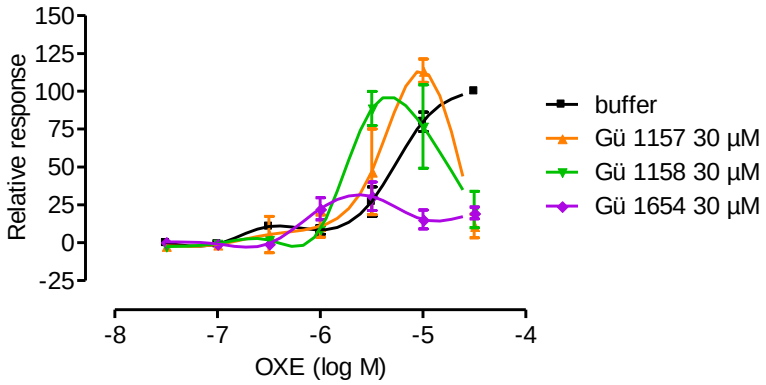

Figure 21: Analysis of antagonistic effects of Gü 1157, Gü 1158 and Gü 1654 on the G_{16} pathway of the OXE-R in DMR assays. PTX-treated HEK-OXE-R-G_{16} cells (50 ng/ml, 18 h) were challenged with increasing concentrations of OXE after pre-incubation with 30 µM of Gü 1157, Gü 1158 and Gü 1654, respectively, or buffer as control. Only Gü 1654 exhibited antagonistic activity on the OXE-R G_{16} DMR response. (**a**) Data points are curve-fitted by non-linear regression. (**b**) Data points are aligned for visualization of the bell-shaped OXE response upon treatment with Gü 1157 and Gü 1158, respectively. Data are mean and SEM of three independent experiments, each performed in triplicates.

Thus, the antagonistic effects of Gü 1157 and Gü 1158 on the G_{16} pathway of the OXE-R discovered in calcium mobilization assays could not be reproduced in DMR assays.

Due to these findings, only Gü 1654 was further analysed in DMR assays for antagonistic effects on the OXE-R in concentrations of 1, 3, 10 and 30 µM, respectively. DMR analysis proved concentration-dependent antagonism of Gü 1654 at the OXE mediated cell response (**fig. 22**), confirming the findings in calcium mobilization assays.

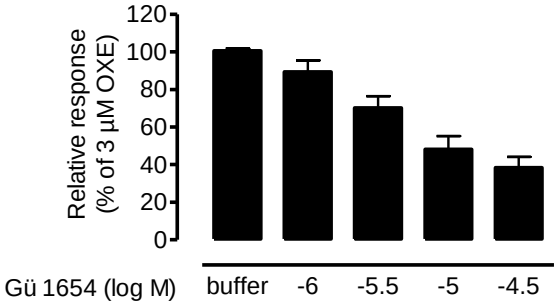

Figure 22: Gü 1654 concentration-dependently inhibits the OXE mediated G_{16} response of the OXE-R in DMR assays. After pre-incubation with Gü 1654 in increasing concentations, PTX-treated HEK-OXE-R-G_{16} cells (50 ng/ml, 18 h) were challenged with 3 µM OXE. The G_{16} mediated DMR responses were concentration-dependently inhibited by increasing concentrations of Gü 1654, and are normalized to the maximum response of 3 µM OXE. Data are mean (+ SEM) of three independent experiments, each performed in triplicates.

3.3.3 Analysis of antagonistic activity of Gü 1654 on the G_i pathway of the OXE-R in DMR assays

Gü 1654 was analysed for its non-antagonistic effect on the G_i pathway of the OXE-R in DMR assays to confirm the hypothesis of "biased antagonism". Because antagonism of Gü 1157 and Gü 1158 on the G_{16} OXE-R pathway had not been confirmed in DMR assays, both compounds were no longer analyzed in DMR assays.

Signaling of the OXE-R transiently expressed in HEK293 cells was visualized upon treatment with OXE in DMR assays yielding an OXE pEC_{50} value of 6.11 ± 0.21. Since the DMR response was completely abolished by PTX pre-treatment (**fig. 23**), the DMR signal was exclusively based on G_i coupling of the OXE-R. The pEC_{50} determined in the DMR assay is in good agreement with the pEC_{50} of 6.67 ± 0.09 obtained for OXE-R G_i signaling in cAMP accumulation assays (section **3.2.2**). Pre-incubation with 30 µM Gü 1654 did not inhibit or attenuate the OXE-R DMR response. These DMR data confirmed the observations made in G_i cAMP accumulation assays: Gü 1654 does not inhibit signaling via the G_i pathway of the OXE-R.

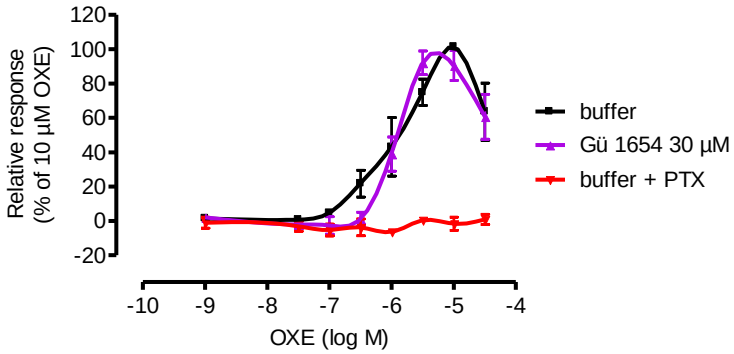

Figure 23: Analysis of Gü 1654 for inhibitory activity on Gi signaling of the OXE-R in DMR assays. HEK293 cells transiently expressing the OXE-R were challenged with increasing concentrations of OXE after pre-incubation with 30 µM Gü 1654, or buffer and PTX (50 ng/ml, 18 h) or buffer as control, for 30 min. Gü 1654 did not affect the OXE mediated G_i response. Data are mean (± SEM) of three independent experiments, each performed in triplicates.

3.3.4 Analysis of specific antagonism of Gü 1654 on the G_{16} pathway of the OXE-R

The possibility that inhibition of the G_{16} response of the OXE-R may be due to universal G_{16} inhibition rather than specific inhibition of G_{16} coupling to the OXE-R was analysed. For analysis of antagonism on the G_{16} response of another receptor, the CRTH2 receptor stably expressed in HEK293 cells was chosen. Upon stimulation with its agonist prostaglandin D2 (PGD2), the CRTH2 receptor couples to G_i (Nagata et al.,

1999a, Nagata et al., 1999b; Hirai et al., 2001), which has already been analysed by Schröder et al. (2010) in DMR assays.

HEK-CRTH2 cells were transiently transfected with the $G\alpha_{16}$ subunit, and cells were stimulated with PGD2 in the presence and absence of PTX. As control, PGD2 mediated DMR responses of non-transfected HEK-CRTH2 cells were measured simultaneously. In the absence of PTX, both the $G\alpha_{16}$-transfected and the non-transfected HEK-CRTH2 cells displayed DMR signals up to 300 pm as cell response to PGD2, whereas in the presence of PTX (50 ng/ml, 18 h) only $G\alpha_{16}$-transfected HEK-CRTH2 cells displayed an immediate DMR response due to G_{16} signaling (**fig. 24c,d**), as compared to HEK-CRTH2 cells without $G\alpha_{16}$ (**fig. 24a,b**).

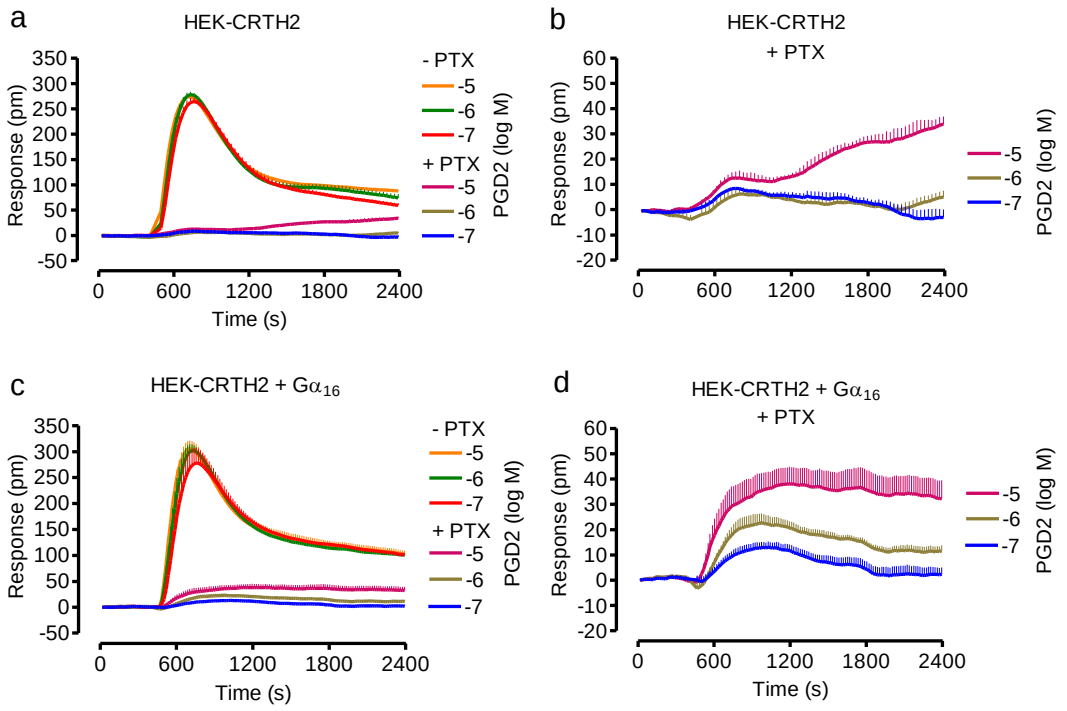

Figure 24: Signaling of CRTH2 funnelled to the G_{16} pathway in DMR assays. HEK-CRTH2 cells transiently expressing $G\alpha_{16}$ are funnelled to the G_{16} pathway after pre-treatment with PTX (50 ng/ml for 18 h), resulting in a prompt and concentration dependent DMR response (**c,d**), in contrast to HEK-CRTH2 cells without $G\alpha_{16}$ (**a,b**). Shown are representative data (mean + SEM) of at least three independent experiments, each performed in triplicates.

Gü 1654 was tested in 3, 10 and 30 µM for inhibitory effects on the PGD2 mediated DMR response of CRTH2 funneled to the G_{16} pathway. After compound pre-incubation for 30 minutes, the PGD2 triggered CRTH2 responses were not affected, as displayed by the bar diagram depicting the CRTH2 responses normalized to 10 µM PGD2 (**fig. 25**).

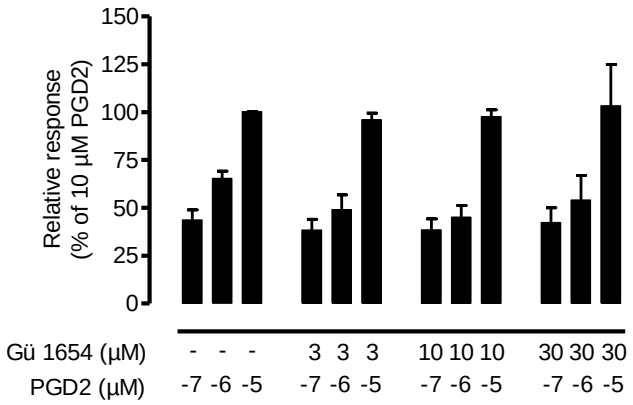

Figure 25: Gü 1654 does not affect the PGD2 mediated G_{16} response of HEK-CRTH2 cells transiently transfected with $G\alpha_{16}$. HEK-CRTH2 cells transiently expressing $G\alpha_{16}$ were funneled to the G_{16} pathway by pre-treatment with PTX (50 ng/ml for 18h) and incubated with increasing concentrations of Gü 1654 for 30 min. The PGD2 triggered G_{16} response was not affected by Gü 1654, as demonstrated by the CRTH2 G_{16} response normalized to 10 µM PGD2 (mean ± SEM) data of at least three independent experiments, each performed in triplicates).

This experiment revealed that Gü 1654 is not a universal G_{16} inhibitor, but specifically inhibits OXE-R G_{16} signaling.

In summary, the findings obtained in DMR assays investigating the putative biased antagonism of Gü 1157, Gü 1158 and Gü 1654 affirmed this hypothesis for at least Gü 1654 to act as a biased antagonist, competent to inhibit OXE-R signaling when coupled to G_{16} but not when coupled to G_i.

3.3.5 Discussion

In DMR assays, Gü 1157, Gü 1158 and Gü 1654, respectively, were investigated for the proposed "biased antagonism" on the G_i and the G_{16} signaling pathway of the OXE-R.

Isolated G_{16} signaling of the OXE-R was measured in DMR assays after PTX treatment of HEK-OXE-R-G_{16} cells, and G_i signaling of the OXE-R could be detected by transient expression of the OXE-R in HEK cells. During the initial DMR experiments for visualizing the distinct OXE-R pathways in HEK-OXE-R-G_{16} cells, two striking observations were made: (i) OXE efficacy obtained for G_{16} signaling of the OXE-R achieved by PTX treatment was higher than OXE efficacy derived from mixed G_i-G_{16} signaling of the OXE-R (**fig. 20d,e**), indicating, that when G_i proteins are inactivated by PTX, the OXE-R signals were reinforced via the G_{16} pathway. In contrast to this finding, only a small DMR response was detectable when CRTH2 was funneled to the

G_{16} pathway by transient G_{16} expression and the use of PTX (**fig.22**). Apparently, the OXE-R has a high efficiency for coupling to $G\alpha_{16}$ subunits.

(ii) Comparison of concentration effect curves of OXE obtained from OXE-R G_{16} signaling in DMR assays and in G_{16} second messenger calcium assays revealed that OXE potency in holistic G_{16} DMR assays was 225 fold decreased compared to that in second messenger G_{16} assays (**fig. 26a**). However, OXE potency for OXE-R G_i mediated DMR responses is quite similar to the OXE potency for G_i mediated inhibition of cAMP production (**fig. 26b**).

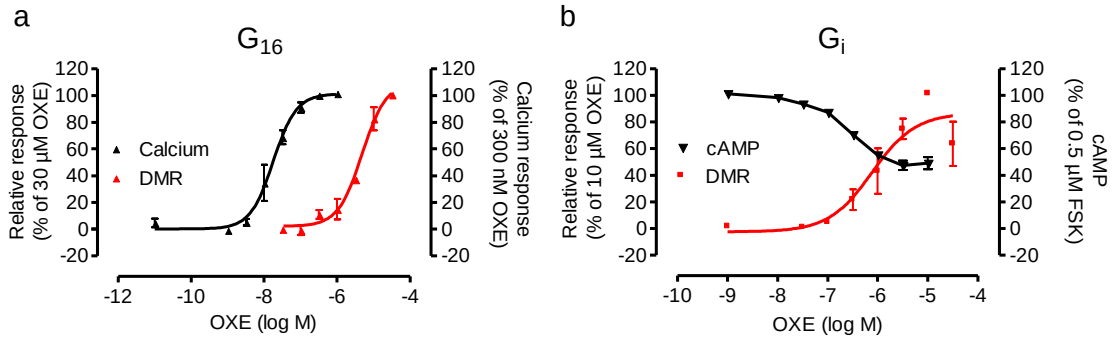

Figure 26: Comparison of concentration effect curves of OXE from OXE-R DMR assays (red signatures) or second messenger assays (black signatures) for G_{16} (a) and G_i (b) signaling of the OXE-R. Comparison of concentration effect curves of OXE derived from OXE-R G_{16} signaling in DMR and calcium mobilization assays (**a**) and OXE-R G_i signaling in DMR and cAMP assays (**b**). For OXE-R G_{16} signaling (**a**), OXE pEC_{50} values are: DMR: 5.39 ± 0.09; calcium: 7.75 ± 0.04, and for OXE-R G_i signaling (**b**), OXE pEC_{50} values are: DMR: 6.11 ± 0.21, cAMP: 6.67 ± 0.09. Data are mean ± SEM of at least three independent experiments, each performed in triplicates.

The discrepancy between OXE potency in G_{16} calcium assays and in G_{16} DMR assays might be due to the different cell responses investigated by each method: while second messenger assays quantify a defined cellular reaction at an early stage of signaling, DMR technology measures the whole-cell response at the end of a signaling cascade, comprising more than one cellular event. Hence, agonist potencies derived from DMR assays and from second messenger assays can converge, but do not have to.

Schröder et al. (2010) evaluated the DMR technology against classical second messenger assays using a set of GPCRs and their corresponding agonists, and by comparing agonist potencies derived from both methods, DMR was found to be as sensitive, or even more, than the according second messenger assay. In another study by Lee et al. (2008), agonist and antagonist potencies derived from DMR and second messenger assays were compared and found to be in good agreement for the most part.

Only the agonist potency of one compound, a synthetic D2 receptor agonist, was more than 1000-fold decreased in DMR assays compared to cAMP assays when tested on CHO-D2 cells. Furthermore, this compound caused DMR responses on CHO-M1 and native CHO cells in micromolar concentrations. It was speculated that the compound might act unspecific due to activation of unknown pathways, thus leading to desensitization of the D2 triggered DMR response of the D2 receptor.

Since it had been determined that OXE did not induce a DMR response on native HEK293 cells (**fig. 20c**) and thus activation of unknown pathways leading to desensitization of the OXE-R can be excluded, the large OXE potency shift between G_{16} DMR and G_{16} calcium mobilization assays might rather be explained by the fact that the G_{16} pathway is not the native pathway of the OXE-R. Obviously, the quick OXE-R G_{16} response observed for nanomolar OXE concentrations in calcium mobilization assays cannot be monitored in DMR assays, proving that the OXE-R G_{16} DMR response follows a different concentration-response relationship.

Unfortunately, of the three compounds tested for inhibitory effects on G_{16} signaling of the OXE-R in DMR assays, only Gü 1654 was found to inhibit the OXE triggered DMR response, whereas no inhibitory effect could be detected for Gü 1157 and Gü 1158. The G_{16} response of the OXE-R was inhibited by Gü 1654 in a concentration dependent manner, while the G_i mediated whole cell response of the OXE-R was not affected by this compound. Furthermore, Gü 1654 was found not to inhibit G_{16} mediated signaling of the CRTH2 receptor, proving that Gü 1654 is not a universal G_{16} inhibitor. Thus, the biased antagonism hypothesis was confirmed for at least this compound.

The next aim of this work was to analyse the OXE-R for recruitment of β-Arrestin and to test Gü 1654 for inhibitory activity on OXE-R β-Arrestin recruitment.

3.4 Investigations of OXE-R β-Arrestin recruitment

Ligand-induced GPCR activation leads to G protein coupling, followed by second messenger production and intracellular signaling. Subsequently after receptor activation, GPCR kinases (GRKs) phosphorylate the receptor, and cytoplasmic proteins called Arrestins, are recruited from the cytoplasm to the cell membrane, where they bind to the receptor and hence inhibit further G protein signaling, resulting in desensitization of GPCR signaling. Thus, Arrestins play an important role in regulating receptor signaling. There are four types of Arrestins, which are also referred to as β-Arrestins1-4. β-Arrestin3 and 4 are expressed only in retinal rods and cones, whereas β-Arrestins1 and β-Arrestin2 are ubiquitously expressed. Recently, new roles for β-Arrestins have been discovered. β-Arrestins are reported to function as scaffold proteins, interacting with GPCRs in a G protein-independent manner, by linking them to cytosolic proteins triggering intracellular signaling targeting mitogen-activated protein kinases (MAPK) like extracellular receptor kinases (ERK) 1/2, as well as JNK3 and p38 MAPK (Wei et al., 2003; Lutrell and Lefkowitz, 2002). In the present chapter of this work, the OXE-R should be analysed for its ability to recruit β-Arrestin in BRET assays. Until now, β-Arrestin recruitment of the OXE-R was mentioned only by Vrecl et al. (2004). In β-Arrestin translocation BRET assays, Vrecl et al. analysed β-Arrestin mutants for enhancement of BRET signals, and the OXE-R *TG1019* was used as a control receptor, also displaying improved BRET signals with a β-Arrestin 2 mutant. As these are the only data in literature concerning β-Arrestin recruitment of the OXE-R, it is unclear whether G_i protein activation is needed for β-Arrestin recruitment to the OXE-R or if the receptor is also able to recruit β-Arrestin independently from G_i. Thus, the OXE-R should be analysed for β-Arrestin recruitment in the presence and absence of G_i protein activation. If β-Arrestin recruitment occurred in the absence of G_i activation, then Gü 1157, Gü 1158 and Gü 1654 should be tested in BRET assays for antagonistic activity on this process.

For performance of OXE-R β-Arrestin recruitment BRET assays, HEK293 cells stably expressing GFP^2-labeled β-Arrestin2 (HEK-ßARR2-GFP^2) were transiently transfected with the OXE-R fused to Renilla luciferase (OXE-R-Rluc). BRET assays were carried out as described in section **2.2.3.3**.

3.4.1 Investigations of OXE-R β-Arrestin recruitment

In BRET assays, at first kinetics of OXE-R β-Arrestin2 recruitment were analysed. HEK-βARR2-GFP^2 cells transiently expressing the OXE-R fused to Rluc were stimulated with 1 µM OXE for 2, 5, 10 and 15 minutes, respectively. Hereafter, Coelenterazine a was added and immediately fluorescence was measured. Increased BRET ratios of approximately 60 mBRET were gained for all agonist stimulation times, as compared to the basal buffer value (**fig. 27a**).

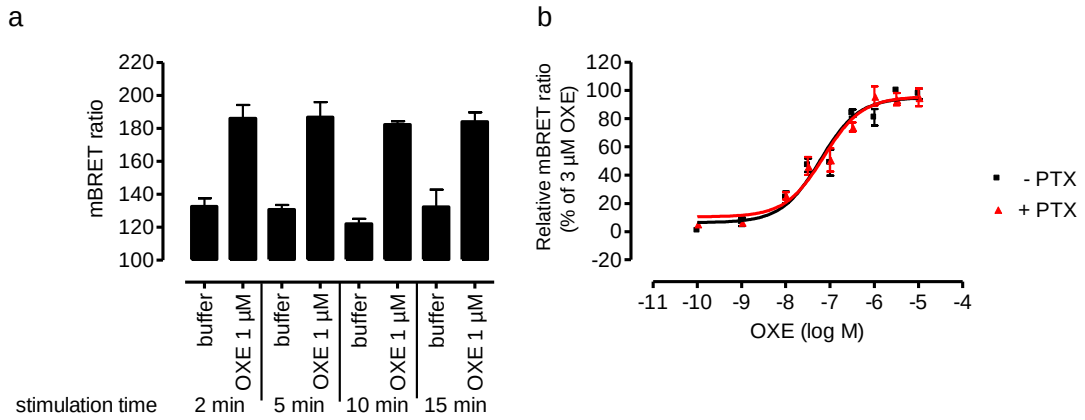

Figure 27: OXE-R β-Arrestin2 recruitment is investigated in BRET assays using HEK-βARR2-GFP^2 cells transiently expressing the OXE-R fused to Rluc. (a) BRET signals of 60 mBRET were obtained after 2,5,10 and 15 minutes of agonist stimulation. (**b**) β-Arrestin2 recruitment was not attenuated after G_i inactivation by PTX pre-treatment (50 ng/ml for 18h). OXE concentration effect curves were established, yielding OXE pEC_{50} values of 7.22 ± 0.1 for PTX-untreated cells and 7.14 ± 0.11 for PTX-treated cells (**b**). In (**a**), representative data (mean + SEM) of three independent experiments are shown, each performed in triplicates. In (**b**), data are mean (± SEM) of at least three independently performed experiments, each in triplicates.

The agonist stimulation time of 10 minutes was chosen for following OXE-R β-Arrestin2 recruitment BRET assays. An OXE concentration effect curve was established by stimulating the cells with increasing concentrations of OXE, yielding an OXE pEC_{50} value of 7.22 ± 0.1 (**fig. 27b,** black trace).

In order to determine whether β-Arrestin2 recruitment to the OXE-R occurs independently from G_i activation, PTX-treated cells (50 ng/ml, 18 h) were challenged with increasing concentrations of OXE (**fig. 27b**, red trace). Data revealed, that β-Arrestin2 recruitment to the OXE-R was not attenuated after inactivation of G_i, and OXE displayed equal potency (pEC_{50} = 7.14 ± 0.11), as compared to OXE potency derived from non-PTX-treated cells. These data suggest that the OXE-R recruits β-Arrestin2 independently from G_i protein activation.

3.4.2 Investigations of antagonistic activity of Gü 1157, Gü 1158 and Gü 1654 on OXE-R β-Arrestin2 recruitment

Gü 1157, Gü 1158 and Gü 1654 were analysed for inhibitory activity on β-Arrestin2 recruitment of the OXE-R. Cells were pre-incubated with increasing concentrations of compounds, or buffer as control, for 30 minutes and agonist concentration effect curves were recorded. Gü 1654 decreased OXE-mediated BRET signals concentration dependently by decreasing the maximal response (**fig. 28a**). Thus, it can be concluded that Gü 1654 acts as an insurmountable antagonist on OXE-R β-Arrestin2 recruitment. However, Gü 1157 and Gü 1158 led to quenched BRET signals, making it impossible to analyse these compounds in BRET assays (data not shown). This phenomenon may be due to the light yellow colouring of the Gü 1157 and Gü 1158 stock solutions. Thus, Gü 1157 and Gü 1158 could not be further evaluated for inhibitory effects on OXE-R β-Arrestin2 recruitment in BRET assays.

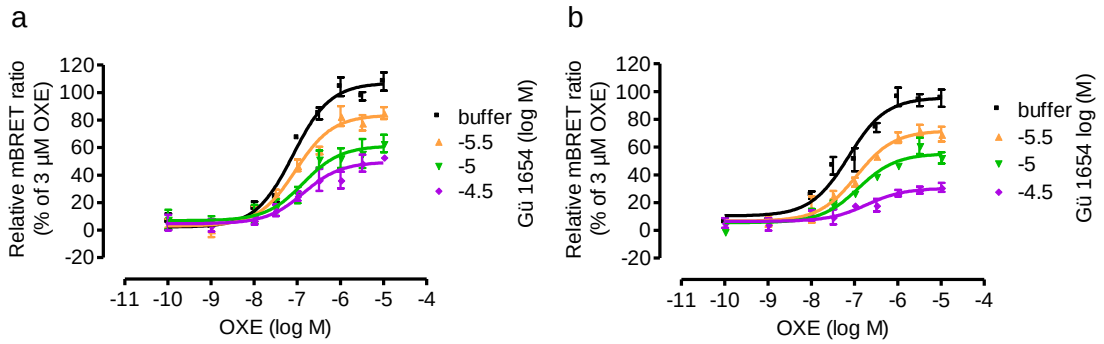

Figure 28: Gü 1654 acts as insurmountable antagonist on OXE-R β-Arrestin2 recruitment. HEK-βARR2-GFP[2] cells transiently expressing the OXE-R linked to Rluc were incubated with Gü 1654 in 3, 10 and 30 µM, respectively, and cells were stimulated with increasing concentrations of OXE. Experiments were performed in the absence (**a**) and presence (**b**) of PTX (50 ng/ml, 18 h). OXE-R β-Arrestin2 recruitment was concentration-dependently inhibited by Gü 1654, and in the absence of active G_i proteins, antagonism was even more pronounced (**b**). Data are mean (± SEM) of at least three independently performed experiments, each in triplicates. BRET ratio is normalized to the maximal concentration of 3 µM OXE.

Interference of Gü 1654 on OXE-R β-Arrestin2 recruitment in the presence of PTX was analysed. OXE concentration effect curves were recorded with PTX-treated cells (50 ng/ml, 18 h) after pre-incubation with Gü 1654 in increasing concentrations. Gü 1654 achieved a concentration dependent decrease of the BRET signals (**fig. 28b**), and it could be observed that antagonism of Gü 1654 in 30 µM appeared even more pronounced in the presence of PTX, as compared to data from PTX-untreated cells (**fig. 28a**).

3.4.3 Investigations of the pharmacology of the OXE-R fused to Rluc in DMR assays

The OXE-R fused to Rluc and transiently expressed in HEK293-βARR2-GFP2 cells was analysed for its signaling function and pharmacology on the G_i pathway, compared to the OXE-R wildtype transiently expressed in HEK293 cells in DMR assays. Cells were pre-treated with 30 µM Gü 1654 or buffer, respectively, and increasing concentrations of OXE were added in the presence and absence of PTX. Concentration effect curves were established, yielding an pEC_{50} value of 6.1 ± 0.14 for the OXE DMR response of the OXE-R-Rluc fusion construct (**fig. 29a**), which was in good agreement with the pEC_{50} value of 6.1 ± 0.08, obtained from the OXE-R wildtype DMR response (**fig. 29b**). G_i signaling of both constructs was confirmed by the use of PTX (50 ng/ml, 18 h), which completely abolished the OXE-mediated response. Signaling of OXE-R fused to Rluc and of OXE-R wildtype was unaffected by 30 µM Gü 1654. Together, OXE-R fusion to Renilla luciferase does not confound the function of the receptor.

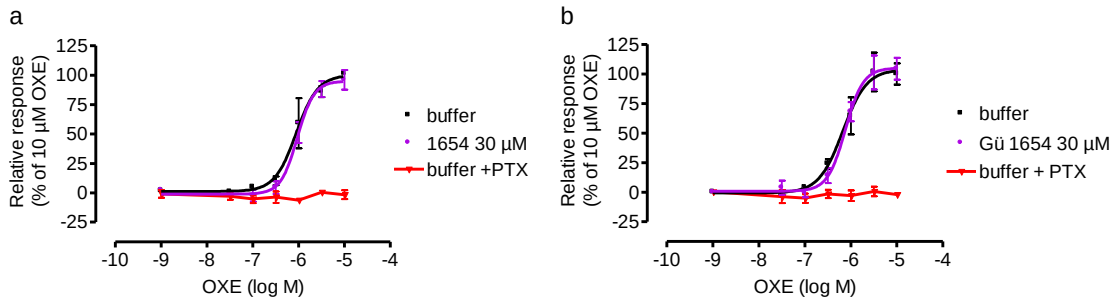

Figure 29: Function and pharmacology of the OXE-R when fused to Renilla luciferase is compared to the OXE-R wildtype in DMR assays. DMR responses of HEK293-βARR2-GFP2 cells transiently expressing the OXE-R fused to Renilla luciferase and HEK293 cells transiently expressing the OXE-R wildtype were compared. OXE-mediated responses obtained from both the OXE-R-Rluc and the OXE-R wildtype construct were Gi-mediated, as confirmed by PTX (50 ng/ml, 18 h) sensitivity, and not affected by 30 µM Gü 1654. The pEC_{50} values of OXE obtained from concentration effect curves were in good agreement (6.1 ± 0.14 for the OXE-R fused to Rluc and 6.1 ± 0.08 for the OXE-R wildtype). Data are mean (± SEM) of three independent experiments, each performed in triplicates. DMR responses are normalized to the maximal concentration of 10 µM OXE.

3.4.4 Investigations of OXE-R specific inhibition of β-Arrestin recruitment by Gü 1654

To confirm that Gü 1654 specifically inhibits β-Arrestin2 recruitment of the OXE-R, Gü 1654 was tested for inhibitory activity on CRTH2 β-Arrestin recruitment in BRET assays. G protein-independent β-Arrestin recruitment by the CRTH2 has previously been reported by Mathiesen et al. (2005). HEK-βARR2-GFP^2-CRTH2-Rluc cells were

pre-incubated with increasing concentrations of Gü 1654 or buffer as control, and were challenged with 100 µM PGD2. BRET data revealed that PGD2-mediated β-Arrestin2 recruitment was not inhibited by Gü 1654 (**fig. 30**).

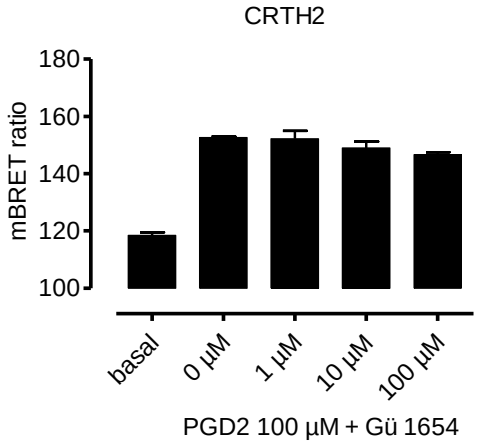

Figure 30: β-Arrestin2 recruitment of the CRTH2 receptor is not inhibited by Gü 1654. After pre-incubation with Gü 1654 in increasing concentrations, stable HEK-ßARR2-GFP2-CRTH2-Rluc cells were challenged with 100 µM PGD2. Gü 1654 did not inhibit PGD2-mediated β-Arrestin2 recruitment. Shown are representative data (mean + SEM) of three independent experiments, each performed in duplicates.

It is concluded that Gü 1654 is indeed a specific inhibitor for the OXE-R since it does not interfere with β-Arrestin2 translocation of the CRTH2.

3.4.5 Discussion

In the present chapter, investigations on β-Arrestin recruitment of the OXE-R in BRET assays are presented. β-Arrestins are cytoplasmic proteins whose function was first found to be terminating GPCR signaling. Nowadays, new findings have emerged concerning functions of β-Arrestins. There is evidence that termination of G protein coupling of some GPCRs can occur independently from GRK phosphorylation and β-Arrestin recruitment (Mathiesen et al., 2005), (Shenoy et al., 2006), moreover, β-Arrestins were discovered to mediate signaling of some GPCRs independently from G proteins by acting as scaffolds, linking the receptor to G protein-independent pathways such as ERK1/2 MAP kinases (Azzi et al., 2003; Wei et al., 2003; Mathiesen et al., 2005). Interestingly, ligands have been reported to act in a biased fashion on GPCR signaling by selectively inducing β-Arrestin-mediated, but not G protein-mediated signaling (Gesty-Palmer et al., 2006), and only recently, a GPCR has been reported to signal exclusively through β-Arrestin without detectable G protein activation (Rajagopal et al., 2010). Furthermore, a biased fashion of antagonism has been described for

antagonists, exhibiting antagonism selectively on β-Arrestin recruitment but not on G protein activation (Mathiesen et al., 2005).

A first hint for β-Arrestin recruitment of the OXE-R was given in a study by Vrecl et al. (2004), but as in this work only briefly β-Arrestin recruitment by the OXE-R was depicted in a control experiment verifying previous findings on a β-Arrestin mutant. The mechanism underlying OXE-R β-Arrestin recruitment would remain unclear.

In this work, OXE-R β-Arrestin recruitment was analysed in β-Arrestin translocation BRET assays, and for the first time it could be demonstrated that the OXE-R recruits β-Arrestin independently from G_i activation. Control experiments in DMR assays proved unaltered function and pharmacology of the OXE-R-Rluc fusion construct, as compared to the OXE-R wildtype. Cell pre-treatment with PTX silenced the DMR response of both OXE-R constructs, proving the OXE triggered response to be G_i-mediated. In addition, the abolished G_i DMR response of HEK293-βARR2-GFP^2 cells transiently expressing the OXE-R-Rluc proved evidence that G_i was indeed silenced in these cells after the same PTX-treatment in β-Arrestin translocation BRET assays.

Moreover, the PTX experiment using HEK293-βARR2-GFP^2 cells transiently expressing the OXE-R fused to Rluc revealed another important finding: As no DMR signal could be observed in the presence of PTX, while in BRET assays with the same cells and the same PTX pre-treatment β-Arrestin translocation was obtained, data revealed that β-Arrestin recruitment cannot be captured by DMR technology.

Gü 1157, Gü 1158 and Gü 1654 were tested in β-Arrestin recruitment BRET assays on the OXE-R. Unfortunately, Gü 1157 and Gü 1158 could not be analysed for inhibitory effects on OXE-R β-Arrestin recruitment in BRET assays, as fluorescence signals were quenched likely due to the yellow colour of the compounds. Gü 1654 exhibited insurmountable antagonism on OXE-R β-Arrestin recruitment in both PTX-treated and untreated cells.

The finding that the OXE-R recruits β-Arrestin independently from G_i proteins, suggests that the OXE-R might utilize β-Arrestin as a scaffold for cellular signaling.

Until now, β-Arrestin signaling of the OXE-R has not been analysed or described in the literature yet.

Studies on general physiological effects related to β-Arrestin signaling have found β-Arrestin to exhibit regulatory functions relevant for cell proliferation (Kim et al., 2008) and heart disease (Noma et al., 2007). Furthermore, β-Arrestin2 was determined to be involved in chemotaxis, as this was demonstrated for the CXCR4 receptor in HeLa and HEK293 cells by Sun et al. (2002). Similar observations have been made by Fong et al. (2002), as they showed that lymphocytes derived from β-Arrestin knock-out mice were impaired in their ability to perform chemotaxis toward a chemotactic gradient. In addition, allergen-sensitized mice lacking β-Arrestin in T cells appeared not to exhibit physiological or inflammatory responses characteristic for asthma (Walker et al., 2003), providing evidence that β-Arrestin2 has a regulatory function for the development of allergic inflammation.

As these findings imply a role for β-Arrestins contributing to cell chemotaxis and to inflammatory processes, it is likely that β-Arrestins might be involved in OXE triggered chemotaxis of neutrophils and eosinophils. In conclusion, OXE-R signaling through β-Arrestin needs to be explored in the future. Evaluation of physiologic or pathophysiologic roles of OXE-R β-Arrestin signaling could be performed by using eosinophils and neutrophils derived from β-Arrestin knock-out mice, e.g. by analysing if these cells have lost their ability to undergo chemotaxis in response to OXE. If OXE triggered chemotaxis of neutrophils and eosinophils turned out to be β-Arrestin-related, Gü 1654 could be a valuable tool to study the pathophysiological role of OXE-R β-Arrestin signaling in asthma or other allergic diseases.

3.5 Investigations of antagonistic activity of Gü 1654 on OXE-R signaling in human primary cells

In cAMP second messenger and DMR assays, Gü 1654 was found to be a selective OXE-R antagonist, competent to discriminate between G_i and G_{16} signaling of the OXE-R. As these findings were observed in recombinant cells overexpressing the OXE-R, it was of great interest to analyse Gü 1654 for inhibitory activity on OXE-R signaling in primary cells and to test, if the compound would retain its ability to discriminate between G_i and non-G_i signaling.

The OXE-R is highly expressed in peripheral leukocytes, lung, kidney, liver and spleen (Hosoi et al., 2002; Jones et al., 2003). As signaling of endogenously expressed OXE-R is mostly analysed in eosinophils and neutrophils, which is due to the high expression of the OXE-R in these cells (Jones et al., 2003; Sturm et al., 2005), eosinophils and neutrophils were selected for analysis of Gü 1654 on OXE-R signaling in primary cells.

O´Flaherty et al. (1996) reported OXE-mediated calcium flux in neutrophils and eosinophils to be PTX sensitive, indicating that OXE-mediated calcium flux is triggered by G_i signaling of the OXE-R in these cells. Thus, calcium flux assays provided the opportunity to analyse the influence of Gü 1654 on the OXE-R G_i pathway.

Analysis of Gü 1654 on OXE-R signaling through another pathway than G_i was attempted to be achieved by DMR assays. Because DMR signals capture the holistic response of a cell, the use of DMR technology was expected to uncover OXE-R signaling beyond the G_i pathway.

The consideration to utilize DMR assays for analysis of OXE-R signaling in neutrophils was supported by DMR data generated by Kathy Dodgson (Astra Zeneca), presenting DMR responses of neutrophils challenged with Interleukin-8, proving that DMR assays offer a chance for the analysis of GPCR signaling in neutrophils.

3.5.1 Investigations of antagonistic activity of Gü 1654 on the OXE-R in neutrophil DMR assays

3.5.1.1 Development of a neutrophil DMR assay

Neutrophil data generated by Kathy Dodgson (Astra Zeneca**)** showed that neutrophils responded with a positive and concentration dependent DMR response to Interleukin-8 (IL-8), the agonist of in neutrophils endogenously expressed chemokine receptors CXCR1 and 2 (**fig. 31**). The IL-8 concentration effect curve generated from these data yielded an EC_{50} value of 1 nM.

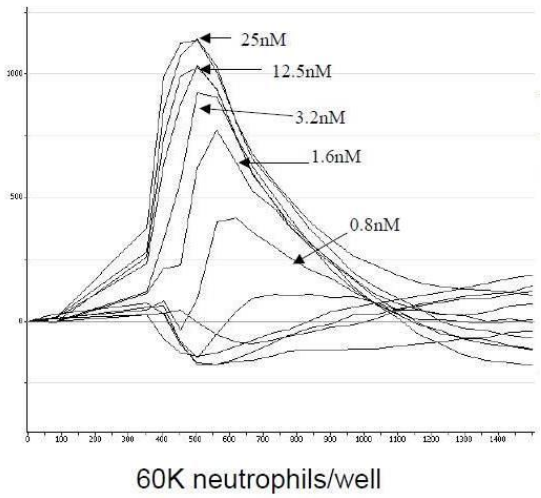

Figure 31: Neutrophils display concentration dependent DMR responses upon stimulaton with IL-8. The image was taken from the ELRIG presentation "Application of the Corning® Epic® System to label-free functional GPCR assays, Kathy Dodgson, Lead Generation Biology, AstraZeneca R&D Charnwood".

Based on these results, IL-8 was chosen as positive control for neutrophil DMR assays. Nicotinic acid was also chosen as control, as expression and functionality of the nicotinic acid receptor HM74A in neutrophils was described by Kostylina et al. (2008).

Peripheral blood from healthy volunteers was collected according to a protocol approved by the Ethics Committee of the medical faculty of the University of Bonn. All volunteers provided informed consent. Neutrophils were isolated from peripheral blood as described in section **2.2.2.8** and cells were seeded with a cell density of 65.000 cells per well into an uncoated biosensor microplate. Because neutrophils are easily activated and therefore should be used within the next few hours after isolation from blood, a short assay pre-incubation time of ten minutes was chosen. During pre-incubation, a

baseline read was performed to control cell reactions, displaying a steady baseline signal that revealed no DMR neutrophil response (**fig. 32a**). IL-8, NA and OXE were added in various concentrations to the cells, and the neutrophil DMR response was recorded. Remarkably, and in contrast to the neutrophil IL-8 DMR data presented by Kathy Dodgson, negative DMR responses were obtained for IL-8 (**fig. 32b**). A negative DMR signal was also obtained for NA (**fig. 32c**), and unfortunately, no DMR response was recorded for OXE (**fig. 32d**).

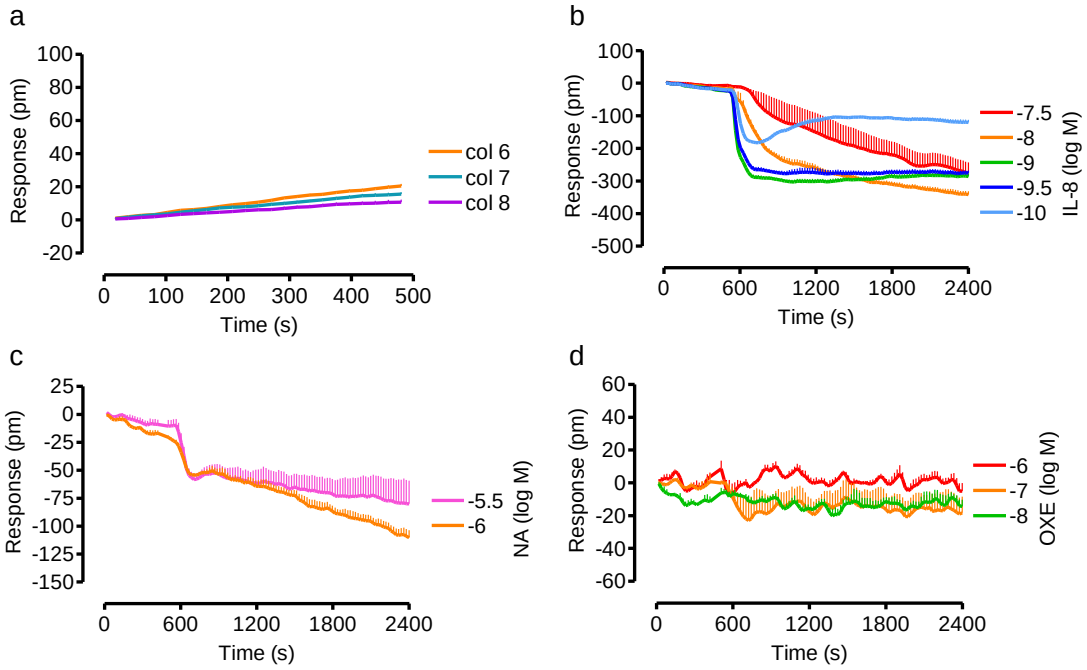

Figure 32: Analysis of neutrophils for DMR responses after stimulation with IL-8, NA and OXE. Neutrophils were seeded into an uncoated biosensor microplate at a cell density of 65.000 cells per well, and DMR responses were analysed during 10 minutes incubation prior to the assay (**a**). Negative DMR responses were recorded after cell stimulation with IL-8 (**b**) and NA (**c**), and no change in baseline signals was recorded after stimulation with OXE (**d**). Shown are data of one experiment (+ SEM) performed in triplicates.

In order to test if a positive DMR response could be obtained by another cell number, different cell numbers of 40.000, 50.000 and 60.000 neutrophils per well were tested in the next experiment. Still, negative DMR responses upon stimulation with IL-8 were recorded for all cell numbers (**fig. 33a,b,c**).

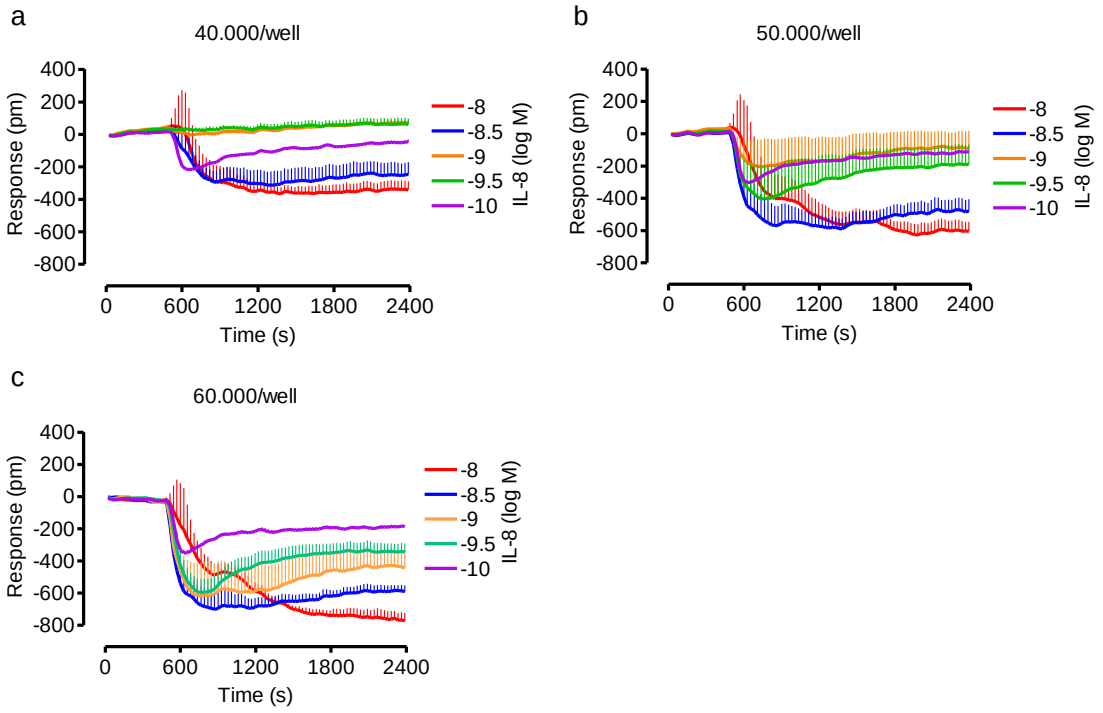

Figure 33: The neutrophil DMR response to IL-8 was analysed using different cell numbers. Neutrophils seeded into an uncoated biosensor microplate at cell numbers of 40.000 (a), 50.000 (b) and 60.000 (c) cells per well were stimulated with IL-8. At all cell numbers, cells responded with a negative DMR response. Depicted are data of one experiment (+ SEM) performed in triplicates.

Because at 60.000 cells per well (**fig. 33c**) the neutrophil DMR response was observed to correspond to the IL-8 concentrations for the most part, this cell number was determined to be used for further experiments. Neutrophil DMR assays were repeated with various incubation times for several experiments to obtain positive neutrophil DMR responses, but although neutrophil isolation and DMR assay conditions were consistent with the protocols used by Kathy Dodgson (personal communication), still negative DMR responses to IL-8 remained (data not shown). Because negative DMRs can indicate cell detachment from the well bottom of the biosensor microplate, in a further experiment neutrophils were seeded into a fibronectin-coated biosensor microplate to enhance cell attachment to the plate bottom. To control cell reactions due to eventual activation by the fibronectin coating, a baseline read was performed during assay pre-incubation of 50 minutes. Indeed, a positive DMR up to 200 pm was observed, which decreased after 600 seconds and changed into a negative DMR (**fig. 34a**). In this assay, IL-8 still induced a negative DMR response (**fig. 34c**), but for the first time, a positive DMR response was obtained for NA (**fig. 34b**). OXE was not applied in this assay.

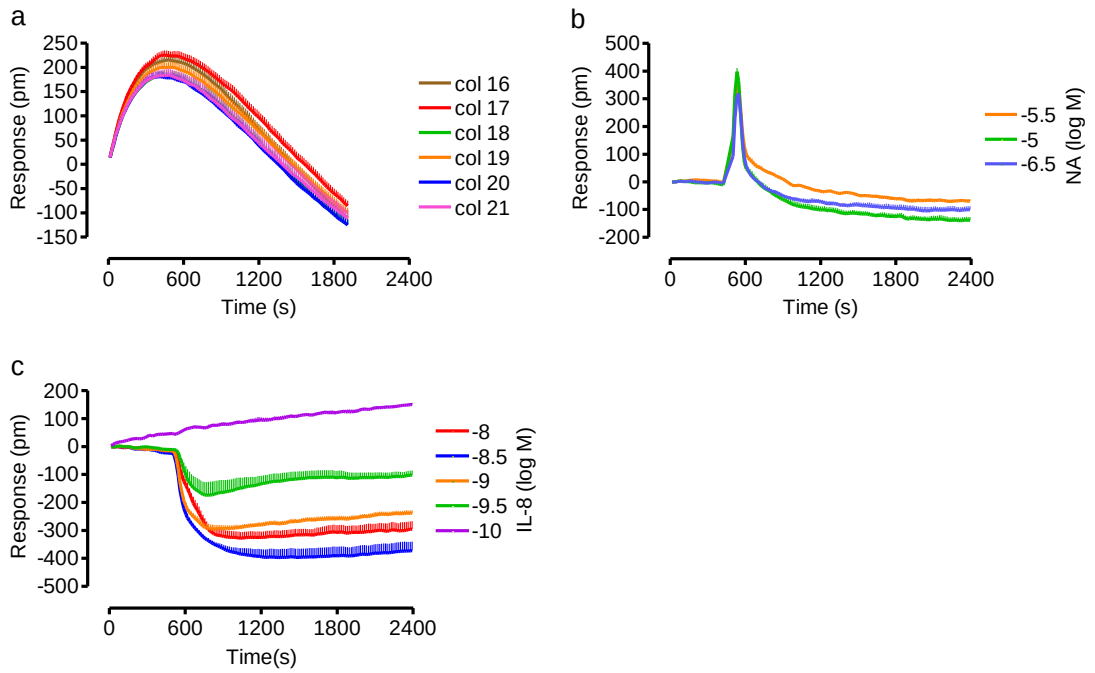

Figure 34: Neutrophil DMR assay using fibronectin-coated biosensor microplates displays a positive DMR for NA. Neutrophils seeded into a fibronectin-coated biosensor microplate showed a positive DMR response during incubation of 50 minutes prior to the assay (**a**). For the first time, NA triggered a positive neutrophil DMR response (**b**), whereas the DMR response to IL-8 remained negative (**c**). Shown are data of a single experiment (+ SEM) performed in triplicates.

In the following experiment using fibronectin-coated biosensor microplates, neutrophils were incubated for 2 hours. Again, cells reacted to fibronectin inducing a positive DMR, but the fibronectin-triggered DMR response declined and stabilized after 2000 seconds (**fig. 35a**). After compound addition, for the first time all agonists induced positive DMR responses. At the positive DMR response for IL-8 (**fig. 35c**), signals increased concentration dependently and an IL-8 concentration effect curve was generated (**fig. 35d**), yielding a pEC_{50} value of 8.35 ± 0.06, which was in good agreement with the IL-8 data by Kathy Dodgson (**fig. 31**). Neutrophils also responded with a positive and concentration dependent DMR signal to NA, from which a concentration effect curve was established, yielding a pEC_{50} of 6.34 ± 0.10 (**fig. 35e**). Surprisingly, cells treated with OXE in various concentrations only responded to the highest agonist concentration of 30 µM, resulting in a positive DMR signal (**fig. 35b**). At lower OXE concentrations, no DMR response could be detected.

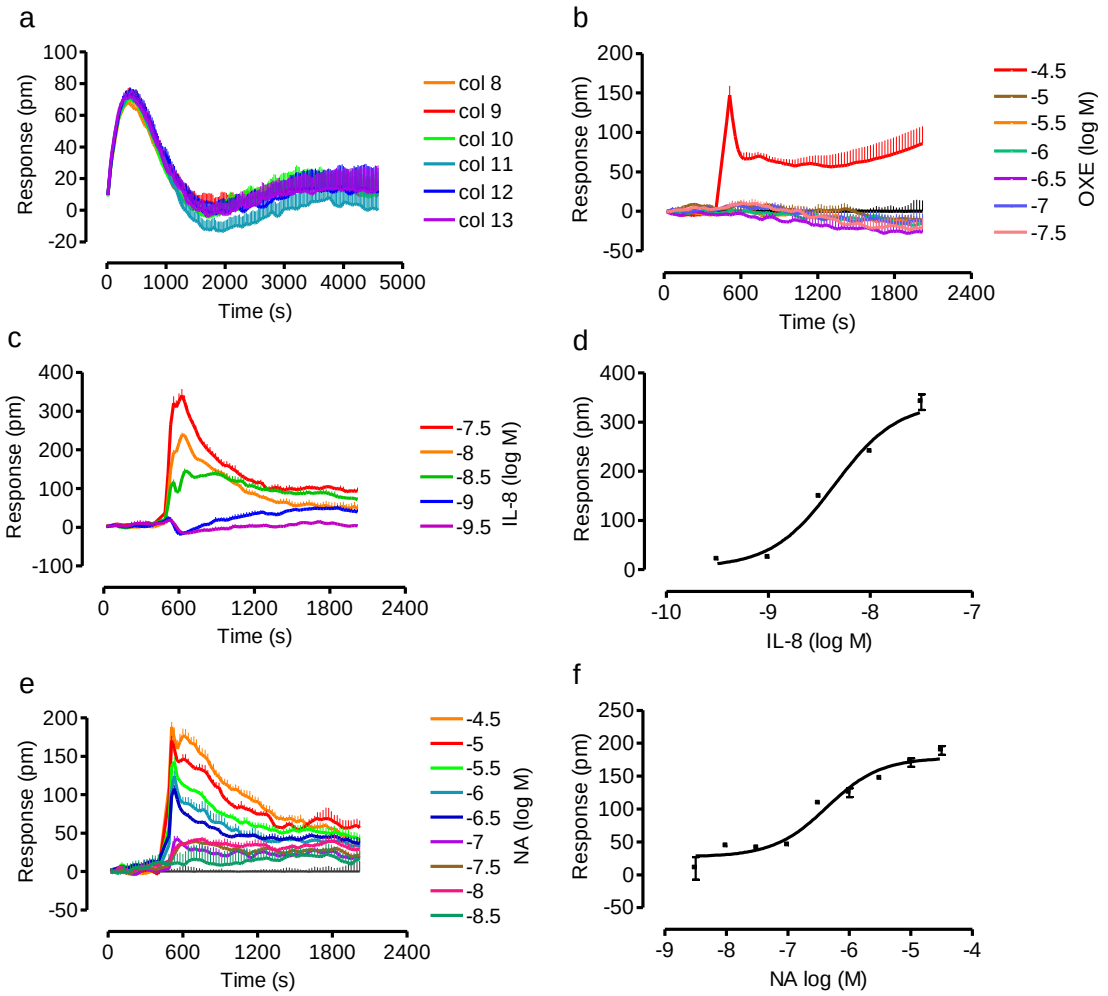

Figure 35: Neutrophils display positive DMR signals after pre-incubation for 2h on fibronectin- coated biosensor microplates. During 2 hours incubation prior to the assay, a positive DMR response was observed, which declined and stabilized after 30 minutes (**a**). Cells responded with positive DMR signals upon agonist stimulation. Signals for IL-8 (**c**) and NA (**e**) were concentration dependent, whereas OXE triggered a DMR signal only at 30 µM (**b**). The pEC_{50} values are: 8.35 ± 0.06 for Il-8 (**d**) and 6.34 ± 0.10 for NA (**f**). Shown is representative data from three independent experiments (+ SEM and mean values), performed in triplicates.

The finding that a neutrophil DMR response could be obtained only at 30 µM OXE was confirmed in several additional assays, where it would remain unclear, why cells did not respond to lower OXE concentrations, while at the same time robust neutrophil responses were obtained for IL-8 and NA at various concentrations.

In calcium flux G_i assays, neutrophil responses due to OXE stimulation are obtained by OXE concentrations ranging from 1 nM to 1 µM (Sturm et al., 2005). Thus, the concentration of 30 µM OXE was fairly high, and it was suggested that the DMR signal obtained at 30 µM OXE might not be mediated by G_i signaling of the OXE-R but by signaling through another pathway. Moreover, it was suggested that this signal might also result from an unspecific cell response triggered by the high OXE concentration.

3.5.1.2 Investigations of inhibitory acitivity of Gü 1654 on the neutrophil DMR response at 30 µM OXE

To evaluate if the DMR signal at 30 µM OXE was produced due to an unspecific cell response triggered by the high OXE concentration, or if the DMR signal might indeed result from OXE-R signaling by another but the G_i pathway, it was analysed if Gü 1654 was able to inhibit the neutrophil DMR response obtained at 30 µM OXE.

Neutrophils were pre-incubated with 30 µM Gü 1654 or buffer as control during the last 30 minutes of a pre-incubation time of 2h, where it could be observed that Gü 1654 did not trigger unspecific neutrophil DMR responses (**fig. 36a**). Remarkably, after addition of OXE to the cells, no DMR response was recorded for cells pre-incubated with Gü 1654 (**fig. 36b**). A DMSO control containing the same DMSO concentration as the buffered solution of Gü 1654 proved, that DMSO did not affect the OXE mediated neutrophil response (**fig. 36b**).

Thus, it was concluded that the abrogated OXE DMR response after pre-incubation with Gü 1654 resulted from inhibitory effects of Gü 1654 and was not due to restricted cell responsiveness caused by DMSO. The inhibitory effect on the 30 µM OXE neutrophil DMR response was also determined for Gü 1654 in 10 µM (**fig. 36c**).

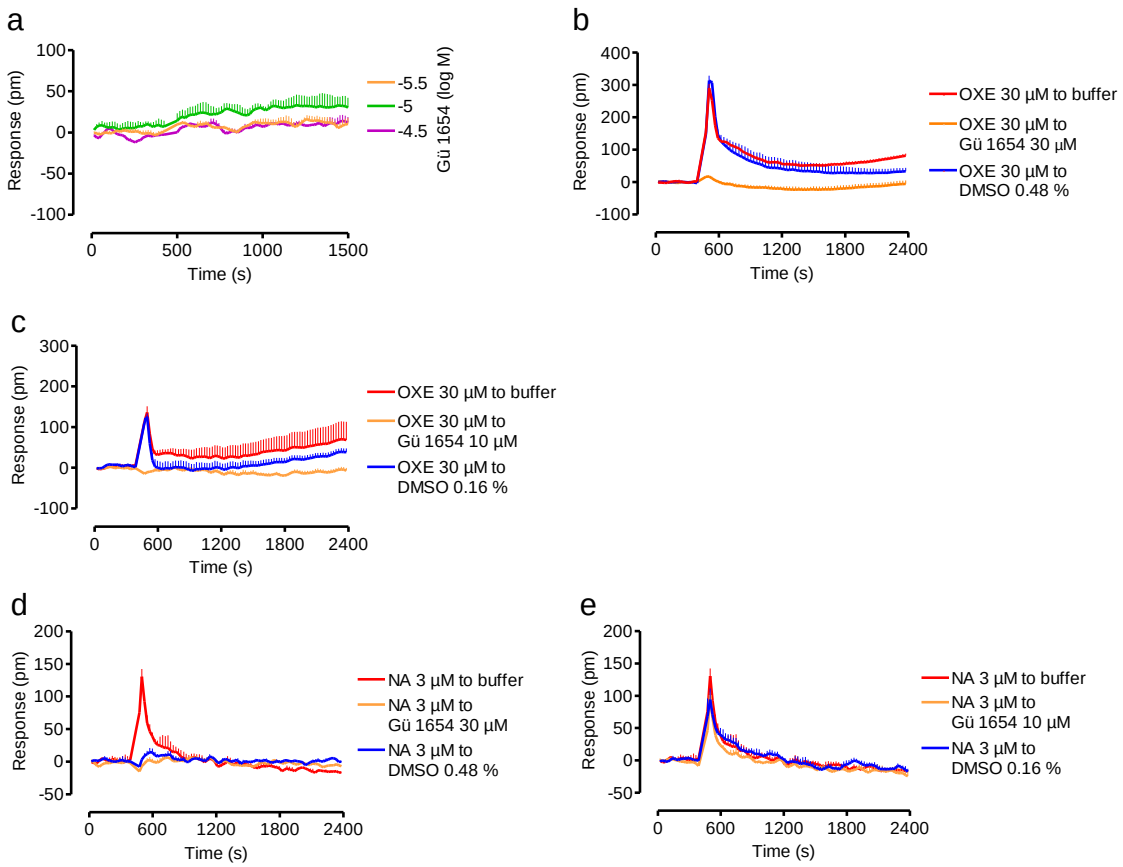

Figure 36: Gü 1654 was analysed for inhibitory effects on the neutrophil DMR response at 30 µM OXE. Neutrophils did not respond to Gü 1654 during pre-incubation for 30 minutes (**a**). The OXE-mediated neutrophil DMR response was inhibited at 30 µM Gü 1654 (**b**) and 10 µM Gü 1654 (**c**). Specific inhibition of the OXE-mediated DMR response by Gü 1654 was analysed at the NA-mediated response: 10 µM Gü 1654 did not inhibit the NA DMR response (**e**), whereas 30 µM Gü 1654 could not be analysed due to DMSO interference with the NA-mediated DMR response (**d**). Shown are representative data (mean + SEM) of one experiment (**d**), two experiments (**c**), and three experiments (**a**,**b**,**e**). Each experiment was performed in triplicates.

The specificity of the inhibitory effect of Gü 1654 on the OXE-mediated cell response was analysed on the neutrophil response mediated by NA. The DMSO control, which was also used here, revealed that the NA-mediated DMR response of neutrophils was sensitive to DMSO at a concentration of 0.48 % (**fig. 36d**). Hence, Gü 1654 was difficult to analyse in 30 µM on the NA neutrophil response.

Analysis of Gü 1654 in 10 µM revealed no antagonistic effects for Gü 1654 on the NA-mediated DMR (**fig. 36e**) and no interaction with the DMSO concentration of 0.16 %, as confirmed by three independent experiments. Thus, specific inhibition of the OXE-mediated DMR response by Gü 1654 could be determined for at least 10 µM Gü 1654.

Based on these results, it was suggested that the neutrophil DMR response at 30 µM OXE was mediated by the OXE-R, as this response was shown to be specifically inhibited by Gü 1654. Also, it was suggested that the neutrophil DMR response at 30 µM OXE resulted from another but the OXE-R G_i pathway. Additional investigations on the OXE-mediated neutrophil DMR response were not performed. DMR assays might be a valuable tool to study signaling of receptors activated by IL-8 or NA in neutrophils, but, however, these assays were determined not to constitute an appropriate method to study OXE-R signaling in neutrophils. Further analysis of OXE-R signaling and inhibitory activity of Gü 1654 on OXE-R signaling in primary cells should be performed using assays approved for analysis of GPCR signaling in leukocytes.

3.5.2 Analysis of Gü 1654 on G_i-mediated signaling of the OXE-R in human primary cells

It was decided to analyse Gü 1654 in calcium mobilization assays using eosinophils and neutrophils in order to investigate if the compound has any influence on the G_i-mediated calcium flux in these primary cells or if Gü 1654 would retain its biased antagonism on OXE-R signaling by showing no inhibition of G_i coupling.

Calcium flux assays on eosinophils and neutrophils were performed by Petra Luschnig from the group of Akos Heinemann, Institute of Experimental and Clinical Pharmacology, Medical University of Graz, Graz, Austria.

3.5.2.1 Investigations of antagonistic activity of Gü 1654 on OXE-R G_i mediated calcium flux in eosinophils and neutrophils

OXE-triggered calcium flux in eosinophils (**fig. 37a)** and neutrophils (**fig. 37c**) was confirmed to be G_i-mediated, as calcium flux was abrogated after cell pre-treatment with PTX (3 µg/ml, 1 h). Cell viability after PTX treatment was confirmed by the Calciumionophore (**fig. 37b,d**), which increases intracellular calcium ions in intact cells and forms stable complexes with divalent cations.

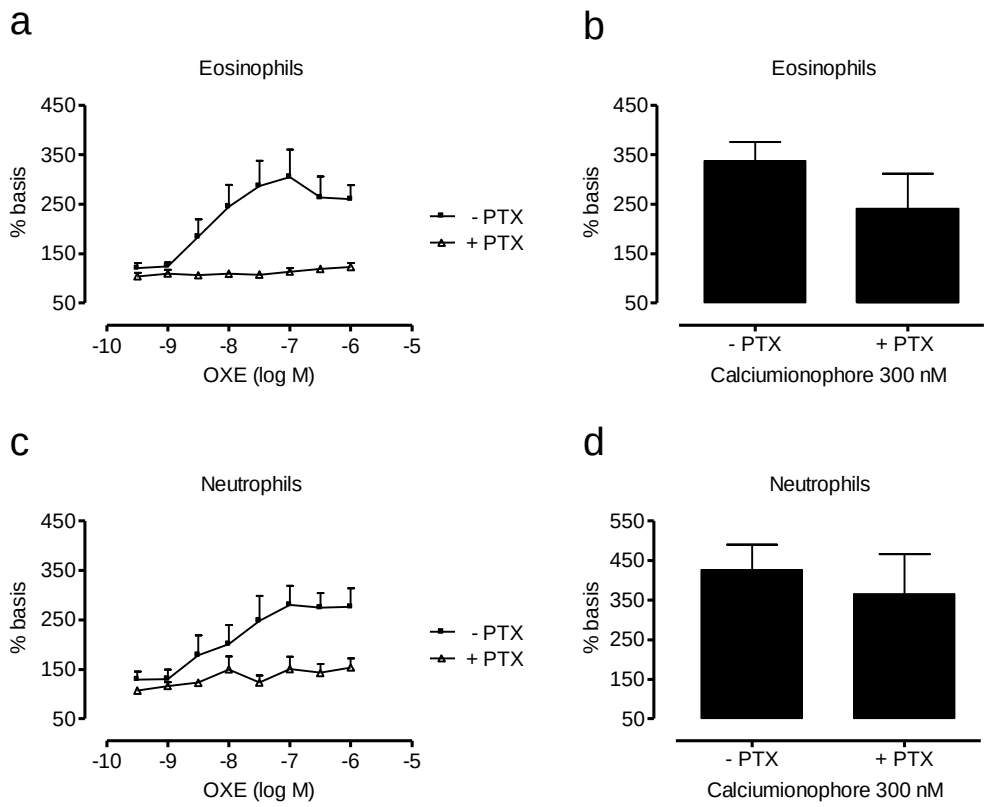

Figure 37: OXE-mediated eosinophil and neutrophil calcium flux is G_i-mediated. Eosinophil (**a**) and neutrophil (**c**) calcium flux upon OXE stimulation was found to be PTX sensitive, and thus Gi mediated. Cells were treated with 3 µM PTX for 1 h. Viability of both eosinophils (**b**) and neutrophils (**d**) after PTX-treatment was confirmed by 300 nM Calciumionophore. Data presented are mean (+ SEM) of four independent experiments, each performed in triplicates.

Gü 1654 was tested for antagonistic activity on G_i-mediated calcium flux in eosinophils and neutrophils. After pre-incubating the cells with 1 µM Gü 1654 for 15 minutes, calcium flux assays were performed as described by Heinemann et al. (2003). Unexpectedly, eosinophil (**fig. 38a**) and neutrophil calcium flux (**fig. 38b**) was completely abrogated at 1 µM Gü 1654.

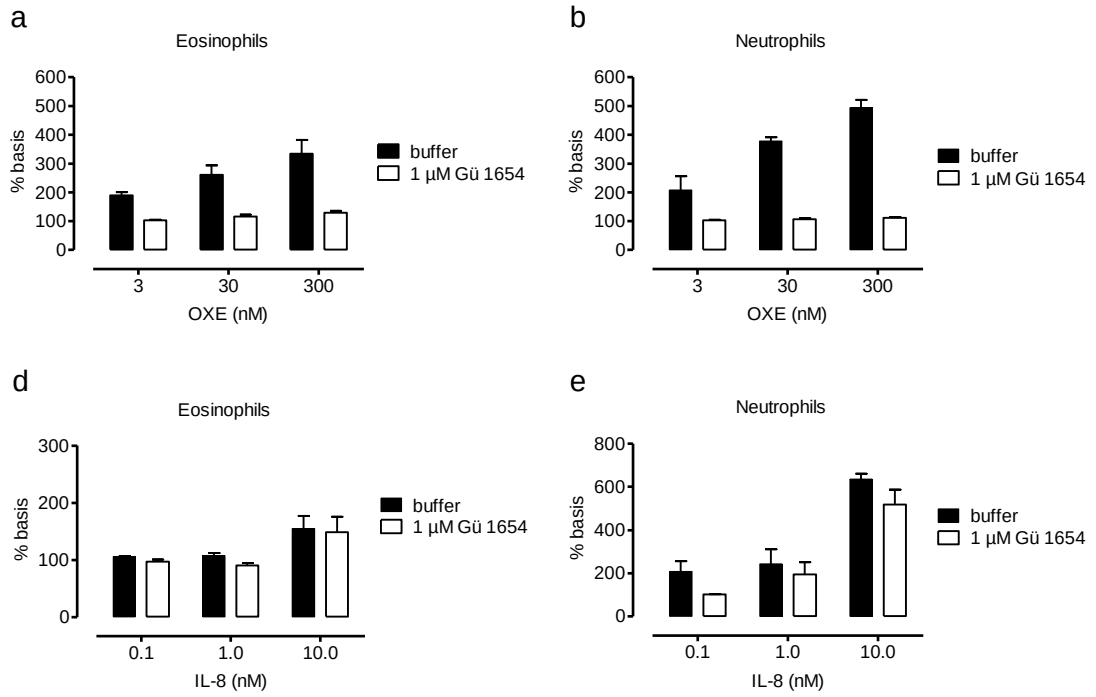

Figure 38: 1 µM Gü 1654 completely inhibits OXE-mediated calcium flux in eosinophils and neutrophils. After pre-incubation with 1 µM Gü 1654 or buffer as control, eosinophils (**a**) and neutrophils (**b**) were challenged with increasing concentrations of OXE. Calcium flux of both eosinophils and neutrophils was completely abolished by Gü 1654. Specificity of Gü 1654 on the OXE-mediated calcium flux was confirmed on IL-8-mediated calcium flux in eosinophils (**c**) and neutrophils (**d**), which was not attenuated after pre-incubation with 1 µM Gü 1654.

To prove receptor specificity of inhibition with Gü 1654, the compound was analysed at G_i-mediated, IL-8 triggered calcium flux of eosinophils and neutrophils (Kernen et al., 1991). IL-8 triggered calcium flux of eosinophils (**fig. 38c**) and neutrophils (**fig. 38d**) was not affected by Gü 1654.

The finding, that Gü 1654 inhibited OXE-R G_i signaling in human primary cells appeared contrary to the findings obtained from cAMP accumulation and DMR assays with HEK293 cells overexpressing the OXE-R, where Gü 1654 was determined not to exhibit antagonism on the OXE-R G_i pathway. Thus, it was initially suggested that Gü 1654 does not maintain its ability to discriminate between the OXE-R signaling via the G_i pathway or another pathway in human primary cells.

However, by comparing the results from cAMP accumulation assays to the results from primary cell calcium flux assays, it became apparent, that, although in both assays G_i signaling of the OXE-R was measured, the recorded G_i signaling in the two different readouts is mediated by two different G_i protein signaling mechanisms: While inhibition of adenylyl cyclase is mediated by $G\alpha_i$ subunits of activated heterotrimeric G_i proteins

(Moxham et al., 1993; Sunahara et al., 1996), calcium flux is mediated by Gβγ subunits of the same activated heterotrimeric G_i protein (Morris and Scarlata, 1996; Hall et al., 1999. Hosoi et al., 2005).

In conclusion, it was suggested that Gü 1654 appeared to exhibit a selective antagonism on OXE-R signaling in leukocytes, by inhibiting receptor signaling via Gβγ subunits but not via $G\alpha_i$ subunits. This putative new mechanism of biased receptor antagonism has not yet been described in literature.

In order to prove this notion, Gü 1654 was tested for antagonism on neutrophil OXE-R $G\alpha_i$ signaling recorded in cAMP accumulation assays.

3.5.2.2 Investigations of antagonistic activity of Gü 1654 on $G\alpha_i$ signaling of the OXE-R in neutrophils using cAMP accumulation assays

Analysis of Gü 1654 on $G\alpha_i$ signaling of in neutrophils endogenously expressed OXE-R was performed in cAMP accumulation assays using the LANCE Ultra cAMP kit (Perkin Elmer), as described in section **2.3.2**.

3.5.2.2.1 Validation of cAMP assay in neutrophils

In order to determine the dynamic range of the LANCE Ultra cAMP assay, a cAMP standard curve was generated according to the *LANCE Ultra cAMP assay development guidelines*. cAMP standard serial solutions were prepared from a cAMP standard and TR-FRET was detected. A cAMP standard curve was established, and the dynamic range was located between -9.45 (IC_{90}) and -8.34 (IC_{10}) (**fig. 39a**).

To determine the optimal cell density to be used in cAMP accumulation assays, forskolin concentration effect curves were generated after 30 minutes of forskolin stimulation using different neutrophil cell densities. The obtained forskolin concentration effect curves were related to the cAMP standard curve. All tested cell numbers provided a response that covered the dynamic range of the cAMP standard curve. Increasing cell numbers yielded an increased assay window with the optimal cell number of 12.000 cell per well while staying within the dynamic range of the cAMP standard curve (**fig. 39b,c**).

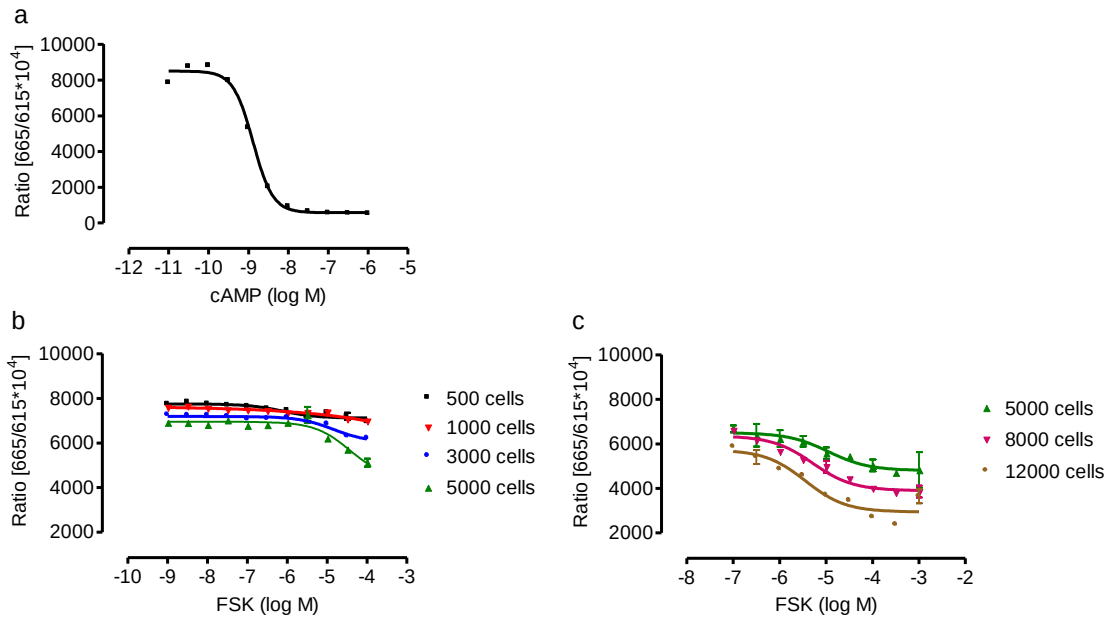

Figure 39: Determination of the dynamic range and the optimal cell number for LANCE Ultra cAMP assays. (**a**) A cAMP standard curve was established, and the dynamic range was located between -9.45 (IC_{90}) and -8.34 (IC_{10}). (**b,c**) In forskolin concentration effect curves, the highest assay window was gained at a cell number of 12.000 cells per well, which proved to be the optimal cell number for neutrophils in LANCE Ultra cAMP assays. Presented data are from a single experiment (+ SEM and mean values, c ± SEM) performed in triplicates.

The optimal cell density used in subsequent experiments was determined to be 12.000 neutrophils per well, since at this cell density the maximal assay window was obtained. For adenylyl cyclase stimulation, the optimal forskolin concentration was determined to be 10 µM.

3.5.2.2.2 Analysis of OXE-R $G\alpha_i$ signaling in neutrophils using cAMP accumulation assays

Neutrophils were analyzed for OXE-mediated inhibition of forskolin-stimulated adenylyl cyclase. In order to investigate if inhibition occurs in a time dependent manner, as it was determined for nicotinic acid-mediated inhibition of forskolin-stimulated adenylyl cyclase (Kostylina et al., 2008), cells were stimulated with agonist for 10 and 30 minutes.

No concentration corresponding inhibition of forskolin stimulated adenylyl cyclase could be determined after neutrophil stimulation with increasing concentrations of OXE for 10 minutes (**fig. 40a**), whereas a concentration dependent inhibition of forskolin-stimulated adenylyl cyclase was observed after cell stimulation with OXE for 30 minutes (**fig. 40b**).

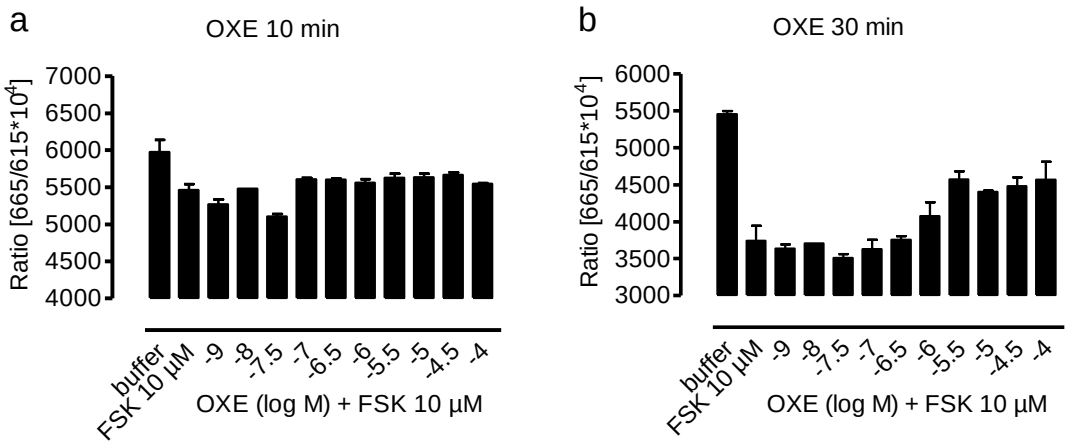

Figure 40: Determination of OXE-mediated inhibition of forskolin-stimulated adenylyl cyclase in neutrophil cAMP accumulation assays. Concentration dependent inbibition of forskolin stimulated adenylyl cyclase was not achieved after 10 minutes stimulation with OXE (**a**), but after 30 minutes (**b**). Presented data are from a single experiment (+ SEM and mean values), each performed in triplicates.

3.5.2.2.3 Analysis of inhibitory activity of Gü 1654 on OXE-R $G\alpha_i$ signaling in neutrophils using cAMP accumulation assays

Prior to antagonism experiments on OXE-R $G\alpha_i$ signaling in neutrophils, Gü 1654 was tested in 30 µM for unspecific effects on neutrophils in cAMP accumulation assays after 15 minutes cell pre-incubation. For cells treated with Gü 1654, no adenylyl cyclase stimulating or inhibiting effects were observed (**fig. 41a**). Subsequently, Gü 1654 was tested at 30 µM for antagonistic acitivity on OXE-R $G\alpha_i$ signaling in cAMP accumulation assays. Data revealed that OXE-mediated inhibition of forskolin-stimulated adenylyl cyclase was not inhibited by 30 µM Gü 1654 (**fig. 41b**), thus confirming the notion that the compound does not inhibit OXE-R $G\alpha_i$ signaling.

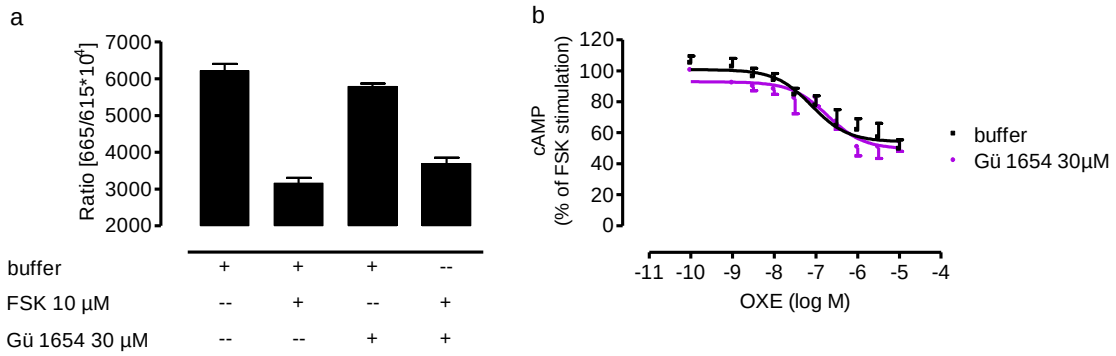

Figure 41: Analysis of inhibitory activity of Gü 1654 on OXE-mediated $G\alpha_i$ signaling in neutrophils. Gü 1654 was found neither to stimulate nor to inhibit adenylyl cyclase activity (**a**). No inhibitory effect on OXE triggered and $G\alpha_i$-mediated inhibition of forskolin-stimulated adenylyl cyclase was detected for Gü 1654 in 30 µM (**b**). (**a**) presents data of a single experiments (+ SEM and mean values) performed in triplicates, and (**b**) presents mean data (± SEM) of four to five independent experiments, each performed in triplicates.

In conclusion, the initial hypothesis that Gü 1654 acts as biased OXE-R antagonist, with inhibitory activity on G_{16}, but not on G_i signaling (section **3.2.2** and **3.3.3**), was extended for the finding, that Gü 1654 is an OXE-R antagonist competent to discriminate between OXE-R signaling via the Gβγ subunit and OXE-R signaling by the $G\alpha_i$ subunit of the same heterotrimeric G_i protein.

It was suggested that these findings uncovered a new mechanism of ligand bias.

3.5.3 Discussion

Analysis of Gü 1654 at OXE-mediated calcium flux in eosinophils and neutrophils uncovered Gü 1654 to inhibit OXE-R signaling via Gβγ subunits, while preserving OXE-R coupling to $G\alpha_i$ subunits of the same heterotrimeric G_i protein. Thus, Gü 1654 was elucidated not to confer biased antagonism on OXE-R signaling via different G protein subfamilies – as previously suggested – but on OXE-R signaling by discriminating between the Gα and Gβγ of G_i proteins.

Strikingly, although in neutrophil cAMP accumulation assays Gü 1654 did not affect $G\alpha_i$ mediated inhibition of cAMP production at the highest concentration of 30 µM - which confirmed the results from HEK293 cell cAMP accumulation assays with overexpressed OXE-R from section **3.2.2** -, Gβγ-mediated calcium flux was already completely abolished by Gü 1654 at a concentration of 1 µM. These findings implied that OXE-R signaling via the G_i protein subunits $G\alpha_i$ and Gβγ might be modulated differentially. Indeed, differential modulation of $G\alpha_i$ and Gβγ effects is not

unprecedented in the literature. About two decades ago, Ashkenazi et al. (1997) appreciated that the muscarinic acetylcholine receptor M2 inhibits adenylyl cyclase and stimulates inositol phosphate (IP) accumulation, and that both processes were mediated via G_i proteins, as evidenced by their sensitivity to PTX pre-treatment. Intriguingly, however, the adenylyl cyclase response was about 10-fold more sensitive to PTX as compared with the IP response. The authors suggested that both effects are differentially coupled via the same G protein. Indeed, inhibition of adenylyl cyclase is mediated via $G\alpha_i$ subunits whereas phosphoinositide hydrolysis is mediated by Gβγ subunits "released" upon $G\alpha_i\beta\gamma$ activation (Camps et al., 1992; Katz et al., 1992). Thereforee, these data provide support for the notion that Gα responses can be differentially modulated over Gβγ responses.

In a further assay, performed by Andreas Bock from the group of Prof. Mohr, Pharmacology and Toxicology Section, Institute of Pharmacy, University of Bonn, selective inhibition of Gβγ signaling of the OXE-R by Gü 1654 was ascertained.
In order to exclusively monitor a Gβγ-mediated downstream event, HEK293 cells were transiently transfected to co-express the OXE-R, Gβ1 and Gγ2, respectively, and Gβγ-mediated inositol phosphate 1 (IP1) production was quantified as a measure of receptor activity. OXE-triggered IP production was highly significant and mediated by Gβγ, since pre-treatment with the small molecule Gβγ inhibitor Gallein (Bonacci et al., 2006) completely abolished the response (**fig. 42**). Gallein, conversely, hardly affected IP1 accumulation induced upon stimulation of endogenous G_q-linked muscarinic receptors in agreement with its inability to dampen G□-mediated cellular responses (Bonacci et al., 2006). Gü1654, which proved to be ineffective when applied alone, completely abrogated OXE-R-mediated IP production, but had no impact on IP1 levels triggered by stimulation of endogenous G_q-linked muscarinic receptors, confirming that inhibition of IP1 production is specific to the OXE-R.

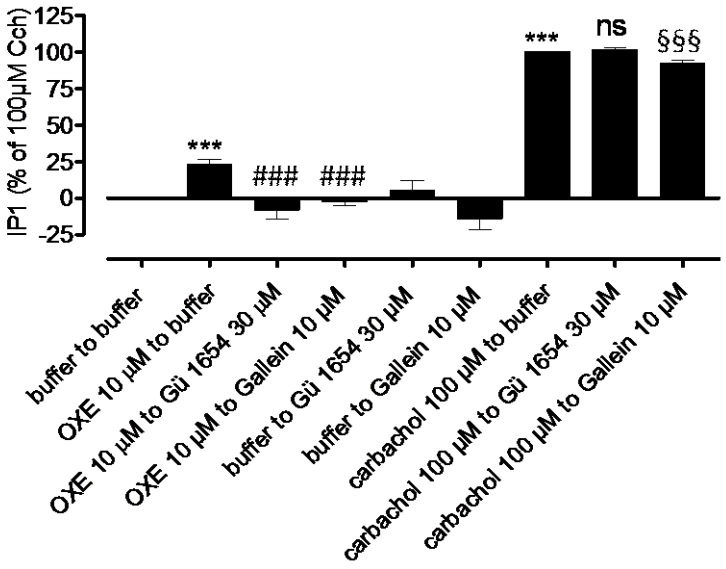

Figure 42: Effects of OXE and carbachol on IP1 generation and their sensitivity to Gallein and Gü 1654 in HEK293 cells transiently expressing the OXE-R, Gβ1 and Gγ2. Shown are mean values ± SEM of 3-8 independent experiments each performed in quadruplicate. ***, significant effect to basal IP1 levels; ###, significant effect to OXE; §§§, significant effect to carbachol; ns, non-significant effect to carbachol. ***, ### and §§§, $p < 0.001$ according to one-way ANOVA with Bonferroni's multiple comparison test. Data was kindly provided by Andreas Bock.

Since no DMR responses could be monitored upon neutrophil stimulation with nanomolar concentrations of OXE, and compared with neutrophil calcium flux and cAMP accumulation assays where OXE in equal concentrations produced robust Gβγ and $G\alpha_i$-mediated responses, respectively, it can be suggested that in DMR assays neither OXE-R Gβγ nor $G\alpha_i$ signaling can be detected. In neutrophil cAMP accumulation assays, OXE-R $G\alpha_i$ signaling results in inhibition of cAMP production, but, however, OXE-R $G\alpha_i$ signaling might probably not result in cellular mass redistribution and therefore cannot be detected by DMR technology. Obviously, OXE-R Gβγ signaling does not trigger DMR reactions either. However, signaling via Gβγ subunits released from activated G_i proteins appears to be a crucial mechanism for OXE-R signaling, in neutrophils as well as in other types of leukocytes (Grant and Powell, 2009).

Originally, G protein βγ subunits were thought to function as terminators of Gα-dependent signaling and to prevent spontaneous Gα activation in the absence of receptor stimulation (Neer, 1995), until Gβγ was found to activate muscarinic K^+ ion

channels in cardiac atrial cells (Logothetis et al., 1987). Nowadays, Gβγ subunits are known to activate various effectors, such as phospholipase C (PLC) β2 (Katz et al., 1992; Sternweis, 1994), adenylyl cyclase (Tang and Gilman, 1991), phosphoinositide 3-kinase (Stephens et al., 1994, Tang and Downes, 1997), and K^+ and Ca^{2+} channels (Logothetis et al., 1987, Reuveny et al., 1994), to name just a few.

G_i protein expression is high and abundant compared with G proteins from other G protein subfamilies, so that the most part of released Gβγ subunits and subsequent signaling of Gβγ is due to G_i protein activation (Clapham and Neer, 1997). Downstream signaling of Gβγ subunits released from G proteins can be attenuated by the Gβγ scavenger $G_t\alpha$, the alpha subunit of transducin (Federman et al., 1992; Ho et al., 1999), or by small molecule Gβγ inhibitors (Bonacchi et al., 2006). By using these Gβγ inhibitors, it could be shown that Gβγ subunits released from chemoattractant G_i coupled receptors are essential for cell chemotaxis (Neptune and Bourne, 1997; Neptune et al., 1999), and neutrophil-dependent inflammation (Lehmann et al., 2007). Signaling by Gβγ subunits has also been reported to be involved in the progression of heart failure (Casey et al., 2010) and in proliferation of the breast cancer cells MDA-MB-231 (Tang et al., 2011). These findings clearly imply a need for therapeutics focusing on inhibition of Gβγ signaling related to disease development.

Two of these Gβγ involved diseases have been reported to be related to OXE-R signaling: Inflammation and cancer. As it is largely known, the chemoattractant OXE-R is expressed on most immune cells and plays a pivotal role in inflammatory reactions (Jones, 2005; Grant and Powell, 2009). Tumor cell proliferation upon OXE stimulation was determined for the breast cancer cell lines MDA-MB-231, MCF7, and SKOV3 (O´Flaherty et al., 2005) and the prostate cancer cell line PC3 (Ghosh and Myers, 1997). OXE-R expression in the breast cancer cell lines was determined by mRNA expression (O´Flaherty et al., 2005), and OXE-R expression in PC3 cells was determined by the use of short-interfering RNA (Sundaram and Ghosh 2006). In conclusion, the finding that Gü 1654 specifically inhibits OXE mediated Gβγ signaling of the OXE-R implies high impact on Gü 1654 to be used as a valuable tool in trials on OXE mediated inflammatory events and OXE-mediated tumor cell proliferation.

4 Final discussion

The aim of the present work was to discover small molecule OXE-R antagonists, to characterize the antagonistic activity of the compounds on the different signaling pathways of the OXE-R, and finally to determine the antagonistic activity in primary cells endogeneously expressing the OXE-R. By use of a biomolecular screening in combination with a virtual screening one compound, Gü 1654, was found to exhibit specific antagonism on G_{16} signaling of the OXE-R when over-expressed in HEK293 cells. Furthermore, antagonistic activity on OXE-R-mediated β-Arrestin2 recruitment could also be determined for Gü 1654 in HEK293 cells. However, this compound was found to exhibit a biased antagonism, because in cAMP accumulation assays using HEK293 cells Gü 1654 did not retain its antagonistic activity on G_i signaling. Finally, and most intriguing, when Gü 1654 was tested for antagonistic activity on OXE-R G_i signaling in human primary cells, antagonism of Gü 1654 was elucidated to selectively inhibit OXE-R Gβγ but not OXE-R $G\alpha_i$ signaling. Thus, Gü 1654 was identified as biased antagonist discriminating between OXE-R signaling via different G protein subunits of the same G protein heterotrimer, which proved a new mechanism of ligand bias.

Ligand bias is a synonym for the ability of a ligand to differentially activate signaling pathways mediated via a single GPCR, which is due to different receptor conformational states induced by the ligand (Vauquelin and Van Liefde, 2005, Urban et al., 2007, Kenakin, 2009). Other terms found to describe this phenomenon, are "stimulus trafficking", "functional selectivity", "agonist-directed trafficking" or "ligand-induced selective signaling (LiSS)". About 15 years ago, the phenomenon of ligand bias was described for the first time. Until then, a receptor was regarded to remain either in an inactive or an active state, and in an active state, induced by agonist binding, the receptor would be able to activate any signaling pathways linked to. Thus, data indicating ligand bias were not compatible with the prevalent pharmacological concepts and were first considered as artefacts resulting from e.g. interactions with unknown receptors, until more and more data emerged pointing at the phenomenon of ligand bias. In conclusion, the two-state receptor conformation model and the concept of "intrinsic efficacy" had to be revised and adapted to a multi-state receptor conformation model.

Ligand bias has been reported for several receptors, e. g. the β2-adrenoceptor (β2-AR) (Woo et al., 2009), the prostaglandin EP4 receptor (Leduc et al., 2009), the serotonin receptors 5-HT2A, 5-HT2B, 5-HT2C-VSV (Cussac et al., 2008), or the sphingosine-1-phosphate receptor subtype 3 (SIP(3)) (Jongsma et al., 2009). Although in literature several reports on ligand biased agonism exist, until now only three cases of ligand biased antagonism have been reported (Mathiesen et al., 2005; Maillet et al., 2007; Dowal et al., 2011). Whereas Mathiesen et al. described biased antagonism of a ligand at the CRTH2 receptor conferring selective inhibition of receptor-β-arrestin recruitment without affecting receptor-G protein activation at the same time, Maillet et al. and Dowal et al. reported biased antagonism for the multi-G protein coupled receptors NK2 and PAR1, respectively, based on selective inhibition of a single G protein pathway while not affecting another G protein pathway. In each of the three studies, the biased antagonism was determined to be induced by antagonists displaying allosteric features. Strikingly, the PAR1 receptor antagonist (Maillet et al., 2007) was even found to bind intracellular to helix 8 of the PAR1 receptor, as determined by point mutation studies.

It is likely, that Gü 1654 might also induce its biased antagonism through allosteric binding to the OXE-R, hereby stabilizing a receptor conformation that preserves activation of $G\alpha_i$-mediated downstream events, but at the same time completely precludes propagation of the Gβγ-mediated signal. In order to evaluate in the future if Gü 1654 might confer its unprecedented mechanism of ligand bias through an allosteric OXE-R binding site, extracellular or even intracellular, mutagenesis studies would have to be performed. Hereby, mutations analogous to those made by Dowal et al. should be considered for generation of OXE-R mutants. An intracellular located allosteric binding site has also been reported for antagonists at the CXCR2 receptor, and domain switching and point mutation studies determined that sensitivity towards the tested CXCR2 antagonists is conferred through the receptor´s C-terminus, as well as through Lys^{320} at the N terminus of helix 8 of CXCR2 (Nicholls et al., 2008; Salchow et al., 2010). Thus, these findings could also provide supporting information regarding mutagenesis studies at the OXE-R.

In BRET studies by Gales et al. (2006), BRET between receptor and Gβγ was analysed and determined to be an indicator of conformational changes propagated from an activated receptor to the G protein. In order to gain additional mechanistic insights into

the mode of biased antagonism of Gü 1654 and to assess, whether Gü 1654 affects proximity between the OXE-R and Gβγ, BRET assays were performed using the same BRET biosensors as Gales et al. These experiments were carried out by Lucas Peters from the group of Prof. Evi Kostenis.

BRET was measured between the OXE-R tagged at its C-terminus with the energy donor Renilla luciferase (RLuc) and the Gγ2 subunit N-terminally fused to the energy acceptor GFP10. Upon stimulation with OXE, robust engagement of Gβγ was observed, which indicated a conformational change between the OXE-R and the Gβγ complex in which energy donor and energy acceptor move closer together (**fig. 43a**). This BRET response was significantly diminished in the presence of increasing concentrations of Gü 1654 (**fig. 43a**), suggesting that Gü 1654 prevents - at least in part - communication between the ligand-activated OXE-R and the Gβγ subunit by altering their proximity or relative orientation, respectively.

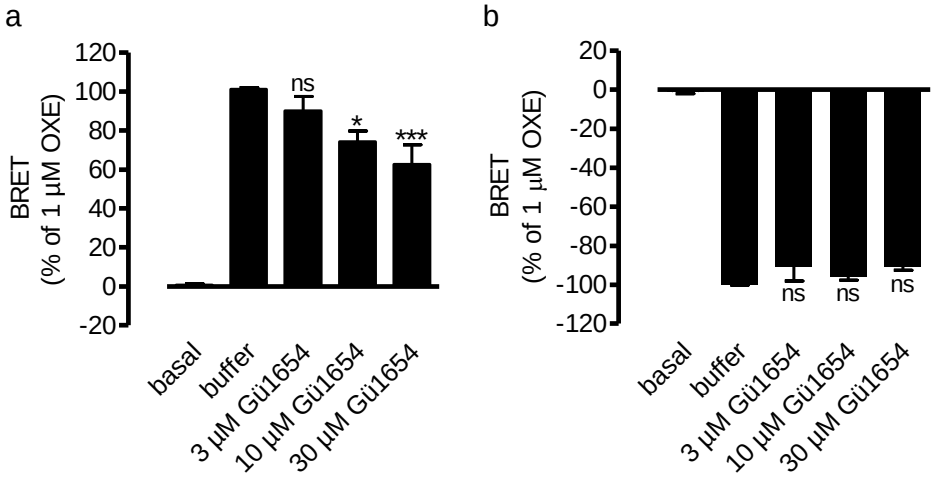

Figure 43: Effects of Gü 1654 on OXE mediated BRET in the presence of Gü 1654. (**a**) OXE-induced BRET between the OXE-R fused to Renilla luciferase (OXE-R-Rluc) and GFP10-labelled Gγ (GFP10-Gγ) was concentration dependently attenuated at increasing concentrations of Gü 1654, as measured in HEK293 cells transiently expressing OXE-R-Rluc, GFP10-Gγ and Gβ. (**b**) The decrease of BRET between $G\alpha_i$ fused to Renilla luciferase ($G\alpha_i$-91-RLuc) and GFP10 labelled Gγ (GFP10-Gγ2) due to OXE-triggered opening of the nucleotide binding pocket of $G\alpha_i$ was not reversed by increasing concentrations of Gü 1654, as measured in HEK293 cells transiently transfected with the OXE-R, $G\alpha_i$-91-RLuc, GFP10-Gγ2 and Gβ. Shown are mean values ± SEM of 5-7 independent experiments each performed in quadruplicate. *** and *, significant effect to OXE; ns, non-significant effect to OXE. *, $p < 0.01$ and ***, $p < 0.001$ according to one-way ANOVA with Bonferroni's multiple comparison test. Data were kindly provided by Lucas Peters.

A control using the HM74A fused to Renilla luciferase proved, that only BRET interaction between the OXE-R and Gβγ was specifically inhibited by Gü 1654 (data not shown). Finally, Gü1654 was completely ineffective when tested for its ability to

inhibit opening of the $G\alpha_i$ nucleotide binding pocket (**Fig. 43b**) as determined in BRET assays where a OXE triggered decrease of BRET between $G\alpha_i$ and $G\beta\gamma$ using the appropriate sensors of $G\alpha_i$ and the $G\beta\gamma$ complex ($G\alpha_i$-91-RLuc, GFP10-Gγ2; Gales et al., 2006) was detected.

As these BRET data showed that contact between the OXE-R and $G\beta\gamma$ is only partially, and not completely diminished in the presence of the highest concentration of Gü 1654, it appeared intriguing that only partially attenuated contact between OXE-R and $G\beta\gamma$ is competent to completely silence downstream signaling of $G\beta\gamma$. But, however, from a different point of view, "only" partial inhibition of receptor-$G\beta\gamma$ contact in the presence of Gü 1654 truly reflects the biased antagonism of Gü 1654 on G_i protein subunit signaling, as probably $G\alpha_i$ activation is only provided due to partially and not completely diminished OXE-R-$G\beta\gamma$ contact.

Models of receptor-mediated G-protein activation presume that $G\beta\gamma$ plays a crucial role in receptor-G protein interaction and G protein activation, and that $G\beta\gamma$ actively participates in receptor-G protein activation (Bourne, 1997; Ford et al., 1998; Iiri et al., 1998). Due to the "lever-arm" (Lichtarge et al., 1996; Rondard et al., 2001) and the "gear-shift" model (Cherfils and Chabre, 2003), $G\beta\gamma$ is involved in mediation of GDP release from the $G\alpha_i$ nucleotide binding pocket, whereas the "C-terminal latch" model (Herrmann et al., 2004; Gautam, 2003; Kisselec and Downs, 2003) presumes the C-terminus of $G\gamma$ to present a receptor contact site before GDP release is enabled. These models imply, that, if the initial contact between agonist stimulated receptor and $G\beta\gamma$ is prevented, – e.g. due to a receptor conformation change induced by an antagonist – G protein activation cannot be initiated.

Indeed, BRET experiments performed by Gales et al. (2006) monitoring interactions between the α_{2A}-adrenoceptor fused to Renilla luciferase and GFP10 labelled $G\beta$ or GFP10 labelled $G\gamma$, respectively, proved that agonist-induced BRET between the α_{2A}-adrenoceptor and the $G\beta\gamma$ dimer was completely abrogated after pre-treatment with the selective α_{2A}-adrenoceptor antagonist RX 821002 (Newman-Tancredi et al., 1998). In the same work, agonist stimulated decrease of BRET between $G\alpha_i$ and $G\gamma$ was also reversed after antagonist pre-treatment indicating the need of receptor-$G\beta\gamma$ interaction for $G\alpha$ activation.

In further experiments, the conformational changes within the G protein heterotrimer induced during receptor-mediated G protein activation were analysed. The results

concerning the structural model of G protein activation were found to be compatible with the “gear-shift” model (Cherfils and Chabre 2003).

Thus, OXE-R BRET assays imply - beneath the finding that obviously partially attenuated contact between OXE-R and Gβγ is competent to completely silence downstream signaling of Gβγ -, that (i) OXE-R-mediated G protein activation is conferred through OXE-R-Gβγ contact, and that (ii) although OXE-R-Gβγ contact is partially diminished in the presence of Gü 1654, the remaining contact between the OXE-R and the Gβγ dimer is still sufficient for activation of $G\alpha_i$.

In conclusion, the identification of the first GPCR antagonist able to discriminate between receptor signaling on the level of an individual Gαβγ heterotrimer can be reported. This unprecedented mechanism of ligand bias suggests an ever increasing number of relevant conformational states that may be adopted by GPCRs and may link them to defined signaling routes. Hence, this new mechanism of ligand bias will state a new paradigm for pathway specific drug design in order to gain allosteric modulators with improved therapeutic window and increased selectivity, and, in addition, offers new implications on the strategy of drug screening, as appropriate assays suited to detect signaling via the Gβγ pathway will need to be established.

5 Summary

The lipid mediator 5-oxo-ETE is a metabolite of the 5-lipoxygenase pathway and acts as a potent chemoattractant on eosinophils and neutrophils. OXE-induced effects are mediated via the G_i coupled 5-oxo-ETE receptor OXE-R, which is mainly expressed on immune cells like eosinophils, neutrophils, basophils and monocytes. The OXE-R is implicated to play a pivotal role in inflammation and inflammatory diseases. For analysis of pathophysiologic effects of OXE-R signaling, an OXE-R antagonist would be needed, but to date, no small molecule OXE-R antagonist has been reported.

In the present thesis, a biomolecular screening in combination with a virtual screening was performed to discover OXE-R antagonists. In calcium mobilization assays, using a human recombinant cell line overexpressing the OXE-R and the promiscuous Gα subunit G_{16}, three compounds were identified with inhibitory effects on the OXE-R G_{16} pathway: Gü 1157, Gü 1158 and Gü 1654. To explore the antagonistic efficacy of the compounds on the various signaling pathways of the OXE-R, a number of functional assays had to be established allowing to monitor G protein-dependent and G protein-independent effector activation of the OXE-R using recombinant cells overexpressing the OXE-R. In cAMP accumulation assays Gü 1157, Gü 1158 and Gü 1654 were analyzed on the native Gi signaling pathway of the OXE-R. Surprisingly, the compounds did not show inhibitory activity on the G_i signaling pathway of the OXE-R, so that Gü 1157, Gü 1158 and Gü 1654 were assumed to exhibit a biased antagonism at OXE-R G_{16} and G_i signaling.To confirm this hypothesis, DMR assays were established and Gü 1157, Gü 1158 and Gü 1654 were analyzed on the discrete OXE-R G_{16} and G_i pathways, respectively. The biased antagonism was confirmed for Gü 1654, but not for Gü 1157 and Gü 1158, which failed to inhibit OXE-R G_{16} DMR responses and were not pursued further.

The OXE-R was analyzed for β-Arrestin recruitment capabilities using BRET assays, and OXE-R β-Arrestin recruitment was uncovered to occur also in the absence of G_i protein activation, which provides evidence for a hitherto unknown G protein-independent signaling pathway of the OXE-R. Analysis of Gü 1654 on OXE-R β-Arrestin translocation revealed inhibitory effects on OXE-mediated β-Arrestin recruitment in the presence and absence of activated G_i proteins, indicating that Gü 1654 is a potent OXE-R antagonist also on a non-Gi-mediated signaling pathway.

It was evaluated if Gü 1654 maintains its biased antagonism on endogenously expressed OXE-R in human primary cells. Intriguingly, analysis of Gü 1654 on OXE-R Gi signaling in eosinophils and neutrophils by using two different assays monitoring G_i-mediated cellular effects uncovered Gü 1654 to inhibit OXE-R Gβγ mediated calcium flux assays but not to inhibit OXE-R $G\alpha_i$ signaling in cAMP assays.

In the present thesis, Gü 1654 was discovered as a novel small molecule OXE-R antagonist which is competent to selectively inhibit OXE-R signaling via different subunits of the same heterotrimeric G_i protein, implying a new mechanism of ligand bias.

6 Abbreviations

AC	adenylyl cyclase
ADP	adenosine 5’-diphosphate
ATP	adenosine 5’-triphosphate
bp	base pairs
BRET	bioluminescence resonance energy transfer
cAMP	cyclic adenosine monophosphate
cDNA	complementary DNA
DAG	diacylglycerol
H_2O	water
DMR	dynamic mass redistribution
DNA	deoxyribonucleic acid
DRC	dose-response curve
EC_{50}	concentration of half maximum effect
ERK	extracellular-signal regulated kinase
FSK	forskolin
g	gram, acceleration by gravity
GDP	guanosine 5′-diphosphate
GFP	green fluorescent protein
GPCR	G protein coupled receptor
G protein	guanine nucleotide-binding protein
GRK	G protein coupled receptor kinases
GTP	guanosine 5′-triphosphate
h	Human, hour
HTRF	homogeneous time resolved fluorescence
IP1	inositol 4-phosphate
IP3	inositol 1,3,4-triphosphate
JNK	c-Jun N-terminal kinase
kb	kilo base(s)
log M	logarithm of molar concentration to base 10
M	molar concentration (mol/liter)
MAPK	mitogen-activated protein kinase

mBRET	milliBRET
min	minute(s)
ml	milliliter
µl	microliter
µM	micromolar
n	number
nm	nanometer
nM	nanomolar
ns	non-significant
OD	optical density
PAR	protease-activated receptor
pEC_{50}	negative logarithm of EC_{50}
PI	phosphatidylinositol
PI3K	phosphatidylinositol 3-kinase
PKA	protein kinase A
PKC	protein kinase C
PLC	phospholipase C
pm	picometer
PTX	Pertussis toxin
RhoA	Ras homolog gene family, member A
RLuc	Renilla luciferase
rpm	rounds per minute
RT	room temperature
RWG	resonant waveguide grating
s	second(s)
SEM	standard error of mean
TM	transmembrane
TR-FRET	time-resolved fluorescence resonance energy transfer
U	unit
UV	ultraviolet
V	volt

7 Literature

Ahmed K; Tunaru S; Offermanns S (2009): GPR109A, GPR109B and GPR81, a family of hydroxy-carboxylic acid receptors. *Trends Pharmacol. Sci.* 30 (11), 557–562.

Arai, H.; Tsou, C. L.; Charo, I. F. (1997): Chemotaxis in a lymphocyte cell line transfected with C-C chemokine receptor 2B: evidence that directed migration is mediated by betagamma dimers released by activation of Galphai-coupled receptors. *Proc. Natl. Acad. Sci. U.S.A* 94 (26), p. 14495–14499.

Ashkenazi, A.; Winslow, J. W.; Peralta, E. G.; Peterson, G. L.; Schimerlik, M. I.; Capon, D. J.; Ramachandran, J. (1987): An M2 muscarinic receptor subtype coupled to both adenylyl cyclase and phosphoinositide turnover. *Science* 238 (4827), p. 672–675.

Azzi, Mounia; Charest, Pascale G.; Angers, Stéphane; Rousseau, Guy; Kohout, Trudy; Bouvier, Michel; Piñeyro, Graciela (2003): Beta-arrestin-mediated activation of MAPK by inverse agonists reveals distinct active conformations for G protein-coupled receptors. *Proc. Natl. Acad. Sci. U.S.A* 100 (20), p. 11406–11411.

Bonacci, Tabetha M.; Mathews, Jennifer L.; Yuan, Chujun; Lehmann, David M.; Malik, Sundeep; Wu, Dianqing et al. (2006): Differential targeting of Gbetagamma-subunit signaling with small molecules. *Science* 312 (5772), p. 443–446.

Bourne HR (1997): How receptors talk to trimeric G proteins. *Curr. Opin. Cell Biol.* 9 (2), p. 134–142.

Brink, Charles; Dahlén, Sven-Erik; Drazen, Jeffrey; Evans, Jilly F.; Hay, Douglas W. P.; Rovati, G. Enrico et al. (2004): International Union of Pharmacology XLIV. Nomenclature for the oxoeicosanoid receptor. *Pharmacol. Rev.* 56 (1), p. 149–157.

Bunemann M; Frank M; Lohse MJ (2003): Gi protein activation in intact cells involves subunit rearrangement rather than dissociation. *Proc Natl Acad Sci U S A* 100 (26), p. 16077–16082.

Burstein ES; Spalding TA; Hill-Eubanks D; Brann MR (1995): Structure-function of muscarinic receptor coupling to G proteins. Random saturation mutagenesis identifies a critical determinant of receptor affinity for G proteins. *J. Biol. Chem.* 270 (7), p. 3141–3146.

Cabrera-Vera TM; Vanhauwe J; Thomas TO; Medkova M; Preininger A; Mazzoni MR; Hamm HE (2003): Insights into G protein structure, function, and regulation. *Endocr. Rev.* 24 (6), p. 765–781.

Camps, M.; Carozzi, A.; Schnabel, P.; Scheer, A.; Parker, P. J.; Gierschik, P. (1992): Isozyme-selective stimulation of phospholipase C-beta 2 by G protein beta gamma-subunits. *Nature* 360 (6405), p. 684–686.

Casey, Liam M.; Pistner, Andrew R.; Belmonte, Stephen L.; Migdalovich, Dmitriy; Stolpnik, Olga; Nwakanma, Frances E. et al. (2010): Small molecule disruption of G beta gamma signaling inhibits the progression of heart failure. *Circ. Res.* 107 (4), p. 532–539.

Cherfils J; Chabre M (2003): Activation of G-protein Galpha subunits by receptors through Galpha-Gbeta and Galpha-Ggamma interactions. *Trends Biochem. Sci.* 28 (1), p. 13–17.

Clapham, D. E.; Neer, E. J. (1997): G protein beta gamma subunits. *Annu. Rev. Pharmacol. Toxicol.* 37, p. 167–203.

Clarke RW; Harris J (2002): RX 821002 as a tool for physiological investigation of alpha(2)-adrenoceptors. *CNS Drug Rev.* 8 (2), p. 177–192.

Cockcroft S; Gomperts BD (1985): Role of guanine nucleotide binding protein in the activation of polyphosphoinositide phosphodiesterase. *Nature* 314 (6011), p. 534–536.

Cussac, Didier; Boutet-Robinet, Elisa; Ailhaud, Marie-Christine; Newman-Tancredi, Adrian; Martel, Jean-Claude; Danty, Nathalie; Rauly-Lestienne, Isabelle (2008): Agonist-directed trafficking of signaling at serotonin 5-HT2A, 5-HT2B and 5-HT2C-VSV receptors mediated Gq/11 activation and calcium mobilisation in CHO cells. *Eur. J. Pharmacol.* 594 (1-3), p. 32–38.

DeFea, K.A (2000): beta-Arrestin-dependent Endocytosis of Proteinase-activated Receptor 2 Is Required for Intracellular Targeting of Activated ERK1/2. *The Journal of Cell Biology* 148 (6), p. 1267–1282.

Digby GJ; Lober RM; Sethi PR; Lambert NA (2006): Some G protein heterotrimers physically dissociate in living cells. *Proc. Natl. Acad. Sci. U S A* 103 (47), p. 17789–17794.

Dowal, Louisa; Sim, Derek S.; Dilks, James R.; Blair, Price; Beaudry, Sarah; Denker, Bradley M. et al. (2011): Identification of an antithrombotic allosteric modulator that acts through helix 8 of PAR1. *Proc. Natl. Acad. Sci. U.S.A* 108 (7), p. 2951–2956.

Erlemann, Karl-Rudolf; Cossette, Chantal; Gravel, Sylvie; Lesimple, Alain; Lee, Gue-Jae; Saha, Goutam et al. (2007): Airway epithelial cells synthesize the lipid mediator 5-oxo-ETE in response to oxidative stress. *Free Radic. Biol. Med.* 42 (5), p. 654–664.

Erlemann, Karl-Rudolf; Rokach, Joshua; Powell, William S. (2004): Oxidative stress stimulates the synthesis of the eosinophil chemoattractant 5-oxo-6,8,11,14-eicosatetraenoic acid by inflammatory cells. *J. Biol. Chem.* 279 (39), p. 40376–40384.

Erlemann KR; Cossette C; Grant GE; Lee GJ; Patel P; Rokach J; Powell WS (2007): Regulation of 5-hydroxyeicosanoid dehydrogenase activity in monocytic cells. *Biochem. J.* 403 (1), p. 157–165.

Erlemann KR; Cossette C; Gravel S; Stamatiou PB; Lee GJ; Rokach J; Powell WS (2006): Metabolism of 5-hydroxy-6,8,11,14-eicosatetraenoic acid by human endothelial cells. *Biochem. Biophys. Res. Commun.* 350 (1), p. 151–156.

Fang Y; Li G; Ferrie AM (2007): Non-invasive optical biosensor for assaying endogenous G protein-coupled receptors in adherent cells. *J. Pharmacol. Toxicol. Methods* 55 (3), p. 314–322.

Federman, A. D.; Conklin, B. R.; Schrader, K. A.; Reed, R. R.; Bourne, H. R. (1992): Hormonal stimulation of adenylyl cyclase through Gi-protein beta gamma subunits. *Nature* 356 (6365), p. 159–161.

Fong, Alan M.; Premont, Richard T.; Richardson, Ricardo M.; Yu, Yen-Rei A.; Lefkowitz, Robert J.; Patel, Dhavalkumar D. (2002): Defective lymphocyte chemotaxis in beta-arrestin2- and GRK6-deficient mice. *Proc. Natl. Acad. Sci. U.S.A* 99 (11), p. 7478–7483.

Ford CE; Skiba NP; Bae H; Daaka Y; Reuveny E; Shekter LR et al. (1998): Molecular basis for interactions of G protein betagamma subunits with effectors. *Science* 280 (5367), p. 1271–1274.

Funk CD (2001): Prostaglandins and leukotrienes: advances in eicosanoid biology. *Science* 294 (5548), p. 1871–1875.

Galandrin, Ségolène; Oligny-Longpré, Geneviève; Bouvier, Michel (2007): The evasive nature of drug efficacy: implications for drug discovery. *Trends Pharmacol. Sci*. 28 (8), p. 423–430.

Gautam N (2003): A conformational switch regulates receptor-G protein interaction. *Structure* 11 (4), p. 359–360.

Gesty-Palmer, Diane; Chen, Minyong; Reiter, Eric; Ahn, Seungkirl; Nelson, Christopher D.; Wang, Shuntai et al. (2006): Distinct beta-arrestin- and G protein-dependent pathways for parathyroid hormone receptor-stimulated ERK1/2 activation. *J. Biol. Chem.* 281 (16), p. 10856–10864.

Gether U; Kobilka BK (1998): G protein-coupled receptors. II. Mechanism of agonist activation. *J. Biol. Chem.* 273 (29), p. 17979–17982.

Ghosh J; Myers CE (1997): Arachidonic acid stimulates prostate cancer cell growth: critical role of 5-lipoxygenase. *Biochem. Biophys. Res. Commun.* 235 (2), p. 418–423.

Ghosh J; Myers CE (1998): Inhibition of arachidonate 5-lipoxygenase triggers massive apoptosis in human prostate cancer cells. *Proc. Natl. Acad. Sci. U S A* 95 (22), p. 13182–13187.

Gilchrist, Annette (2010): GPCR molecular pharmacology and drug targeting. Shifting paradigms and new directions. Hoboken, N.J: Wiley. Online at http://www.worldcat.org/oclc/489623096.

Graham, François D.; Erlemann, Karl-Rudolf; Gravel, Sylvie; Rokach, Joshua; Powell, William S. (2009): Oxidative stress-induced changes in pyridine nucleotides and chemoattractant 5-lipoxygenase products in aging neutrophils. *Free Radic. Biol. Med.* 47 (1), p. 62–71.

Grant, Gail E.; Gravel, Sylvie; Guay, Julie; Patel, Pranav; Mazer, Bruce D.; Rokach, Joshua; Powell, William S. (2011): 5-Oxo-ETE is a major oxidative stress-induced arachidonate metabolite in B lymphocytes. *Free Radic. Biol. Med*.

Grant, Gail E.; Rokach, Joshua; Powell, William S. (2009): 5-Oxo-ETE and the OXE receptor. *Prostaglandins Other Lipid Mediat.* 89 (3-4), p. 98–104.

Grant, Gail E.; Rubino, Stephen; Gravel, Sylvie; Wang, Xiaoping; Patel, Pranav; Rokach, Joshua; Powell, William S. (2011): Enhanced formation of 5-oxo-6,8,11,14-eicosatetraenoic acid by cancer cells in response to oxidative stress, docosahexaenoic acid, and neutrophil-derived 5-hydroxy-6,8,11,14-eicosatetraenoic acid. *Carcinogenesis*.

Gravel, J.; Falgueyret, J. P.; Yergey, J.; Trimble, L.; Riendeau, D. (1993): Identification of 5-keto-(7E,9E,11Z,14Z)-eicosatetraenoic acid as a novel nonenzymatic rearrangement product of leukotriene A4. *Arch. Biochem. Biophys.* 306 (2), p. 469–475.

Guilbert, M.; Ferland, C.; Bossé, M.; Flamand, N.; Lavigne, S.; Laviolette, M. (1999): 5-Oxo-6,8,11,14-eicosatetraenoic acid induces important eosinophil transmigration

through basement membrane components: comparison of normal and asthmatic eosinophils. *Am. J. Respir. Cell Mol. Biol* 21 (1), p. 97–104.

Heinemann A; Ofner M; Amann R; Peskar BA (2003): A novel assay to measure the calcium flux in human basophils: effects of chemokines and nerve growth factor. *Pharmacology* 67 (1), p. 49–54.

Herrmann R; Heck M; Henklein P; Kleuss C; Hofmann KP; Ernst OP (2004): Sequence of interactions in receptor-G protein coupling. *J. Biol. Chem.* 279 (23), p. 24283–24290.

Ho, B. Y.; Uezono, Y.; Takada, S.; Takase, I.; Izumi, F. (1999): Coupling of the expressed cannabinoid CB1 and CB2 receptors to phospholipase C and G protein-coupled inwardly rectifying K+ channels. *Recept. Channels* 6 (5), p. 363–374.

Holst, B.; Hastrup, H.; Raffetseder, U.; Martini, L.; Schwartz, T. W. (2001): Two active molecular phenotypes of the tachykinin NK1 receptor revealed by G-protein fusions and mutagenesis. *J. Biol. Chem.* 276 (23), p. 19793–19799.

Hosoi, Takeshi; Koguchi, Yutaka; Sugikawa, Emiko; Chikada, Aiko; Ogawa, Koji; Tsuda, Naoki et al. (2002): Identification of a novel human eicosanoid receptor coupled to G(i/o). *J. Biol. Chem.* 277 (35), p. 31459–31465.

Hosoi, Takeshi; Sugikawa, Emiko; Chikada, Aiko; Koguchi, Yutaka; Ohnuki, Tetsuo (2005): TG1019/OXE, a Galpha(i/o)-protein-coupled receptor, mediates 5-oxo-eicosatetraenoic acid-induced chemotaxis. *Biochem. Biophys. Res. Commun* 334 (4), p. 987–995.

Hurowitz EH; Melnyk JM; Chen YJ; Kouros-Mehr H; Simon MI; Shizuya H (2000): Genomic characterization of the human heterotrimeric G protein alpha, beta, and gamma subunit genes. *DNA Res.* 7 (2), p. 111–120.

Iikura, Motoyasu; Suzukawa, Maho; Yamaguchi, Masao; Sekiya, Takashi; Komiya, Akiko; Yoshimura-Uchiyama, Chitose et al. (2005): 5-Lipoxygenase products regulate basophil functions: 5-Oxo-ETE elicits migration, and leukotriene B(4) induces degranulation. *J. Allergy Clin. Immunol.* 116 (3), p. 578–585.

Iiri T; Farfel Z; Bourne HR (1998): G-protein diseases furnish a model for the turn-on switch. *Nature* 394 (6688), p. 35–38.

Im, Dong-Soon (2009): New intercellular lipid mediators and their GPCRs: an update. *Prostaglandins Other Lipid Mediat.* 89 (3-4), p. 53–56.

Irwin JJ; Shoichet BK (2005): ZINC--a free database of commercially available compounds for virtual screening. *J. Chem. Inf. Model.* 45 (1), p. 177–182.

Jacoby E; Bouhelal R; Gerspacher M; Seuwen K (2006): The 7 TM G-protein-coupled receptor target family. *Chem.Med.Chem.* 1 (8), p. 761–782.

Janetopoulos C; Jin T; Devreotes P (2001): Receptor-mediated activation of heterotrimeric G-proteins in living cells. *Science* 291 (5512), p. 2408–2411.

Johnston CA; Siderovski DP (2007): Receptor-mediated activation of heterotrimeric G-proteins: current structural insights. *Mol. Pharmacol.* 72 (2), p. 219–230.

Jones, Carol E. (2005): The OXE receptor: a new therapeutic approach for asthma? *Trends Mol. Med.* 11 (6), p. 266–270.

Jones, Carol E.; Holden, Suzanne; Tenaillon, Laurent; Bhatia, Umesh; Seuwen, Klaus; Tranter, Pamela et al. (2003): Expression and characterization of a 5-oxo-

6E,8Z,11Z,14Z-eicosatetraenoic acid receptor highly expressed on human eosinophils and neutrophils. *Mol. Pharmacol.* 63 (3), p. 471–477.

Jongsma, M.; van Unen, J.; van Loenen, P. B.; Michel, M. C.; Peters, S. L. M.; Alewijnse, A. E. (2009): Different response patterns of several ligands at the sphingosine-1-phosphate receptor subtype 3 (S1P(3)). *Br. J. Pharmacol.* 156 (8), p. 1305–1311.

Kaslow HR; Lim LK; Moss J; Lesikar DD (1987): Structure-activity analysis of the activation of pertussis toxin. *Biochemistry* 26 (1), p. 123–127.

Katz, A.; Wu, D.; Simon, M. I. (1992): Subunits beta gamma of heterotrimeric G protein activate beta 2 isoform of phospholipase C. *Nature* 360 (6405), p. 686–689.

Kelly P; Casey PJ; Meigs TE (2007): Biologic functions of the G12 subfamily of heterotrimeric g proteins: growth, migration, and metastasis. *Biochemistry* 46 (23), p. 6677–6687.

Kenakin, Terry (2009): Biased agonism. *F1000 Biol Rep* 1.

Kenakin, Terry; Jenkinson, Stephen; Watson, Christian (2006): Determining the potency and molecular mechanism of action of insurmountable antagonists. *J. Pharmacol. Exp. Ther.* 319 (2), p. 710–723.

Kernen, P.; Wymann, M. P.; Tscharner, V. von; Deranleau, D. A.; Tai, P. C.; Spry, C. J. et al. (1991): Shape changes, exocytosis, and cytosolic free calcium changes in stimulated human eosinophils. *J. Clin. Invest.* 87 (6), p. 2012–2017.

Kim, Jihee; Zhang, Lisheng; Peppel, Karsten; Wu, Jiao-Hui; Zidar, David A.; Brian, Leigh et al. (2008): Beta-arrestins regulate atherosclerosis and neointimal hyperplasia by controlling smooth muscle cell proliferation and migration. *Circ. Res* 103 (1), p. 70–79.

Kisselev OG; Downs MA (2003): Rhodopsin controls a conformational switch on the transducin gamma subunit. *Structure* 11 (4), p. 367–373.

Koike, Daigo; Obinata, Hideru; Yamamoto, Atsushi; Takeda, Shigeki; Komori, Hironobu; Nara, Futoshi et al. (2006): 5-Oxo-eicosatetraenoic acid-induced chemotaxis: identification of a responsible receptor hGPCR48 and negative regulation by G protein G(12/13). *J. Biochem.* 139 (3), p. 543–549.

Kostylina, G.; Simon, D.; Fey, M. F.; Yousefi, S.; Simon, H. U. (2008): Neutrophil apoptosis mediated by nicotinic acid receptors (GPR109A). *Cell Death Differ.* 15 (1), p. 134–142.

Kristiansen K (2004): Molecular mechanisms of ligand binding, signaling, and regulation within the superfamily of G-protein-coupled receptors: molecular modeling and mutagenesis approaches to receptor structure and function. *Pharmacol. Ther.* 103 (1), p. 21–80.

Krupnick JG; Benovic JL (1998): The role of receptor kinases and arrestins in G protein-coupled receptor regulation. *Annu. Rev. Pharmacol. Toxicol.* 38, p. 289–319.

Kurose H (2003): Galpha12 and Galpha13 as key regulatory mediator in signal transduction. *Life Sci.* 74 (2-3), p. 155–161.

Lagerstrom MC; Schioth HB (2008): Structural diversity of G protein-coupled receptors and significance for drug discovery. *Nat. Rev. Drug Discov.* 7 (4), p. 339–357.

Langlois, Anick; Chouinard, Francois; Flamand, Nicolas; Ferland, Claudine; Rola-Pleszczynski, Marek; Laviolette, Michel (2009): Crucial implication of protein kinase C (PKC)-delta, PKC-zeta, ERK-1/2, and p38 MAPK in migration of human asthmatic eosinophils. *J. Leukoc. Biol.* 85 (4), p. 656–663.

Lappano, Rosamaria; Maggiolini, Marcello (2011): G protein-coupled receptors: novel targets for drug discovery in cancer. *Nat. Rev. Drug Discov.* 10 (1), p. 47–60.

Leduc, Martin; Breton, Billy; Galés, Céline; Le Gouill, Christian; Bouvier, Michel; Chemtob, Sylvain; Heveker, Nikolaus (2009): Functional selectivity of natural and synthetic prostaglandin EP4 receptor ligands. *J. Pharmacol. Exp. Ther.* 331 (1), p. 297–307.

Lehmann, D. M.; Seneviratne, A. M. P. B.; Smrcka, A. V. (2008): Small molecule disruption of G protein beta gamma subunit signaling inhibits neutrophil chemotaxis and inflammation. *Mol. Pharmacol.* 73 (2), p. 410–418.

Lichtarge O; Bourne HR; Cohen FE (1996): Evolutionarily conserved Galphabetagamma binding surfaces support a model of the G protein-receptor complex. *Proc. Natl. Acad. Sci. U S A* 93 (15), p. 7507–7511.

Logothetis, D. E.; Kurachi, Y.; Galper, J.; Neer, E. J.; Clapham, D. E.: The beta gamma subunits of GTP-binding proteins activate the muscarinic K+ channel in heart. *Nature* 325 (6102), p. 321–326.

Lundstrom K (2006): Latest development in drug discovery on G protein-coupled receptors. *Curr. Protein Pept. Sci.* 7 (5), p. 465–470.

Luttrell, Louis M.; Lefkowitz, Robert J. (2002): The role of beta-arrestins in the termination and transduction of G-protein-coupled receptor signals. *J. Cell. Sci.* 115 (Pt 3), p. 455–465.

MacLeod, R. J.; Lembessis, P.; Hamilton, J. R.; Powell, W. S. (1999): 5-Oxo-6,8,11,14-eicosatetraenoic acid stimulates isotonic volume reduction of guinea pig jejunal crypt epithelial cells. *J. Pharmacol. Exp. Ther.* 291 (2), p. 511–516.

Maillet, Emeline L.; Pellegrini, Nadia; Valant, Celine; Bucher, Bernard; Hibert, Marcel; Bourguignon, Jean-Jacques; Galzi, Jean-Luc (2007): A novel, conformation-specific allosteric inhibitor of the tachykinin NK2 receptor (NK2R) with functionally selective properties. *FASEB J* 21 (9), p. 2124–2134.

Marti-Renom MA; Stuart AC; Fiser A; Sanchez R; Melo F; Sali A (2000): Comparative protein structure modeling of genes and genomes. *Annu. Rev. Biophys. Biomol. Struct.* 29, p. 291–325.

Mathews, Jennifer L.; Smrcka, Alan V.; Bidlack, Jean M. (2008): A novel Gbetagamma-subunit inhibitor selectively modulates mu-opioid-dependent antinociception and attenuates acute morphine-induced antinociceptive tolerance and dependence. *J. Neurosci.* 28 (47), p. 12183–12189.

Mathiesen, Jesper Mosolff; Christopoulos, Arthur; Ulven, Trond; Royer, Julia F.; Campillo, Mercedes; Heinemann, Akos et al. (2006): On the mechanism of interaction of potent surmountable and insurmountable antagonists with the prostaglandin D2 receptor CRTH2. *Mol. Pharmacol.* 69 (4), p. 1441–1453.

Mathiesen, Jesper Mosolff; Ulven, Trond; Martini, Lene; Gerlach, Lars Ole; Heinemann, Akos; Kostenis, Evi (2005): Identification of indole derivatives exclusively interfering with a G protein-independent signaling pathway of the prostaglandin D2 receptor CRTH2. *Mol. Pharmacol.* 68 (2), p. 393–402.

Mercier, Frederic; Morin, Caroline; Cloutier, Martin; Proteau, Sonia; Rokach, Joshua; Powell, William S.; Rousseau, Eric (2004): 5-Oxo-ETE regulates tone of guinea pig airway smooth muscle via activation of Ca2+ pools and Rho-kinase pathway. *Am. J. Physiol. Lung Cell Mol. Physiol.* 287 (4), p. L631-40.

Millar, Robert P.; Newton, Claire L. (2010): The year in G protein-coupled receptor research. *Mol. Endocrinol.* 24 (1), p. 261–274.

Milligan G; Kostenis E (2006): Heterotrimeric G-proteins: a short history. *Br. J. Pharmacol.* 147 Suppl 1, p. S46-55.

Morin, Caroline; Rousseau, Eric (2007): Effects of 5-oxo-ETE and 14,15-EET on reactivity and Ca2+ sensitivity in guinea pig bronchi. *Prostaglandins Other Lipid Mediat.* 82 (1-4), p. 30–41.

Morin, Caroline; Sirois, Marco; Echave, Vincent; Gomes, Marcio M.; Rousseau, Eric (2007): Relaxing effects of 5-oxo-ETE on human bronchi involve BK Ca channel activation. *Prostaglandins Other Lipid Mediat.* 83 (4), p. 311–319.

Morris, A. J.; Malbon, C. C. (1999): Physiological regulation of G protein-linked signaling. *Physiol. Rev.* 79 (4), p. 1373–1430.

Moxham, C. M.; Hod, Y.; Malbon, C. C. (1993): Gi alpha 2 mediates the inhibitory regulation of adenylylcyclase in vivo: analysis in transgenic mice with Gi alpha 2 suppressed by inducible antisense RNA. *Dev. Genet.* 14 (4), p. 266–273.

Muro, Shigeo; Hamid, Qutayba; Olivenstein, Ronald; Taha, Rame; Rokach, Joshua; Powell, William S. (2003): 5-oxo-6,8,11,14-eicosatetraenoic acid induces the infiltration of granulocytes into human skin. *J. Allergy Clin. Immunol.* 112 (4), p. 768–774.

Murphy, Robert C.; Zarini, Simona (2002): Glutathione adducts of oxyeicosanoids. *Prostaglandins Other Lipid Mediat.* 68-69, p. 471–482.

Nanoff C; Koppensteiner R; Yang Q; Fuerst E; Ahorn H; Freissmuth M (2006): The carboxyl terminus of the Galpha-subunit is the latch for triggered activation of heterotrimeric G proteins. *Mol. Pharmacol.* 69 (1), p. 397–405.

Navé, J. F.; Jacobi, D.; Gaget, C.; Dulery, B.; Ducep, J. B. (1991): Evaluation of 5- and 6-fluoro derivatives of arachidonic acid and 5,8,14-eicosatrienoic acid as substrates and inhibitors of 5-lipoxygenase. *Biochem. J.* 278 (Pt 2), p. 549–555.

Neer, E. J. (1995): Heterotrimeric G proteins: organizers of transmembrane signals. *Cell* 80 (2), p. 249–257.

Neptune, E. R.; Iiri, T.; Bourne, H. R. (1999): Galphai is not required for chemotaxis mediated by Gi-coupled receptors. *J. Biol. Chem.* 274 (5), p. 2824–2828.

Newman-Tancredi A; Nicolas JP; Audinot V; Gavaudan S; Verriele L; Touzard M et al. (1998): Actions of alpha2 adrenoceptor ligands at alpha2A and 5-HT1A receptors: the antagonist, atipamezole, and the agonist, dexmedetomidine, are highly selective for alpha2A adrenoceptors. *Naunyn Schmiedebergs Arch. Pharmacol.* 358 (2), p. 197–206.

Nicholls DJ; Tomkinson NP; Wiley KE; Brammall A; Bowers L; Grahames C et al. (2008): Identification of a putative intracellular allosteric antagonist binding-site in the CXC chemokine receptors 1 and 2. *Mol. Pharmacol.* 74 (5), p. 1193–1202.

Nishimura A; Kitano K; Takasaki J; Taniguchi M; Mizuno N; Tago K et al. (2010): Structural basis for the specific inhibition of heterotrimeric Gq protein by a small molecule. *Proc. Natl. Acad. Sci. U S A* 107 (31), p. 13666–13671.

Noma, Takahisa; Lemaire, Anthony; Naga Prasad, Sathyamangla V.; Barki-Harrington, Liza; Tilley, Douglas G.; Chen, Juhsien et al. (2007): Beta-arrestin-mediated beta1-adrenergic receptor transactivation of the EGFR confers cardioprotection. *J. Clin. Invest.* 117 (9), p. 2445–2458.

O'Flaherty, J. T.; Kuroki, M.; Nixon, A. B.; Wijkander, J.; Yee, E.; Lee, S. L. et al. (1996): 5-Oxo-eicosanoids and hematopoietic cytokines cooperate in stimulating neutrophil function and the mitogen-activated protein kinase pathway. *J. Biol. Chem.* 271 (30), p. 17821–17828.

O'Flaherty, Joseph T.; Rogers, LeAnn C.; Paumi, Christian M.; Hantgan, Roy R.; Thomas, Lance R.; Clay, Carl E. et al. (2005): 5-Oxo-ETE analogs and the proliferation of cancer cells. *Biochim. Biophys. Acta* 1736 (3), p. 228–236.

Oldham WM; Hamm HE (2008): Heterotrimeric G protein activation by G-protein-coupled receptors. *Nat. Rev. Mol. Cell Biol.* 9 (1), p. 60–71.

Overington JP; Al-Lazikani B; Hopkins AL (2006): How many drug targets are there? *Nat. Rev. Drug Discov.* 5 (12), p. 993–996.

Patel, Pranav; Cossette, Chantal; Anumolu, Jaganmohan R.; Erlemann, Karl-Rudolf; Grant, Gail E.; Rokach, Joshua; Powell, William S. (2009): Substrate selectivity of 5-hydroxyeicosanoid dehydrogenase and its inhibition by 5-hydroxy-Delta6-long-chain fatty acids. *J. Pharmacol. Exp. Ther.* 329 (1), p. 335–341.

Patel, Pranav; Cossette, Chantal; Anumolu, Jaganmohan R.; Gravel, Sylvie; Lesimple, Alain; Mamer, Orval A. et al. (2008): Structural requirements for activation of the 5-oxo-6E,8Z, 11Z,14Z-eicosatetraenoic acid (5-oxo-ETE) receptor: identification of a mead acid metabolite with potent agonist activity. *J. Pharmacol. Exp. Ther.* 325 (2), p. 698–707.

Pfleger KD; Seeber RM; Eidne KA (2006): Bioluminescence resonance energy transfer (BRET) for the real-time detection of protein-protein interactions. *Nat. Protoc.* 1 (1), p. 337–345.

Pitcher, J. A.; Inglese, J.; Higgins, J. B.; Arriza, J. L.; Casey, P. J.; Kim, C. et al. (1992): Role of beta gamma subunits of G proteins in targeting the beta-adrenergic receptor kinase to membrane-bound receptors. *Science* 257 (5074), p. 1264–1267.

Popova JS; Johnson GL; Rasenick MM (1994): Chimeric G alpha s/G alpha i2 proteins define domains on G alpha s that interact with tubulin for beta-adrenergic activation of adenylyl cyclase. *J. Biol. Chem.* 269 (34), p. 21748–21754.

Powell, W. S.; Ahmed, S.; Gravel, S.; Rokach, J. (2001): Eotaxin and RANTES enhance 5-oxo-6,8,11,14-eicosatetraenoic acid-induced eosinophil chemotaxis. *J. Allergy Clin. Immunol.* 107 (2), p. 272–278.

Powell, W. S.; Boismenu, D.; Khanapure, S. P.; Rokach, J. (2001): Quantitative analysis of 5-oxo-6,8,11,14-eicosatetraenoic acid by electrospray mass spectrometry using a deuterium-labeled internal standard. *Anal. Biochem.* 295 (2), p. 262–266.

Powell, W. S.; Chung, D.; Gravel, S. (1995): 5-Oxo-6,8,11,14-eicosatetraenoic acid is a potent stimulator of human eosinophil migration. *J. Immunol.* 154 (8), p. 4123–4132.

Powell, W. S.; Gravel, S.; Gravelle, F. (1995): Formation of a 5-oxo metabolite of 5,8,11,14,17-eicosapentaenoic acid and its effects on human neutrophils and eosinophils. *J. Lipid Res.* 36 (12), p. 2590–2598.

Powell, W. S.; Gravel, S.; Halwani, F. (1999): 5-oxo-6,8,11,14-eicosatetraenoic acid is a potent stimulator of L-selectin shedding, surface expression of CD11b, actin polymerization, and calcium mobilization in human eosinophils. *Am. J. Respir. Cell Mol. Biol.* 20 (1), p. 163–170.

Powell, W. S.; Gravel, S.; Halwani, F.; Hii, C. S.; Huang, Z. H.; Tan, A. M.; Ferrante, A. (1997): Effects of 5-oxo-6,8,11,14-eicosatetraenoic acid on expression of CD11b, actin polymerization, and adherence in human neutrophils. *J. Immunol.* 159 (6), p. 2952–2959.

Powell, W. S.; Gravel, S.; Khanapure, S. P.; Rokach, J. (1999): Biological inactivation of 5-oxo-6,8,11,14-eicosatetraenoic acid by human platelets. *Blood* 93 (3), p. 1086–1096.

Powell, W. S.; Gravel, S.; MacLeod, R. J.; Mills, E.; Hashefi, M. (1993): Stimulation of human neutrophils by 5-oxo-6,8,11,14-eicosatetraenoic acid by a mechanism independent of the leukotriene B4 receptor. *J. Biol. Chem.* 268 (13), p. 9280–9286.

Powell, W. S.; Gravel, S.; Stamatiou, P.; MacLeod, R. J. (1995): Effects of 5-oxo-ETE on neutrophils, eosinophils, and intestinal epithelial cells. *Adv. Prostaglandin Thromboxane Leukot. Res.* 23, p. 431–433.

Powell, W. S.; Gravelle, F.; Gravel, S. (1992): Metabolism of 5(S)-hydroxy-6,8,11,14-eicosatetraenoic acid and other 5(S)-hydroxyeicosanoids by a specific dehydrogenase in human polymorphonuclear leukocytes. *J. Biol. Chem.* 267 (27), p. 19233–19241.

Powell, W. S.; Gravelle, F.; Gravel, S. (1994): Phorbol myristate acetate stimulates the formation of 5-oxo-6,8,11,14-eicosatetraenoic acid by human neutrophils by activating NADPH oxidase. *J. Biol. Chem.* 269 (41), p. 25373–25380.

Powell, W. S.; Gravelle, F.; Gravel, S.; Hashefi, M.: Metabolism of 5(S)-hydroxyeicosanoids by a specific dehydrogenase in human neutrophils. *J. Lipid Mediat.* 6 (1-3), p. 361–368.

Powell, W. S.; MacLeod, R. J.; Gravel, S.; Gravelle, F.; Bhakar, A. (1996): Metabolism and biologic effects of 5-oxoeicosanoids on human neutrophils. *J. Immunol.* 156 (1), p. 336–342.

Powell, W. S.; Zhang, Y.; Gravel, S. (1994): Effects of phorbol myristate acetate on the synthesis of 5-oxo-6,8,11,14-eicosatetraenoic acid by human polymorphonuclear leukocytes. *Biochemistry* 33 (13), p. 3927–3933.

Powell, William S.; Gravel, Sylvie; Rokach, Joshua (2002): Interactions between 5-oxo-ETE and chemokines in stimulating eosinophils. *Adv. Exp. Med. Biol.* 507, p. 237–242.

Powell, William S.; Rokach, Joshua: Biochemistry, biology and chemistry of the 5-lipoxygenase product 5-oxo-ETE. *Prog. Lipid Res.* 44 (2-3), p. 154–183.

Rajagopal, Sudarshan; Kim, Jihee; Ahn, Seungkirl; Craig, Stewart; Lam, Christopher M.; Gerard, Norma P. et al. (2010): Beta-arrestin- but not G protein-mediated signaling by the "decoy" receptor CXCR7. *Proc. Natl. Acad. Sci. U.S.A* 107 (2), p. 628–632.

Rebecchi, M. J.; Pentyala, S. N. (2000): Structure, function, and control of phosphoinositide-specific phospholipase C. *Physiol. Rev.* 80 (4), p. 1291–1335.

Reuveny, E.; Slesinger, P. A.; Inglese, J.; Morales, J. M.; Iñiguez-Lluhi, J. A.; Lefkowitz, R. J. et al. (1994): Activation of the cloned muscarinic potassium channel by G protein beta gamma subunits. *Nature* 370 (6485), p. 143–146.

Rondard P; Iiri T; Srinivasan S; Meng E; Fujita T; Bourne HR (2001): Mutant G protein alpha subunit activated by Gbeta gamma: a model for receptor activation? *Proc. Natl. Acad. Sci. U S A* 98 (11), p. 6150–6155.

Rosenzweig DH; Nair KS; Wei J; Wang Q; Garwin G; Saari JC et al. (2007): Subunit dissociation and diffusion determine the subcellular localization of rod and cone transducins. *J. Neurosci.* 27 (20), p. 5484–5494.

Rubin, Paul; Mollison, Karl W. (2007): Pharmacotherapy of diseases mediated by 5-lipoxygenase pathway eicosanoids. *Prostaglandins Other Lipid Mediat.* 83 (3), p. 188–197.

Salchow K; Bond ME; Evans SC; Press NJ; Charlton SJ; Hunt PA; Bradley ME (2010): A common intracellular allosteric binding site for antagonists of the CXCR2 receptor. *Br. J. Pharmacol.* 159 (7), p. 1429–1439.

Sasaki, Yoshinori; Tsujii, Takashi; Takeda, Shigeki; Obinata, Hideru; Izumi, Takashi; Yamada, Keiichi; Katakai, Ryoichi (2008): Identification of novel peptide agonists from a random peptide library for a 5-oxo-ETE receptor, a receptor for bioactive lipids. *J. Pept. Sci.* 14 (12), p. 1251–1258.

Schratl, Petra; Sturm, Eva M.; Royer, Julia F.; Sturm, Gunter J.; Lippe, Irmgard T.; Peskar, Bernhard A.; Heinemann, Akos (2006): Hierarchy of eosinophil chemoattractants: role of p38 mitogen-activated protein kinase. *Eur. J. Immunol.* 36 (9), p. 2401–2409.

Schwenk, U.; Schröder, J. M. (1995): 5-Oxo-eicosanoids are potent eosinophil chemotactic factors. Functional characterization and structural requirements. *J. Biol. Chem.* 270 (25), p. 15029–15036.

Shenoy, Sudha K.; Drake, Matthew T.; Nelson, Christopher D.; Houtz, Daniel A.; Xiao, Kunhong; Madabushi, Srinivasan et al. (2006): beta-arrestin-dependent, G protein-independent ERK1/2 activation by the beta2 adrenergic receptor. *J. Biol. Chem.* 281 (2), p. 1261–1273.

Siehler, Sandra; Milligan, Graeme (2011): G protein-coupled receptors. Structure, signaling, and physiology. Cambridge ;, New York: Cambridge University Press. Online at http://www.worldcat.org/oclc/649795882.

Siehler S (2009): Regulation of RhoGEF proteins by G12/13-coupled receptors. *Br. J. Pharmacol.* 158 (1), p. 41–49.

Simon MI; Strathmann MP; Gautam N (1991): Diversity of G proteins in signal transduction. *Science* 252 (5007), p. 802–808.

Sozzani, S.; Zhou, D.; Locati, M.; Bernasconi, S.; Luini, W.; Mantovani, A.; O'Flaherty, J. T. (1996): Stimulating properties of 5-oxo-eicosanoids for human monocytes: synergism with monocyte chemotactic protein-1 and -3. *J. Immunol.* 157 (10), p. 4664–4671.

Stamatiou, P.; Hamid, Q.; Taha, R.; Yu, W.; Issekutz, T. B.; Rokach, J. et al. (1998): 5-oxo-ETE induces pulmonary eosinophilia in an integrin-dependent manner in Brown Norway rats. *J. Clin. Invest.* 102 (12), p. 2165–2172.

Stamatiou, Panagiota B.; Chan, Chi-Chung; Monneret, Guillaume; Ethier, Diane; Rokach, Joshua; Powell, William S. (2004): 5-oxo-6,8,11,14-eicosatetraenoic acid stimulates the release of the eosinophil survival factor granulocyte/macrophage colony-stimulating factor from monocytes. *J. Biol. Chem.* 279 (27), p. 28159–28164.

Stephens, L.; Smrcka, A.; Cooke, F. T.; Jackson, T. R.; Sternweis, P. C.; Hawkins, P. T. (1994): A novel phosphoinositide 3 kinase activity in myeloid-derived cells is activated by G protein beta gamma subunits. *Cell* 77 (1), p. 83–93.

Sternweis, P. C. (1994): The active role of beta gamma in signal transduction. *Curr. Opin. Cell Biol.* 6 (2), p. 198–203.

Sturm, Gunter J.; Schuligoi, Rufina; Sturm, Eva M.; Royer, Julia F.; Lang-Loidolt, Doris; Stammberger, Heinz et al. (2005): 5-Oxo-6,8,11,14-eicosatetraenoic acid is a potent chemoattractant for human basophils. *J. Allergy Clin. Immunol.* 116 (5), p. 1014–1019.

Sun, Yue; Cheng, Zhijie; Ma, Lan; Pei, Gang (2002): Beta-arrestin2 is critically involved in CXCR4-mediated chemotaxis, and this is mediated by its enhancement of p38 MAPK activation. *J. Biol. Chem.* 277 (51), p. 49212–49219.

Sun Y; McGarrigle D; Huang XY (2007): When a G protein-coupled receptor does not couple to a G protein. *Mol. Biosyst.* 3 (12), p. 849–854.

Sunahara, R. K.; Dessauer, C. W.; Gilman, A. G. (1996): Complexity and diversity of mammalian adenylyl cyclases. *Annu. Rev. Pharmacol. Toxicol.* 36, p. 461–480.

Sundaram S; Ghosh J (2006): Expression of 5-oxoETE receptor in prostate cancer cells: critical role in survival. *Biochem. Biophys. Res. Commun.* 339 (1), p. 93–98.

Swift, Steven; Leger, Andrew J.; Talavera, Joyce; Zhang, Lei; Bohm, Andrew; Kuliopulos, Athan (2006): Role of the PAR1 receptor 8th helix in signaling: the 7-8-1 receptor activation mechanism. *J. Biol. Chem.* 281 (7), p. 4109–4116.

Tang, W. J.; Gilman, A. G. (1991): Type-specific regulation of adenylyl cyclase by G protein beta gamma subunits. *Science* 254 (5037), p. 1500–1503.

Tang, X.; Downes, C. P. (1997): Purification and characterization of Gbetagamma-responsive phosphoinositide 3-kinases from pig platelet cytosol. *J. Biol. Chem.* 272 (22), p. 14193–14199.

Topiol S; Sabio M (2009): X-ray structure breakthroughs in the GPCR transmembrane region. *Biochem. Pharmacol.* 78 (1), p. 11–20.

Urban, Jonathan D.; Clarke, William P.; Zastrow, Mark von; Nichols, David E.; Kobilka, Brian; Weinstein, Harel et al. (2007): Functional selectivity and classical concepts of quantitative pharmacology. *J. Pharmacol. Exp. Ther.* 320 (1), p. 1–13.

Vauquelin, G.; van Liefde, I. (2005): G protein-coupled receptors: a count of 1001 conformations. *Fundam. Clin. Pharmacol.* 19 (1), p. 45–56.

Vauquelin, G.; van Liefde, I.; Birzbier, B. B.; Vanderheyden, P. M. L. (2002): New insights in insurmountable antagonism. *Fundam. Clin. Pharmacol.* 16 (4), p. 263–272.

Vauquelin, Georges; Mentzer, Bengt von (2007): G protein-coupled receptors. Molecular pharmacology from academic concept to pharmaceutical research. Chichester, England ;, Hoboken, NJ: John Wiley & Sons. Online at http://www.worldcat.org/oclc/144568185.

Vauquelin, Georges; Szczuka, Anna (2007): Kinetic versus allosteric mechanisms to explain insurmountable antagonism and delayed ligand dissociation. *Neurochem. Int.* 51 (5), p. 254–260.

Vauquelin, Georges; van Liefde, Isabelle; Vanderheyden, Patrick (2002): Models and methods for studying insurmountable antagonism. *Trends Pharmacol. Sci.* 23 (11), p. 514–518.

Vrecl, Milka; Jorgensen, Rasmus; Pogacnik, Azra; Heding, Anders (2004): Development of a BRET2 screening assay using beta-arrestin 2 mutants. *J. Biomol. Screen.* 9 (4), p. 322–333.

Walker, Julia K. L.; Fong, Alan M.; Lawson, Barbara L.; Savov, Jordan D.; Patel, Dhavalkumar D.; Schwartz, David A.; Lefkowitz, Robert J. (2003): Beta-arrestin-2 regulates the development of allergic asthma. *J. Clin. Invest.* 112 (4), p. 566–574.

Walters, Robert W.; Shukla, Arun K.; Kovacs, Jeffrey J.; Violin, Jonathan D.; DeWire, Scott M.; Lam, Christopher M. et al. (2009): beta-Arrestin1 mediates nicotinic acid-induced flushing, but not its antilipolytic effect, in mice. *J. Clin. Invest.* 119 (5), p. 1312–1321.

Wei, Huijun; Ahn, Seungkirl; Shenoy, Sudha K.; Karnik, Sadashiva S.; Hunyady, László; Luttrell, Louis M.; Lefkowitz, Robert J. (2003): Independent beta-arrestin 2 and G protein-mediated pathways for angiotensin II activation of extracellular signal-regulated kinases 1 and 2. *Proc. Natl. Acad. Sci. U.S.A* 100 (19), p. 10782–10787.

Wilkie TM; Scherle PA; Strathmann MP; Slepak VZ; Simon MI (1991): Characterization of G-protein alpha subunits in the Gq class: expression in murine tissues and in stromal and hematopoietic cell lines. *Proc. Natl. Acad. Sci. U S A* 88 (22), p. 10049–10053.

Woehler A; Ponimaskin EG (2009): G protein--mediated signaling: same receptor, multiple effectors. *Curr. Mol. Pharmacol.* 2 (3), p. 237–248.

Woo, Anthony Yiu-Ho; Wang, Tian-Bing; Zeng, Xiaokun; Zhu, Weizhong; Abernethy, Darrell R.; Wainer, Irving W.; Xiao, Rui-Ping (2009): Stereochemistry of an agonist determines coupling preference of beta2-adrenoceptor to different G proteins in cardiomyocytes. *Mol. Pharmacol.* 75 (1), p. 158–165.

Worzfeld T; Wettschureck N; Offermanns S (2008): G(12)/G(13)-mediated signaling in mammalian physiology and disease. *Trends Pharmacol. Sci.* 29 (11), p. 582–589.

Wu B; Chien EY; Mol CD; Fenalti G; Liu W; Katritch V et al. (2010): Structures of the CXCR4 chemokine GPCR with small-molecule and cyclic peptide antagonists. *Science* 330 (6007), p. 1066–1071.

Ye RD; Boulay F; Wang JM; Dahlgren C; Gerard C; Parmentier M et al. (2009): International Union of Basic and Clinical Pharmacology. LXXIII. Nomenclature for the formyl peptide receptor (FPR) family. *Pharmacol. Rev.* 61 (2), p. 119–161.

Zarini, Simona; Murphy, Robert C. (2003): Biosynthesis of 5-oxo-6,8,11,14-eicosatetraenoic acid from 5-hydroperoxyeicosatetraenoic acid in the murine macrophage. *J. Biol. Chem.* 278 (13), p. 11190–11196.

Zhang, Y.; Styhler, A.; Powell, W. S. (1996): Synthesis of 5-oxo-6,8,11,14-eicosatetraenoic acid by human monocytes and lymphocytes. *J. Leukoc. Biol.* 59 (6), p. 847–854.

Zhao, Ming; Wimmer, Antonia; Trieu, Khanh; Discipio, Richard G.; Schraufstatter, Ingrid U. (2004): Arrestin regulates MAPK activation and prevents NADPH oxidase-dependent death of cells expressing CXCR2. *J. Biol. Chem.* 279 (47), p. 49259–49267.

Zimpfer; Hofmann; Dichmann; Schopf; Norgauer (1998): Synthesis, biological effects and pathophysiological implications of the novel arachidonic acid metabolite 5-oxo-eicosatetraenoic acid (Review). *Int. J. Mol. Med.* 2 (2), p. 149–153.

Zimpfer, U.; Dichmann, S.; Termeer, C. C.; Simon, J. C.; Schröder, J. M.; Norgauer, J. (2000): Human dendritic cells are a physiological source of the chemotactic arachidonic acid metabolite 5-oxo-eicosatetraenoic acid. *Inflamm. Res.* 49 (11), p. 633–638

Appendix

Chemical structures of compounds tested in HEK-OXE-R-G_{16} calcium mobilization assays (section 3.1.2, 3.1.4, 3.1.5).

compound name	chemical structure
Gü 259	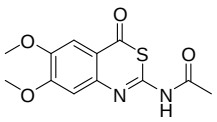
Gü 292	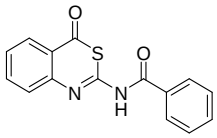
Gü 295	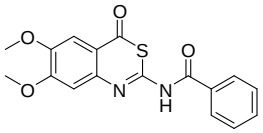
Gü 304	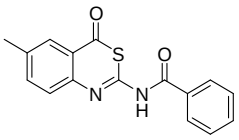
Gü 314	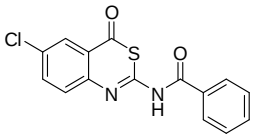
Gü 315	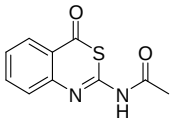
Gü 1028	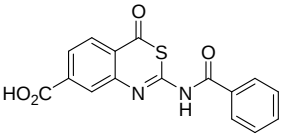

compound name	chemical structure
Gü 1142	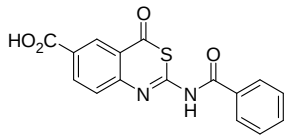
682471	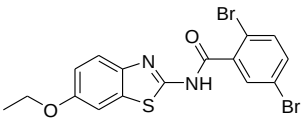
938141	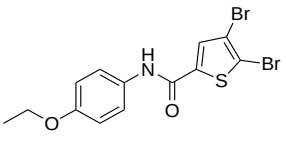
1071153	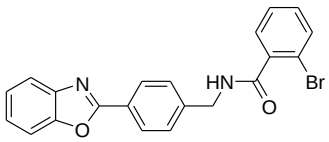
3022900	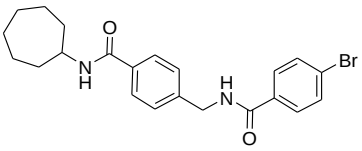
9030109	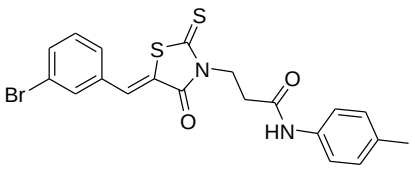
1087122	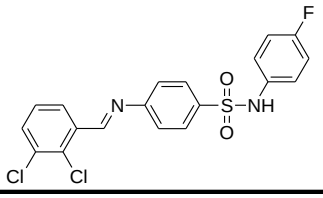

compound name	chemical structure
Gü 1635	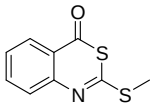
Gü 1650	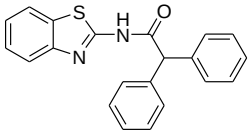
Gü 1651	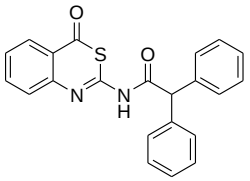
Gü 1652	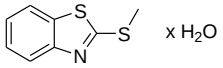
Gü 1653	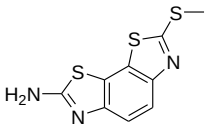
Gü 1655	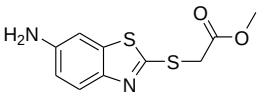
Gü 1656	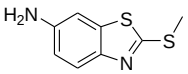
Gü 1657	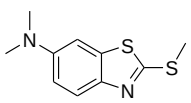

compound name	chemical structure
Gü 1678	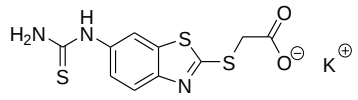
Gü 1679	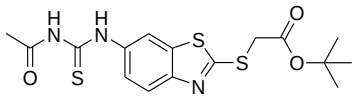
Gü 1680	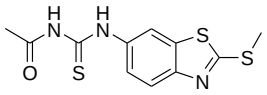
Gü 1681	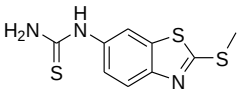
Gü 1682	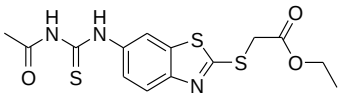
Gü 1683	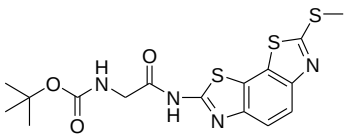
Gü 1684	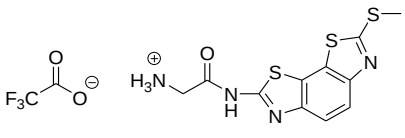

Publications

Schröder R, Janssen N, Schmidt J, Kebig A, Merten N, Hennen S, Müller A, **Blättermann S**, Mohr-Andrä M, Zahn S, Wenzel J, Smith NJ, Gomeza J, Drewke C, Milligan G, Mohr K, Kostenis E. (2010) Deconvolution of complex G protein-coupled receptor signaling in live cells using dynamic mass redistribution measurements. *Nature Biotechnology, Volume: 28, Pages: 943–949*

Balenga NA, Aflaki E, Kargl J, Platzer W, Schröder R, **Blättermann S**, Kostenis E, Brown AJ, Heinemann A, Waldhoer M. (2011) GPR55 regulates cannabinoid 2 receptor-mediated responses in human neutrophils. *Cell Research.*

Schröder R, Schmidt J, **Blättermann S**, Peters L, Janssen N, Grundmann M, Seemann W, Kaufel D, Merten N, Drewke C, Gomeza J, Milligan G, Mohr K, Kostenis E. (2011) Applying label-free dynamic mass redistribution technology to frame signaling of G protein-coupled receptors non-invasively in living cells. (*Nature Protocols*, in press)

Tyagi R, **Blättermann S**, Kostenis E, Ulven T. (2011) A concise method for synthesis of the potent inflammatory mediator 5-oxo-eicosa-6*E*,8*Z*,11*Z*,14*Z*-tetraenoic acid (5-oxo-ETE). (submitted)

Blättermann S, Peters L, Luschnig P, Ottersbach P, Bock A, Gonzalez A, Schröder R, Tyagi R, Gäb J, Hennen S, Ulven T, Pardo L, Mohr K, Gütschow M, Heinemann A, Kostenis E. (2011) Differential inhibition of Gbetagamma but not Galpha signaling by a small molecule antagonist provides evidence for a new mechanism of ligand bias at a G protein coupled receptor. (in preparation)

Erklärung

Hiermit erkläre ich, dass ich die vorliegende Dissertation selbständig angefertigt habe. Es wurden nur die in der Arbeit ausdrücklich benannten Quellen und Hilfsmittel benutzt. Wörtlich oder sinngemäß übernommenes Gedankengut habe ich als solches kenntlich gemacht.

Ort, Datum	Unterschrift

Acknowledgments

I wish to express my sincere gratitude to Prof. Dr. Evi Kostenis, who constantly guided, encouraged and supported me through this work. Without her, this work would not have been possible. I thank her for inspiring discussions, for her contagious enthusiasm on GPCR research and for personal care.

I would like to thank Prof. Dr. Mohr for cooperation, for providing the opportunity to work in his lab facilities and for officiating as second referee.

I would like to thank Prof. Dr. Gütschow for cooperation and for participation at the examination committee.

I thank Prof. Dr. Bönisch for participation at the examination committee.

I am grateful to Dr. Petra Luschnig and Prof. Dr. Akos Heinemann, Institute of Experimental and Clinical Pharmacology, Medical University of Graz, Austria, for collaboration and for providing the assays in primary human eosinophils and neutrophils.

I would like to thank Angel Gonzalez and Prof. Dr. Leonardo Pardo, Laboratory of Computational Medicine, Universitat Autònoma de Barcelona, Barcelona, Spain, for the computational modeling and the virtual screening.

I would like to thank Rahul Tyiagi and Prof. Dr. Trond Ulven, Department of Physics and chemistry, Syddansk Universitet, Odense, Denmark, for kindly providing 5-oxo-ETE.

A special thank you goes to Philipp Ottersbach for the fragment based synthesis of potential OXE receptor antagonists and for support on compound structures.

I would like to thank Andreas Bock for excellent cooperation and for providing the IP1 data.

I am grateful to Uli Rick and Marianne Vasmer-Ehses for outstanding experimental support.

I am grateful to Lucas Peters for outstanding support on the last experiments of this work and for providing the BRET data.

I would like to thank Dr. Jesús Gomeza for support in molecularbiological and other matters.

I thank Dr. Christel Drewke for support in different matters and for proof-reading this thesis.

I would like to thank Dr. Nicole Merten for support in all kinds of experimental matters and for proof-reading this thesis.

A special thank you goes to Elke Gassen for support in administrative matters, to Edith Neu for support in order affairs and to Thomas Kögler for support in many different matters.

I am grateful to the whole working group of Prof. Mohr for cooperation and for support in many matters.

I would like to thank Dr. Stefan Kehraus for support in different matters and for creating a good working atmosphere at student classes.

I would like to thank all members of the institute of Pharmaceutical Biology for cooperation and support in different matters.

A very special thank you goes to all my colleagues for creating an excellent working atmosphere in the lab, for mutual assistance and for enjoyable gatherings outside the lab: Katrin Bell, Manuel Grundmann, Stephanie Hennen, Waltraud Läer, Dr. Nicole Merten, Julia Morschel, Anke Müller, Lucas Peters, Ulrike Rick, Johannes Schmidt, Ralf Schröder, Daniel Schulz, Andreas Spinrath and Marianne Vasmer-Ehses.

Last, but not least, I am grateful to my sister Anne and to my parents who always support me in every situation under any circumstances.